UNIVERSITE D'ABOMEY -CALAVI (UAC)

INSTITUT NATIONAL DE L'EAU

Registered under N° 502-24/UAC/VR-AA/SA

A DISSERTATION

Submitted

In partial fulfillment of the requirements for the degree of

DOCTOR of Philosophy (PhD) of the University of Abomey-Calavi (Benin Republic)

In the framework of the

Graduate Research Program on Climate Change and Water Resources (GRP-CCWR)

By

Moustapha TALL

Public defense on: 01/20/2021

======

INTEGRATION OF LAND SURFACE MODELING, DATA ASSIMILATION AND CLIMATE CHANGE IN ASSESSING PAST AND FUTURE HYDROCLIMATIC CONDITIONS OVER BURKINA FASO, WEST AFRICA

======

Supervisors

Luc O. SINTONDJI, Full Professor, University of Abomey-Calavi, Bénin
Amadou T. GAYE, Full Professor, University Cheikh Anta Diop, Sénégal

Fabien C. C. HOUNTONDJI, Associate Professor, University of Parakou, Bénin

======

Reviewers:

Arouna DIEDHIOU	Research Director, Institut de la Recherche Pour le Développement, France	Reviewer
Jean-Marie DIPAMA	Full Professor, University of Joseph Ki-Zerbo, Burkina-Faso	Reviewer
Eric A. Alamou	Associate Professor, Université Nationale des Sciences, Technologies, Ingénierie et Mathématiques, Bénin	Reviewer

======

JURY

Jean Bio CHABI OROU	Full Professor, University of Abomey-Calavi, Bénin	President
Arouna DIEDHIOU	Research Director, Institut de la Recherche pour le Développement, France	Reviewer
Jean-Marie DIPAMA	Full Professor, University of Joseph Ki-Zerbo, Burkina-Faso	Reviewer
Eric A. Alamou	Associate Professor, Université Nationale des Sciences, Technologies, Ingénierie et Mathématiques, Bénin	Examiner
Amadou T. Gaye	Full Professor, University of Cheikh Anta Diop, Sénégal	Co-supervisor
Fabien C. C. Hountondji	Associate Professor, University of Parakou, Bénin	Co-supervisor
Luc O. SINTONDJI	Full Professor, University of Abomey-Calavi, Bénin	Supervisor

Dedication

To my family

Acknowledgements

This thesis is realized in the framework of the West African Science Service Centre on Climate Change and Adapted Land use (WASCAL) with financial aid from the German Ministry of Education and Research (BMBF) in collaboration with the Benin Ministry of High Education and Scientific Research (MESRS). Special thanks to the BMBF and WASCAL for providing the scholarship and financial support throughout this thesis.

I would like to first say a very big thank to my supervisors and advisors Prof Luc Olivier Sintondji, Prof Amadou Thierno Gaye and Prof Fabien C. C. Hountondji, for all the support and encouragement they gave me, during the whole process of this thesis. Without their guidance and valuable feedbacks, this PhD would not have been achievable.

I greatly appreciate the support received through the collaborative work undertaken with the Centre National de Recherches Météorologiques (CNRM) based at Toulouse in France, especially with Dr Clément Albergel and Dr Françoise Guichard. Thank you, dear Clément, for introducing me in the fascinating world of data assimilation in hydrological research. I really appreciate your support and close assistance during all my visits to the VEGEO group of Météo-France. Same appreciation goes also to Françoise whose contributions and exciting scientific discussions helped considerably.

My gratitude also goes to the administrative team of WASCAL Graduate Research Program (GRP) of University of Abomey Calavi in Benin Republic, especially to the Director Prof Julien Adounkpe and the Deputy Director of the program Prof Emmanuel Lawin for their advices and directives, as well as the staff members of the GRP, Mr Salem and Mrs Djagoun.

I would also like to thank my colleagues Djan'na Koubodana, Oumou Diancoumba, Abdou Boko, Abdelaziz Kouakou, Femi Adeyeri, Isaac Larbi, Rita Houngue, Adama Jallow and Samiratou Oueremi. I will never forget all the good —and challenging—time we shared together.

I cannot finish without mentioning how helpful was my local laboratory (LPAO-SF) based in Cheikh Anta Diop University in terms of facilities and infrastructures provided. I therefore would deeply thank everyone working in the lab, from the Director to all associates, post-graduates, graduates and staff as well as the alumni members.

Most importantly, a big thank to my family, especially my parents, their love and support over the years has meant a great deal to me. Time spent with family and friends

throughout this process always reminded me of what is most important in life, and they have all contributed in some way to my achievements.

Abstract

Estimating climate change impacts on water resources in West Africa has been challenged by hydrological data scarcity and inconsistencies in the available climate projections. In this thesis, an integrated approach involving land surface modelling, data assimilation and multi-model ensemble of the most recent regional climate model output is used to simulate the hydroclimatic impacts of climate change over Burkina Faso. To this end, high-resolution simulations from the CO_2-responsive versions of the Interactions between Soil, Biosphere, and Atmosphere (ISBA), the global Land Data Assimilation System (LDAS-Monde) and a multi-model ensemble based on the most recent version of the Regional Climate Model (RegCM4) under two Representative Concentration Pathways (RCP4.5 and RCP8.5) are used. ISBA estimates are assessed through its forcings (ERA5 and ERA-Interim reanalyses) for precipitation and solar radiation variables. First, it is shown that both reanalyses present a good performance in representing precipitation variability and incoming solar radiation (with better score for ERA5). This highlights a good calibration and the potential of ISBA to provide good quality estimates of land surface estimates such as Leaf Area Index (LAI) and Surface Soil Moisture (SSM). Then, within LDAS-Monde, SSM and LAI observations from the Copernicus Global Land Service (CGLS) are assimilated with a simplified extended Kalman filter (SEKF) using ISBA over a long period (2001-2018). Results of four experiments are then compared: Open-loop simulation (i.e., model run with no assimilation) and analysis (i.e., joint assimilation of SSM and LAI) both forced by either ERA5 or ERA-Interim. After jointly assimilating SSM and LAI, sensitivity study of the model to the observations permits to notice that the assimilation is able to impact soil moisture in the first top soil layers (mainly up the first 20 cm), but also in deeper soil layers (from 20 cm to 60 cm and below), as reflected by the structure of the SEKF Jacobians. The benefit of using ERA5 reanalysis over ERA-Interim when used in LDAS-Monde is highlighted. The assimilation is able to improve the simulation of both SSM and LAI: the analyses add skills to both configurations, indicating the good behaviour of LDAS-Monde. For LAI in particular, the southern region of Burkina Faso (dominated by a Sudan-Guinean climate) highlights a strong impact of the assimilation compared to the other two sub-regions of Burkina Faso (dominated by Sahelian and Sudan-Sahelian climates). In the southern part of the domain, differences between the model and the observations are the largest, prior to any assimilation. These differences are linked to the model failing to represent the behaviour of some specific vegetation species, which are known to produce leaves before the first rains of the season. The LDAS-Monde analysis is very efficient at compensating for this model weakness.

Evapotranspiration estimates from the Global Land Evaporation Amsterdam Model (GLEAM) project as well as upscaled carbon uptake from the FLUXCOM project and sun-induced fluorescence from the Global Ozone Monitoring Experiment-2 (GOME-2) are used in the evaluation process, again demonstrating improvements in the representation of evapotranspiration and gross primary production from assimilation. Finally, the impact of anthropogenic climate change in the hydroclimatology of Burkina Faso for the middle (2041–2060) and late (2080–2099) 21st century has been investigated with regard to the historical period (2001-2018). The results indicate that an increased warming, leading to substantial increase of atmospheric water demand, is projected over all Burkina Faso areas. In addition, mean precipitation unveils contrasting changes with wetter conditions (for all three climatic zones) by the middle of the century and drier conditions during the late twenty-first century (mostly for the Sahelian zone). Such changes cause more/less evapotranspiration and soil moisture respectively during the two future periods. Furthermore, surface runoff shows a tendency to increase and decrease along with short spatial gradients regardless whether the region receives more or less precipitation. Finally, it is found that while dry and semi-arid conditions develop in the RCP4.5 scenario, generalized arid conditions prevail over the whole Burkina Faso for RCP8.5. It is thus evident that these future climate conditions substantially threaten water resources availability for the country as well as agricultural activities. Therefore, strong strategedies are needed to help design response options to cope with the challenges posed by the projected climate change for the country.

Keywords: Land surface modelling, data assimilation, evapotranspiration; leaf area index, runoff, surface soil moisture.

Synthèse de la thèse

Résumé

La présente thèse vise à évaluer les conditions hydroclimatiques historiques et futures du Burkina Faso en utilisant une approche intégrée impliquant la modélisation des variables d'état de surface, l'assimilation de données et les changements climatiques. Pour cela, des simulations à haute résolution (0.25°) de la version sensible au CO_2 du modèle ISBA (Interaction Sol-Biosphère-Atmosphère), du système global d'assimilation de données de surfaces terrestres (LDAS-Monde) et d'un ensemble multi-modèle basé sur la version la plus récente du modèle climatique régional (RegCM4) considérant deux profils représentatifs d'évolution de concentration (RCP4.5 et RCP8.5) sont utilisées. La validation du modèle ISBA se fait indirectement en évaluant la qualité de ses forçages atmosphériques (les ré-analyses ERA5 et ERA-Interim) pour la pluie et le rayonnement solaire pour la période 2010-2016. Tout d'abord, il est démontré que les deux ré-analyses présentent une bonne performance dans la représentation de la variabilité des précipitations et du rayonnement solaire entrant (avec un meilleur score pour ERA5). Cela met en évidence un bon potentiel de ISBA à fournir de raisonnables estimations des variables d'état de surface telles que l'indice de surface foliaire (LAI, en anglais) et l'humidité superficielle du sol (SSM, en anglais). Ensuite, dans le système d'assimilation LDAS-Monde, les observations satellitaires de SSM et LAI du Copernicus Global Land Service (CGLS) sont assimilées à l'aide d'un Filtre de Kalman Simplifié Etendu (SEKF, en anglais) en utilisant ISBA sur une longue période (2001-2018). Les résultats de quatre expériences sont ensuite comparés : deux simulations « en boucle-ouverte » (c'est-à-dire modèles sans assimilation) et deux analyses (c'est-à-dire assimilation conjointe de SSM et de LAI dans le modèle) respectivement forcées par les ré-analyses atmosphériques ERA5 et ERA-Interim. Après l'assimilation conjointe de SSM et de LAI, l'étude de la sensibilité du modèle aux observations permet de constater que l'assimilation peut avoir un impact positif sur l'humidité du sol dans les premières couches supérieures (principalement jusqu'aux 20 premiers cm), mais aussi dans les couches plus profondes (de 20 cm à 60 cm et en dessous), comme le reflète la structure des Jacobiens du SEKF. La valeur ajoutée de la ré-analyse ERA5 par rapport à ERA-Interim lorsqu'elle est utilisée dans LDAS-Monde est mise en évidence. L'assimilation est capable d'améliorer la simulation de SSM et de LAI : les analyses ajoutent de la compétence aux deux configurations, indiquant un comportement adéquat de LDAS-Monde. Pour le LAI en particulier, la région Sud du Burkina Faso (dominée par un climat soudano-guinéen) met en évidence un fort impact de l'assimilation par rapport aux deux autres sous-régions du Burkina

Faso (dominées par les climats sahélien et soudano-sahélien). Dans la partie Sud, les différences entre le modèle et les observations sont les plus importantes, ceci avant toute assimilation. Ces différences sont liées au fait que le modèle ne représente pas le comportement de certaines espèces végétales spécifiques, qui sont connues par leur capacité à produire du feuillage avant les premières pluies de la saison. L'analyse de LDAS-Monde est très efficace pour compenser cette faiblesse observée dans le comportement du modèle de surface ISBA. Des estimations d'évapotranspiration provenant du projet GLEAM (Global Land Evaporation Amsterdam Model) ainsi que des produits de carbone assimilé du projet FLUXCOM et la fluorescence induite par le soleil de l'expérience GOME-2 (Global Ozone Monitoring Experiment) sont utilisées dans le processus d'évaluation, démontrant encore une fois des améliorations dans la représentation de l'évapotranspiration et de la production primaire brute après assimilation. Enfin, les impacts du changement climatique anthropique sur l'hydroclimatologie du Burkina Faso pour la moitié (2041-2060) et la fin (2080-2099) du 21^{e} siècle ont été analysés par rapport à la période historique (2001-2018). Les résultats indiquent qu'un réchauffement élevé, entraînant une augmentation substantielle de la demande en eau atmosphérique, est prévu sur l'ensemble du Burkina Faso. En outre, les précipitations moyennes révèlent des changements contrastés avec des conditions plus humides au milieu du siècle (pour toutes les zones climatiques) et des conditions plus sèches (plus particulieremnt dans la zone sahélienne) à la fin du 21^{e} siècle. De tels changements entraînent une évapotranspiration et une humidité du sol plus ou moins importantes au cours des deux périodes futures. En outre, le ruissellement de surface aurait, en partie, tendance à augmenter et à diminuer avec un imporatant gradient spatial, tenant compte de la quantité de pluie reçue par le pays. Enfin, on constate que si des conditions sèches et semi-arides se développent dans le scénario RCP4.5, des conditions arides généralisées prévalent sur l'ensemble du Burkina Faso pour le RCP8.5. Il est donc évident que ces conditions climatiques futures menaceront considérablement la disponibilité des ressources en eau pour le pays ainsi que les activités agricoles. Par conséquent, des stratégies adaptées sont nécessaires pour aider à concevoir des options de réponse afin de faire face aux défis posés par le changement climatique prévu pour le pays.

Mots clés : Modélisation des surfaces terrestres, assimilation de données, évapotranspiration, indice de surface foliaire, ruissellement, humidité de surface.

Introduction

Les variables d'état de surface permettent de caractériser la dynamique des surfaces continentales et de l'atmosphère, jouant ainsi un rôle clé dans notre système hydroclimatique.

L'initialisation des modèles de variables d'état de surface (LSM, en anglais pour *Land Surface Model*) pour une représentation optimale des variables d'états de surface est donc pertinente pour le suivi des variables de surface terrestre et bien sur, leur prévision. Dans un contexte de changement climatique et d'augmentation probable dans le futur de la fréquence et de l'intensité des événements extrêmes, des sécheresses agricoles en particulier, il est nécessaire de mieux représenter la réponse des variables hydroclimatiques. Le suivi de l'impact des événements extrêmes sur les surfaces terrestres fait intervenir de nombreuses variables du système sol-plante, comme le contenu en eau des sols et l'indice de surface foliaire (LAI) de la végétation. Ces variables peuvent être suivies de deux façons : (1) en utilisant le volume d'observations sans précédent fourni par la flotte de satellites d'observation de la Terre, et (2) en utilisant des modèles de surfaces terrestres. Il existe une troisième solution qui consiste à combiner l'ensemble de l'information disponible en intégrant les observations satellitaires dans les modèles. Ce processus s'appelle l'assimilation de données. Elle produit une analyse des variables terrestres qui constitue la meilleure estimation possible car les informations de départ sont pondérées de façon à prendre en compte les incertitudes.

Outre le contexte de la surveillance climatique et hydrologique, l'amélioration de la prévision des paramètres de surface terrestre - en particulier dans les zones pauvres en données comme le Sahel en Afrique - est également pertinente pour toute une série d'autres problèmes dont la solution dépend d'informations précises et opportunes sur le bilan hydrique et énergétique de la surface terrestre. Pour ces raisons, il a été largement proposé dans cette thèse une stratégie effective pour mieux représenter les paramètres clés pour le suivi des ressources en eau, comme l'humidité du sol. Enfin, il sera fourni des projections robustes de paramètres clés permettant d'analyser la disponibilité future des ressources en eau pour le Burkina Faso. Les objectifs spécifiques de cette thèse sont : (i) évaluer la qualité des simulations de ISBA à travers la performance des ré-analyses ERA5 et ERA-Interim ; (ii) évaluer la capacité de LDAS-Monde à fournir une ré-analyse à long terme des variables hydroclimatiques à travers l'assimilation conjointe d'observations de LAI et d'humidité superficielle du sol ; et enfin (iii) évaluer les changements potentiels sur les variables hydroclimatiques telles que l'évapotranspiration, le ruissellement de surface, et l'humidité du sol.

Contexte général et revue de littérature

Ce chapitre a donné des informations détaillées basées sur la littérature. Ces informations sont fondées sur des études antérieures et sont pertinentes pour les objectifs mis en évidence dans le chapitre d'introduction. Il a également été noté un manque de connaissances

dans le contexte de la recherche sur l'assimilation des données dans les modèles de surface dans un cadre plus large - que le cadre de modélisation réalisé ici contribue à étoffer. La littérature suggère également la nécessité de progresser vers l'utilisation de schémas d'assimilation de données plus optimaux tels que le KF (filtre de Kalman), afin de mieux gérer les différents produits de données de surface terrestre de plus en plus disponibles. Le SEKF (filtre de Kalman étendu simplifié) est donc un choix approprié à utiliser pour l'assimilation séquentielle de l'humidité du sol et des produits de végétation dans cette thèse. De nombreuses études d'assimilation publiées ont examiné l'assimilation de données sur l'humidité du sol, la température du sol ou la végétation dans une série d'études. Inversement, les recherches sur l'assimilation des données de SSM et de LAI sont limitées dans la littérature, plus particulèrement, le potentiel de l'utilisation conjointe de ces données pour améliorer les prévisions de SSM et de LAI ainsi que les flux tels que l'évapotranspiration. C'est pourquoi cette thèse a cherché à produire une ré-analyse de qualité de paramètres d'état de surface pour enfin, faire un suivi des impacts des changements climatiques futurs sur l'hydroclimatologie du pays.

Présentation de la zone d'étude

La zone d'étude est le Burkina Faso (Burkina Faso) et couvre environ 274 000 km^2 pour une population estimée à 20 millions d'habitants (largement plus concentre au Sud). Le pays est situé entre le désert du Sahara et le Golfe de Guinée, au sud du fleuve Niger, entre les latitudes 9° et 15°N, et les longitudes 6°W et 3°E. Le Burkina Faso possède des plans d'eau tels que des lacs et des bassins fluviaux sur l'ensemble de son territoire. Toutefois, le plus grand réseau d'eau se trouve dans le sud du pays, qui présente trois principaux bassins fluviaux : la Volta, la Comoé et le Niger. L'altitude moyenne du pays est de 400 m et la différence entre le relief le plus élevé et le plus bas ne dépasse pas 600 m. Ainsi, le Burkina Faso est considéré comme un pays relativement plat. En termes de climat, le Burkina Faso est principalement marqué par un climat tropical avec deux saisons. Pendant la saison des pluies, le pays reçoit entre 600 et 900 mm de précipitations ; tandis que la saison sèche est caractérisée par un vent chaud et sec en provenance du Sahara caractérisant ainsi trois zones climatiques : climat sahélien (SH), climat Soudano-Sahélien (SS) et climat Soudano-Guinéen (SG).

Matériels et méthodes

Ce chapitre a présenté les différents jeux de données et modèles utilisés dans cette thèse. Ce sont entre autre les données in-situ de pluie et radiation solaire de l'ANAM (Agence Nationale de la Météorologie) du Burkina Faso, les données de télédétection d'indice de surface foliaire (LAI) et d'humidité du sol (SSM) issues du CGLS (Copernicus Global Land Service,

en anglais), les ré-analyses atmosphériques ERA-Interim et ERA5 du centre européen pour les prévisions météorologiques à moyen terme (ECMWF, anglais), le modèle de surface ISBA ainsi que le système d'assimilation de données terrestres LDAS-Monde mis en place pour améliorer la représentation des variables d'état de surface. Il s'y ajoute la dernière version du modèle régional climatique RegCM4 développée par le centre international de physique théorique (ICTP, en anglais) utilisée pour l'analyse des projections hydroclimatiques futures. Le filtre de Kalman Etendu Simplifié (SEKF) a été utilisé comme méthode dans le cadre des expériences d'assimilation afin d'intégrer les données d'observation (LAI et SSM) dans le modèle ISBA afin de permettre à LDAS-Monde de produire des ré-analyses de surface telles que l'humidité du sol. Ces sorties du système LDAS-Monde sont soumises à des stratégies d'évaluation pour apprécier leur qualité et performance. Ces stratégies mettent en jeu des scores statistiques tels que la corrélation (R), l'erreur quadratique moyen ou RMSD ainsi que le RMSD non biaisé (ubRMSD), le biais et la différence des écart-types (SDD). Afin d'aborder les questions de disponibilité future de l'eau pour le Burkina Faso dans le cadre du changement climatique, nous avons étudié dans quelle mesure le changement climatique anthropique modifie l'hydroclimatologie du pays. Pour ce faire, la méthode du changement de signal appelée aussi Méthode du Delta (futur - présent) a été utilisée. Plus précisément, il a examiné comment les différents forçages RCPs (RCP4.5 & RCP8.5) impactent les températures, les précipitations, l'évapotranspiration, l'humidité du sol, le ruissellement de surface dans un futur proche et à la fin du 21^{e} siècle. Enfin, l'aridité du Burkina Faso a été étudiée à travers une approche multivariée, utilisant la classification révisée de l'humidité de Thornthwaite combinée à l'indice développé par Wilmot et Feddema pour la période de référence (2001-2018), le proche avenir (2041-2060) et la fin du 21^{e} siècle (2080-2099), ainsi que pour la RCP4.5 et la RCP8.5.

Résultats et discussions

Les résultats de la thèse sont largement basés sur la modélisation des variables d'état de surface, l'assimilation de données et les changements climatiques.

En premier lieu, cette étude s'est accentuée sur la validation des ré-analyses atmosphériques ERA5 et ERA-Interim à controller les sorties du modèle ISBA à l'aide de mesures in situ de pluie et de rayonnement solaire entrant (SW_{in}). Cette approche représente une évaluation indirecte des simulations d'ISBA pour des variables comme le LAI et le SSM qui sont principalement conditionnées par la qualité des forçages atmosphériques comme la pluie et la radiation solaire. La qualité d'ERA5 par rapport à l'ancienne réanalyse ERA-Interim a été aussi évaluée en meme temps. Les valeurs médianes de R, ubRMSD, biais et RMSD pour la série chronologique (2001 à 2018) des précipitations mensuelles totales sont respectivement

de 0.82 ± 0.009, 52.02 ± 1.390 mm/mois, - 15.00 ± 3.270 mm/mois, et 56.15 ± 3.600 mm/mois pour ERA5, et 0.77 ± 0.010, 58.44 ± 1.420 mm/mois, - 19.85 ± 3.770 mm/mois, et 63.89 ± 3.250 mm/mois pour ERA-Interim avec un intervalle de confiance estimé à 95 %. Ces résultats indiquent une meilleure performance avec la réanalyse ERA5 dans la représentation de la variabilité des précipitations comparée à ERA-Interim. De plus, ERA5 est plus performant qu'ERA-Interim pour 84% des stations de mesure des précipitations pour les valeurs de R, 89% pour les valeurs de ubRMSD, 83% pour les valeurs de biais et 86% pour les valeurs de RMSD. Les mêmes conclusions ont été illustrées par les cartes de la Figure 1, où les symboles en forme de triangle (cercle) indiquent les stations où l'ERA5 est plus performant (moins performant) que l'ERA-Interim en termes de R (Figure 1a) et de ubRMSD (Figure 1b).

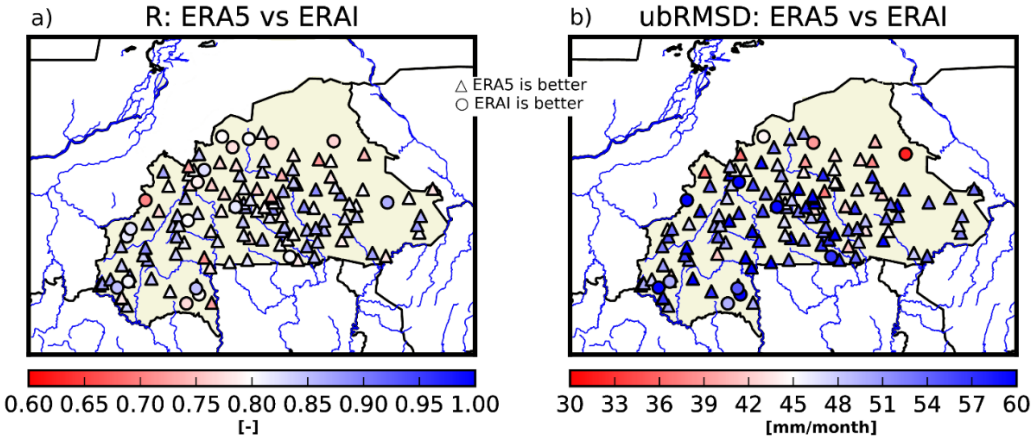

Figure 1 : *Cartes de corrélation (R) sur les séries chronologiques de précipitations (a) et de ubRMSD (mm/mois) sur les séries chronologiques de précipitations (b) entre les mesures in situ des précipitations et les deux reanalyses ERA-Interim et ERA5.*

Des améliorations substantielles d'ERA5 par rapport à ERA-interim pour la variable SW_{in} (sur 2017) ont aussi été obtenues en utilisant les mêmes métriques statistiques que pour les précipitations. Median R, ubRMSD, bias, and RMSD values along with their 95% confidence interval are 0.59 ± 0.070, 36.23 ± 6.480 W/ m^2, 19.40 ± 32.430 W/m^2, and 42.24 ± 21.760 W/m^2 for ERA5, and 0.46 ± 0.150, 41.03 ± 4.220 W/m^2, 28.12 ± 29.800 W/m^2, and 50.72 ± 18.630 W/m^2 for ERA-Interim. ERA5 et ERA-Interim montrent donc une bonne abilité pour forcer le modèle de surface ISBA afin de produire des simulations adéquates de variables d'état de surface.

Dans une seconde partie, des expériences d'assimilation ont été menées avec le système LDAS-Monde intégrant les données d'observations LAI et de SSM dans le modèle ISBA. Les principaux résultats ont démontré une bonne qualité des ré-analyses LDAS-Monde pour surveiller les conditions de surface continentale à différentes échelles de temps (mensuelle,

annuelle, saisonnière, etc.) sur le Burkina Faso avec une gamme d'incertitudes adéquates. Ensuite, une évaluation comparative des performances de LDAS-Monde a été réalisée en utilisant les deux ré-analyses atmosphériques précédents forçant le modèle ISBA. Les deux configurations conduisent dans un premier temps à de bonnes estimations, par exemple, sur la variable LAI avec un avantage utilisant ERA5 comme forçage du système (Figure 2). Néanmoins, la comparaison effectuée entre le modèle (sans assimilation) et le LAI observé a mis en évidence l'absence de processus dans la représentation de la phénologie de la végétation. Cependant, l'assimilation conjointe de LAI et SSM a permis de corriger ce manquement du modèle ISBA par l'amélioration des corrélations et la réduction des RMSD avec LDAS-Monde (Figure 2). Concernant l'humidité de surface du sol, l'assimilation a permis d'améliorer sa représentation en utilisant soit ERA5, soit ERA-Interim. Cela a mis en évidence que l'assimilation ajoute de la "compétence" aux deux configurations et a prouvé le comportement sain du système LDAS-Monde. En outre, d'importantes améliorations dans la représentation des variables (LAI, SSM, l'évapotranspiration et la production primaire brute) ont été obtenues avec de meilleurs scores pour l'analyse que pour le modèle équivalent (sans assimilation). En particulier, l'analyse du LAI a très bien compensé les défauts du modèle ISBA, comme l'incapacité à capturer l'apparition de la végétation avant les premières pluies pour certaines espèces de plantes.

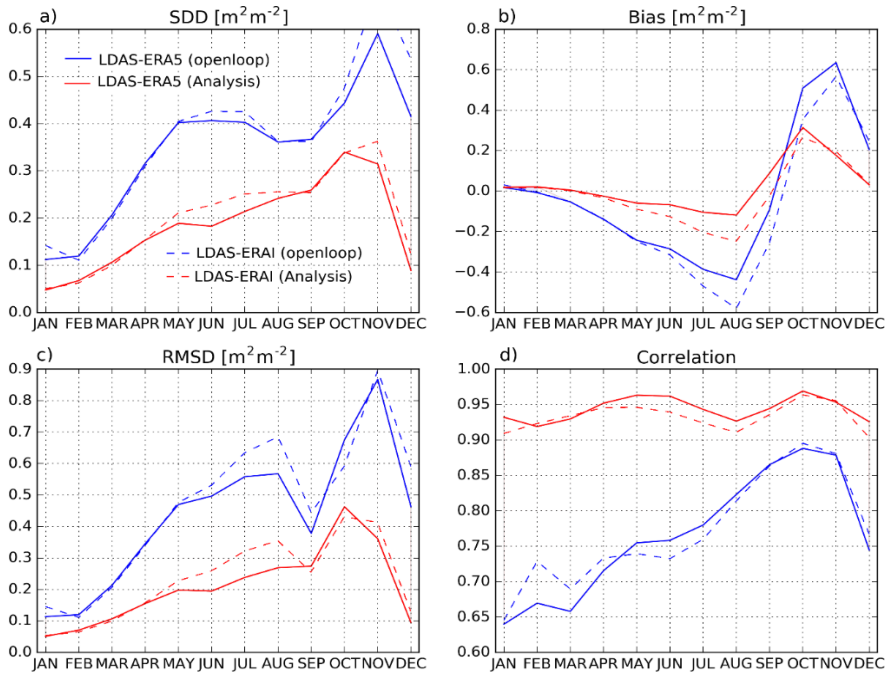

Figure 2 : *(a) SDD (b) biais (c) RMSD et (d) corrélation (R) saisonniers entre le LAI provenant soit de la configuration LDAS-ERA5 (lignes continues) ou de LDAS-ERAI (lignes pointillées) et le LAI observé entre janvier 2001 et juin 2018.*

Enfin, l'impact du changement climatique anthropique sur l'hydroclimatologie du Burkina Faso a été analysé utilisant un ensemble multi-modèle basé sur des simulations climatiques régionales du modèle RegCM4 considèrant les scénarios RCP4.5 et RCP8.5. Les principaux résultats montrent une augmentation généralisée du réchauffement sur tout le Burkina Faso (1 à 6.5 °C). Pour les précipitations, des changements contrastés ont été notés : des conditions plus humides (10 à 50 %) au milieu du siècle (2041-2060) et des conditions plus sèches (plus de 30 %) à la fin du 21^{e} siècle (2080-2099). Ces modifcations projetées sur la température et les précipitations pourraient occasionner une augmentation (et une dimunition) de l'évapotranspiration et de l'humidité du sol plus ou moins importantes pour le milieu (et la fin) du siècle pour les deux scénarios considèrés. De plus, une tendance à la hausse (et à la baisse) du ruissellement de surface a été projetée avec un important gradient spatial, c'est à dire sur de très petites distances (Figure 3).

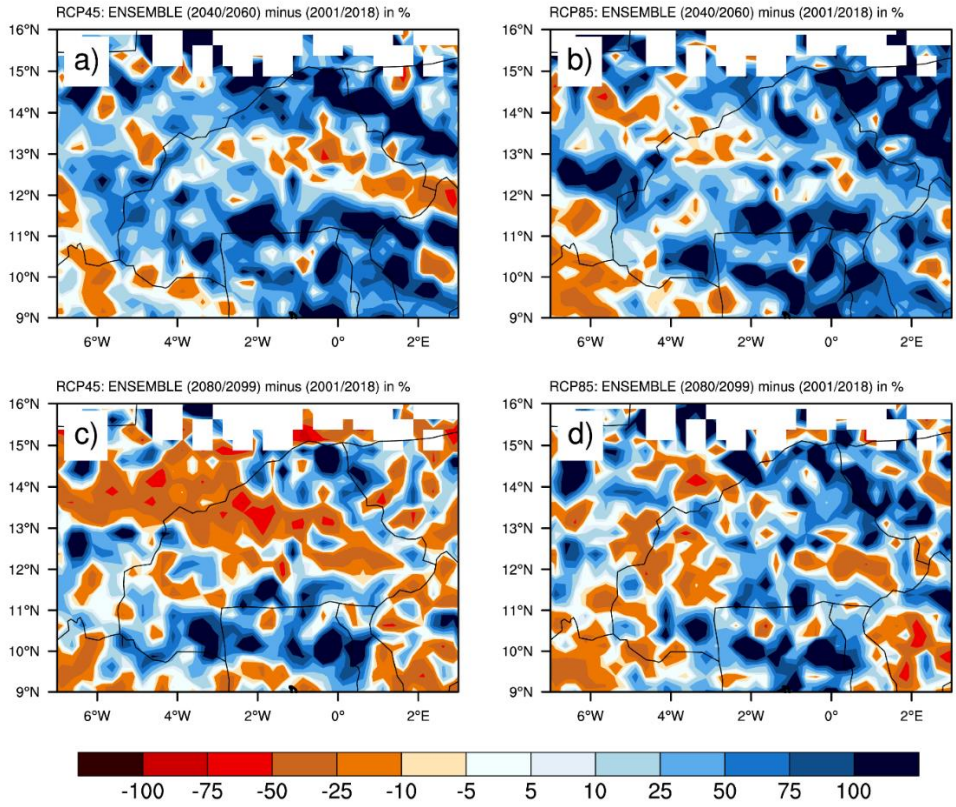

Figure 3 : *Évolution des écarts (par rapport à la période de référence) du ruissellement annuel moyen (en %) pour le futur proche (2041-2060, panneaux supérieurs) et le futur lointain (2080-2099, panneaux inférieurs) et pour la RCP4.5 (panneaux gauches) et la RCP8.5 (panneaux droits).*

Pour examiner comment ces changements combinés affecteront les conditions d'humidité du Burkina Faso, une approche multivariée a été utilisée, en l'occurence la classification révisée de l'humidité de Thornthwaite, pour dériver un indice d'aridité pour le

pays suivant Feddema (2005). L'indice d'aridité est présenté à la figure 4 pour l'historique, le proche avenir et la fin du 21e siècle, ainsi que pour la RCP4.5 et la RCP8.5. La période historique montre que Burkina Faso est essentiellement un pays semi-aride. Dans un avenir proche, cette semi-aridité est moins étendue pendant que certaines conditions sèches et, dans une moindre mesure, humides apparaissent dans les régions du sud. Cependant, pour la fin du 21e siècle et pour les deux scénarios, les régions du centre et du nord du pays montrent des conditions arides (Figure 4).

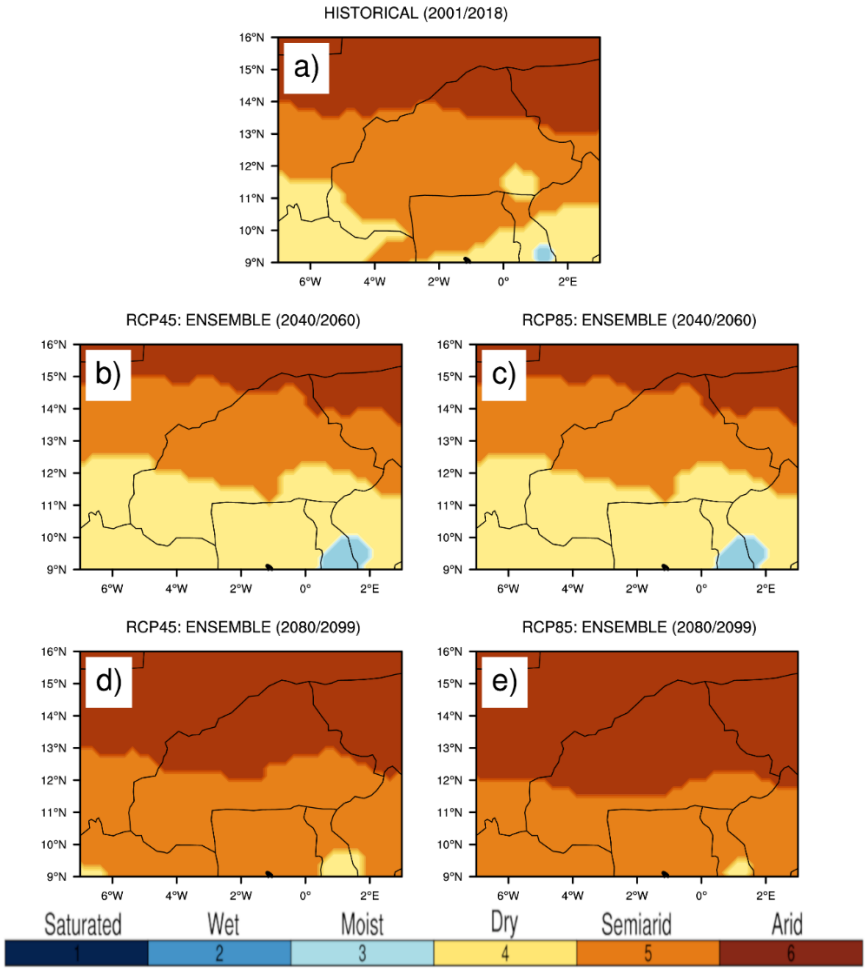

Figure 4 : *Distribution de l'indice d'aridité pour l'historique (2001-2018, panneau supérieur), le futur proche (2041-2060, panneaux du milieu) et le futur lointain (2080-2099, panneaux inférieurs) et pour le RCP4.5 (panneaux de gauche) et le RCP8.5 (panneaux de droite).*

Conclusion

Cette thèse a permis d'avoir une meilleure connaissance de la modélisation des variables d'état de surface et de l'assimilation de données au Burkina Faso. Elle a aussi contribué à fournir des informations sur les changements climatiques futurs qui pourraient affecter les ressources en eau du pays. L'étude de la comparaison des deux forçages atmosphériques a donné deux résultats clés : des améliorations importantes ont été constatées avec ERA5 par rapport à ERA-

Intérim pour les précipitations ainsi que pour la variable du rayonnement solaire. Ensuite, une évaluation comparative des performances de LDAS-Monde a été réalisée en utilisant les deux réanalyses atmosphériques précédents forçant le modèle ISBA. Les deux configurations conduisent à un bon modèle de première estimation (avec un avantage utilisant ERA5 comme forçage du système LDAS-Monde). L'assimilation conjointe de LAI et SSM a aussi permis de mettre en évidence l'absence de processus physiques dans le modèle ISBA comme l'abscence de représentation de la phénologie de certains types de végétation propres au Sud du Burkina Faso. La représentation de l'humidité superficielle du sol a aussi été améliorée par l'assimilation ainsi que l'évapotranspiration.

De par ces améliorations apportées par le système d'assimilation LDAS-Monde, ce dernier peut être utilisé pour résoudre certains problèmes liés aux ressources en eau, tels que la surveillance et la prévision du débit des cours d'eau, en mettant à jour les données d'entrée à l'échelle d'un bassin versant ou pour des zones plus larges. En outre, il a aussi été démontré que les changements climatiques affecteront considérablement l'hydroclimatologie du Burkina Faso dans un avenir proche, avec une diminution de la quantité d'eau de surface et une diminution généralisée de la disponibilité en eau à la fin du 21^{e} siècle (diminution du ruissellement de surface et augmentation de l'évapotranspiration). De tels changements pourraient intensifier le stress des activités agricoles dans le pays à une période où les cultures auront besoin de plus d'eau en raison de l'augmentation des conditions de sécheresses (plus prononcée dans le Nord). Par conséquent, des mesures d'adaptation et d'atténuation fiables doivent être mises au point afin de faire face aux futurs changements hydroclimatiques dans le contexte du réchauffement climatique.

List of contents

List of Acronyms

AMMA	African Monsoon Multidisciplinary Analysis
ALMIP	AMMA Land surface Models Intercomparison Project
AMSR-E	C-band Advanced Microwave Scanning Radiometer
ANAM	Agence Nationale de la Météorologie, Burkina Faso
ASCAT	Advanced Scatterometer
BATS	Biosphere-Atmosphere Transfer Scheme
BMBF	German Ministry of Education and Research
CC	Correlation Coefficient
CCDAS	Carbon Cycle Data Assimilation System
CGLS	Copernicus Global Land Service
CLVLDAS	Coupled Land Vegetation Land Data Assimilation System
CLM	Community Land Model
CMIP	Coupled Model Intercomparison Project
CNRM	Centre National de Recherches Météorologiques
ECMWF	European Centre for Medium-Range Weather Forecasts
EKF	Extended Kalman Filter
EnKF	Ensemble Kalman Filter
ESM	Earth System Modeling
FAO	Food and Agriculture Organization
FLDAS	FEWS (Famine early warning system) - Land Data Assimilation System
GAI	Green Area Index
GCM	Global Climate Model
GFDL	Geophysical Fluid Dynamics Laboratory

GHG	Greenhouse Gas
GLACE	Global Land-Atmosphere Coupling Experiment
GLDAS	Global Land Data Assimilation System
GLEAM	Global Land Evaporation Amsterdam Model
GOME	Global Ozone Monitoring Experiment
GPP	Gross Primary Production
GRP	Graduate Research Program
ICTP	International Centre for Theoretical Physics
IFS	Integrated Forecast System
INSD	Institut National de la Statistique et de la Démographie
IPCC	Intergovernmental Panel on Climate change
IRIN	Integrated Regional Information Networks
ISBA	Interactions between Soil, Biosphere, and Atmosphere
KF	Kalman Filter
LAI	Leaf Area Index
LDAS-Monde	Land Data Assimilation System – Monde
LPAO-SF	Laboratory of Atmospheric and Ocean Physics – Siméon Fongang
LSM	Land Surface Model
LSV	Land Surface Variable
MA	Ministère de l'Agriculture Burkinabé
MEE	Ministère de l'Eau et de l'Environnement Burkinabé
MetOP	Meteorological Operational satellite
MESRS	Ministère de l'Enseignement Supérieure et de la Recherche Scientifique
MIT	Massachusetts Institute of Technology
NASA	National Aeronautics and Space Administration

NCA-LDAS	National Climate Assessment - Land Data Assimilation System
PAR	Photosynthetically-Active Radiation
PROBA-V	Project for On-Board Autonomy – Vegetation
PSU	Pensylvania State University
RCM	Regional Climate Model
RCP	Representative Concentration Pathways
RMSD	Root Mean Square Difference
RZSM	Root Zone Soil Moisture
SEKF	Simplified Extended Kalman Filter
SG	Sudan-Guinea
SiB	Simple Biosphere
SIF	Solar-Induced chlorophyll Fluorescence
SDD	Standard Deviation of Differences
SSM	Surface Soil Moisture
SURFEX	SURFace Externalisée
SMAP	Soil Moisture Active Passive
SMOS	Soil Moisture and Ocean Salinity
SH	Sahel
SS	Sudan-Sahel
SPOT-VGT	Satellite Pour l'Observation de la Terre – Vegetation
SWI	Soil Water Index
UbRMSD	unbiased Root Mean Square Difference
UNEP	United Nations Environment Program
UTC	Coordinated Universal Time
WASCAL	West African Science Service Centre on Climate Change and Adapted Land Use

List of figures

List of tables

Chapter 1: General Introduction

This chapter gives a general survey of the thesis. It outlines the research project from the beginning, the gaps to be filled, the objectives, the literature review on recent studies linked to the thesis as well as the expected results.

1.1. General Context and problem statement

Surface state variables charecterize the dynamics of the continental surface and atmosphere, thus playing a key role in our hydroclimatic system. Initializing Land Surface Models (LSMs) and Regional Climate Models (RCMs) for optimal land surface conditions representation is therefore relevant for land surface variables monitoring as well as climate change projections. The overall aim of this thesis is to contribute to existing knowledge on the best ways to optimise the representation of land surface parameters from LSMs using remotely sensed observations through a data assimilation framework and ultimately provide high-resolution regional climate projections for water resources parameters over Burkina Faso. In addition to the climate and hydrological monitoring context, improving land surface parameters prediction—especially in data-problem areas such as Sub-Saharan Africa—is also relevant for a range of other problems that depend on accurate and timely land surface water and energy balance information for their solution.

1.2. Literature review

An accurate representation of land surface variables (LSVs), such as soil moisture or vegetation cover, is critical in climate science as well as environmental monitoring and prediction (e.g., in order to cope with drought, flood, or other extreme events). To that end, land surface models (LSMs) have been widely used to simulate and predict the Earth's water storage and energy budgets over a broad range of time scales (Rodell et al. 2004; Schellekens et al. 2017; Dirmeyer et al. 2006; Albergel et al. 2018). For instance, the AMMA (African Monsoon Multidisciplinary Analysis) Land Surface Model Intercomparison Project (ALMIP) used a set of LSMs forced in offline mode by a combination of satellite products and high quality in situ measurements in order to better apprehend LSVprocesses and their representation (Boone et al. 2009). These LSMs are intended to reproduce LSVs, such as surface and root zone soil moisture (SSM and RZSM, respectively), vegetation biomass, and leaf area index (LAI), together with surface energy fluxes and streamflow simulations.

Over the last two decades, much progress has been made on the degree to which realistic land surface initialization contributes to the skill and performance of sub-seasonal land-related predictability as documented by Koster et al., (2011, 2009) in the Global Land-Atmosphere Coupling Experiment (GLACE). LSMs have subsequently benefited from the growing development of observational networks. Unfortunately, those are not evenly spaced and data sparse regions remain very difficult to model with accuracy. This is the case of West Africa (Boone et al., 2009; Diallo et al., 2017), where LSVs are of primary importance, as emphasized by many studies, (see, e.g. Charney, 1975; Taylor et al., 2011).

In addition, data assimilation field of research has earned increasing consideration over the previous decades through largely by its potential for providing improved estimates of land surface states related to energy and water balance which can be used for both weather and hydrological forecasting and monitoring (Balsamo et al., 2007; Mahfouf, 2010; Reichle et al., 2007; Van Den Hurk et al., 2002). These estimates are crucial for water resources management especially in data-sparse region like Africa. Furthermore, the increasing pace in the availability of different satellite-based observations that are linked to both land surface water and energy balances – including near-surface soil moisture from microwave sensors and vegetation products (Kerr, 2007; Owe et al., 2008) facilitates the growth consideration on land data assimilation. Certain type of these data have not been thoroughly investigated for LSM assimilation applications and, in particular, there are very few published examples assimilating LAI and SSM over Africa. In the context of West Africa, LSM applications is very relevant because of the low-availability of data in the region. LSMs are intended to reproduce Land Surface Variables (LSVs), such as surface and root zone soil moisture (SSM and RZSM, respectively), vegetation biomass, and leaf area index (LAI), together with surface energy fluxes and streamflow simulations.

An important LSM is the ISBA (Interactions between Soil, Biosphere, and Atmosphere), which is part of the SURFEX modelling system (SURFace Externalisée, Massson et al. 2013). The CO_2-responsive version of ISBA (Calvet et al., 1998; Masson et al., 2013; Noilhan and Planton, 1989) is used in this work for assimilating satellite-based observations. It models leaf-scale physiological processes and plant growth. Transfer of water and heat in the soil rely on a multilayer diffusion scheme. LSM data assimilation is seen as an integral part of hydrological system and monitoring, yet its application over Africa undergone very few studies.

The ability to consistently improve soil moisture estimates and fluxes like evapotranspiration through the assimilation of key remote sensing observations will ultimately

lead to better water management strategies and optimal monitoring of key essential climate variables. Ultimately, examining the joint assimilation impacts of LAI and SSM would lead to an improved monitoring of key land parameters relevant for extreme events coping especially drought and floods as well as for hydroclimatic change monitoring.

1.2.1 Importance of land-atmosphere feedback system

The principal role of a LSM in hydroclimatic prediction systems is to evaluate latent and sensible heat flux feedbacks in the lower atmosphere. These fluxes depict transfer of energy into latent heat in the form of water vapour and sensible heat from the land surface to the atmosphere (Brutsaert, 2005). Consequent condensation of the evaporated/vegetation-transpired water into cloud – leading to precipitation – is associated with a release of heat energy, which together with near surface heat conductance produce atmospheric convection, and thus controlling the thermodynamics of the atmosphere and hence our hydroclimatic system (Brutsaert, 2005; Pitman, 2003).

As a fundamental water supply for evapotranspiration, soil moisture is a key variable in hydrological processes (runoff, evaporation from bare soil and transpiration from the vegetation cover), impacts plant growth and carbon fluxes (Dirmeyer et al., 1999; Entekhabi et al., 1999). Soil moisture is also important on its own for monitoring land surface conditions that trigger extreme events such as droughts, floods, and heatwaves. As a consequence, a significant amount of studies has been conducted to obtain soil moisture estimates. It was shown that, land surface modelling (e.g. Dirmeyer et al., 1999; Georgakakos and Carpenter, 2006) and remote sensing techniques (Kerr, 2007, 2007; Kerr et al., 2001; Njoku et al., 2003) have a great potential to provide reliable estimates of soil moisture.

1.2.2 The land surface

In general, the term ‘land surface’ employed here refers to the earth’s landscapes at the interface with the atmosphere, inclusive of vegetation and the unsaturated soil zone between the soil surface and the groundwater table. Water and energy transfers between the land surface and the atmosphere are connected, and the fundamentals of the science behind our current understanding of these continuous processes can be found in introductory texts on hydrology such as those of Beven, (2012) and Brutsaert, (2005).

1.2.2.1 The water balance

Most of the natural water supply to the land surface comes from precipitation in the form of rainfall. Rainfall either directly reaches the soil surface or is intercepted by vegetation cover from where it can evaporate or drip through to the soil surface. At the soil surface it either evaporates, infiltrates into the soil or becomes gravity-driven surface runoff which flows into topographic depressions or waterways. For rainfall to become surface runoff there needs to be a sufficient surface gradient and the rate of rainfall needs to exceed the rate of infiltration (which typically decreases with increasing volumetric soil moisture content i.e. θ), and if the soil is saturated (maximum θ) there is no infiltration and practically all rainfall becomes runoff (Beven, 2012). Therefore, θ is a very important state in the overall water balance given its effect on different hydrologic processes such as vegetation and moisture parameters.

θ is defined as in the same notation from (Brutsaert, 2005),

$$\theta = \lim_{V_{H_2O} \to \theta_{sat}} \left(\frac{V_{H_2O}}{\Delta\lambda}\right) \qquad \text{(Equation 1.1)}$$

is the total volume of water (V_{H_2O}) contained in the pore space of a given bulk soil sample, per total volume of that sample $\Delta\lambda$. The maximum possible θ (being for saturated soil: θ_{sat}) is equivalent to the soil porosity, or the volume of pore space between solid particles (with volume solids V_{solids}) where

$$\theta_{sat} = 1 - \left(\frac{V_{solids}}{\Delta\lambda}\right) \qquad \text{(Equation 1.2)}$$

Based on soil type, pore space varies due to differing proportions of different sized soil particles (i.e. sand, clay and silt) and it is a pathway for infiltrated water to percolate through. The rate of infiltration is dependent on the soil hydraulic conductivity (K), potential gradient (ψ) and rainfall rate. For ψ, the holding force between water and the soil matrix (e.g. capillarity) is the dominant factor, with the terms pressure head, matric potential or soil suction commonly used for it. As soils drain post saturation, a balance between gravity and the capillary forces in the pores is eventually reached, and the term for θ when this occurs is the field capacity (θ_{FC}). Wilting point (θ_{Wilt}) refers to a lower limit of θ beyond which plants can no longer extract water and they wilt. The range of θ between θ_{FC} and θ_{wilt} defines the available water capacity, which is generally accepted as an approximation of the range within which water is available for

extraction by plant roots (McKenzie et al., 2000), and is therefore important with regard to Evapotranspiration (ET).

Richards' equation (Richards, 1931) which is a well-established is used for vertical water flux through pore space of unsaturated soils, as a function of key soil properties:

$$\frac{\partial\theta}{\partial t} = -\frac{\partial}{\partial z}(K(\theta) + D(\theta)\frac{\partial\theta}{\partial z}) \quad \text{(Equation 1.3)}$$

The term z represents the vertical distance below the land surface while D(θ) is the soil moisture diffusivity where,

$$D(\theta) = -K(\theta)\frac{\partial\Psi(\theta)}{\partial\theta} \quad \text{(Equation 1.4)}$$

Solving Equation (2.3) therefore relies on relationships between θ, ψ and K such as that of Brooks and Corey, (1964), with

$$\frac{\theta-\theta_{res}}{\theta_{sat}-\theta_{res}} = (\frac{\Psi_{aep}}{\Psi})^{b} \quad \text{(Equation 1.5)}$$

and,

$$\frac{K}{K_s} = (\frac{\theta-\theta_{res}}{\theta_{sat}-\theta_{res}})^{3+2b} \quad \text{(Equation 1.6)}$$

In Equation 1.5, ψ_{aep} represents air entry potential (also referred to as the suction at saturation) and K_s in Equation 1.6 is the hydraulic conductivity at saturation, while θ_{res} is the residual or air-dry soil moisture content (for ψ approaching infinity). The term b is a non-dimensional constant, sometimes called the pore size index (Beven, 2012) or Campbell b parameter (Williams et al., 1992) in relation to the work of (Campbell, 1974) where the following was used:

$$\Psi = \Psi_{aep}(\frac{\theta}{\theta_{sat}})^{-b} \quad \text{(Equation 1.7)}$$

Equation 1.7, in addition to:

$$K = K_s(\frac{\theta}{\theta_{sat}})^{3+2b} \quad \text{(Equation 1.8)}$$

are the relationships of Clapp and Hornberger, (1978) for solving Richards' equation. They are a slight variation on the Brooks and Corey, (1964) relationships (Equation 1.5) and Equation 1.6, with the difference being that θ_{res} is made redundant for a smoother parabolic function relating the full range of values for θ, ψ and K. The van Genucthen model (van Genuchten, 1980) is another representation of soil-water retention that is widely referenced in the literature, and is expressed as:

$$\theta = \theta_{res} + \frac{\theta_{sat} - \theta_{res}}{[1+(\alpha\Psi)^n]^{1-1/n}} \quad \text{(Equation 1.9)}$$

In Equation 1.9, the parameters α and n relate to ψ_{aep} and pore size distribution respectively.

The heterogeneity of the land surface as shown previously includes variation in soil type and therefore some of the key properties such as θ_{sat}, K, ψ, θ_{FC} and θ_{Wilt} can vary both laterally and with depth down to sub 1 metre scale. This can contribute to high spatial variability of θ, which in combination with varying vegetation type and cover, and associated plant water use, may also contribute to the spatial variability of heat fluxes (Kalma et al., 2008). On the angle of spatial variability, these quantities add to the challenge of estimating them over large spatial regions and over long time periods, especially in data-sparse region.

1.2.2.2 The energy balance

A schematic description of the major land surface energy balance components discussed here is presented in Figure 2.1. Surface albedo is impacted by land cover and represents the fraction of total incoming shortwave (solar) radiation that is reflected away from it, while the remaining fraction is absorbed. Some generic albedo values given by Brutsaert (2005) for different surfaces include: ~0.8-0.9 (highly reflective) for fresh snow; ~0.05-0.15 (minimal reflection and high absorption) for moist dark soil; and, ~ 0.15-0.25 for green grass. Longwave radiation (or thermal infrared energy) plays a key role in the energy balance, with the land surface emitting it and absorbing it from the atmosphere. Boltzmann law is employed to describe emitted longwave radiation from the land surface.

$$\uparrow LW = \epsilon \sigma T_{sk}^4 \qquad \text{(Equation 1.10)}$$

where $\uparrow LW$ represents the emitted longwave radiation, ϵ the emissivity, σ the Stefan Boltzmann constant (= $5.67*10^{-8} Js^{-1}m^{-2}K^{-4}$) and T_{sk} the radiative temperature of the land surface (representing contributions from soil and vegetation surfaces), which is referred to hereon in as the skin temperature. For a perfect black body the value of ϵ is 1 and approximate values for some different surfaces from Brutsaert (2005) include: ~0.99 for fresh snow; ~0.95-0.98 for bare soil; 0.96-0.97 for tree vegetation; and, ~0.97-0.98 for grassy vegetation.

The total sum of the major vector quantities of radiation – incoming shortwave (↓SW), incoming longwave (↓LW), reflected shortwave (↑SW) and emitted longwave (↑LW) – defines the net radiation (R_N) that is available to the land surface, so

$$R_N = \downarrow SW - \uparrow SW + \downarrow LW - \uparrow LW \qquad \text{(Equation 1.11)}$$

The soil type, terrain, and vegetation type and cover of the land surface typically varies over a range of spatial scales (Richter et al., 2004; Yates et al., 2003) which translates to variations in albedo and emissivity. This spatial heterogeneity implies that there can be significant variation in R_N across landscapes which receive similar amounts of incoming radiation.

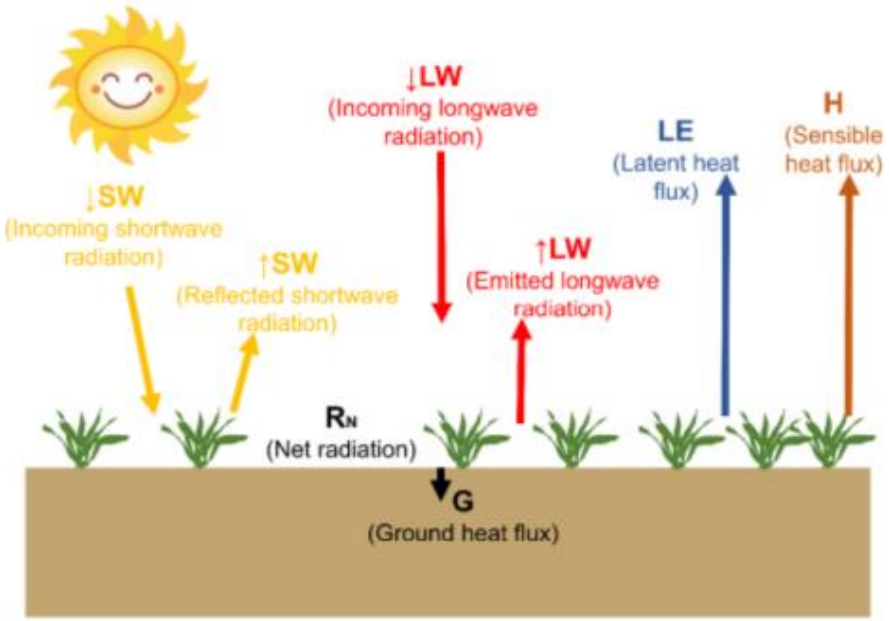

(Source: https://climate.ncsu.edu/edu/EnergyBalance)

Figure 1.1: *Schematic of the major energy balance components at the land surface.*

Most of the R_N available to the land surface is subsequently partitioned to produce either latent (*LE*) or sensible (*H*) heat flux feedbacks to the atmosphere, in addition to a residual (typically smaller) energy flux into the soil termed the soil heat flux (*G*) as illustrated in Figure 2.1. From Hsieh et al., (2009), *G* can be up to 50% of the R_N for dry soil surfaces in some conditions. Soil temperature (T_{Soil}) shares a strong relationship with *G* and is an important state of the land surface energy balance (De Ridder, 2009).

From much of the literature (e.g. Beven, 2012; Brutsaert, 2005; Ladson and Weinmann, 2008), LE, H and G are the main quantities resulting from R_N partitioning at the land surface (Fig. 2.10. and Eq. (2.11)) and hence the energy balance can be expresseed as:

$$R_N = LE + H + G \qquad \text{(Equation 1.12)}$$

A major factor controlling the partitioning of R_N, and an important link between the land surface energy and water balances, is the amount of soil moisture available for soil evaporation (*E*) and plant transpiration via root uptake (in combination referred to as evapotranspiration or *ET*), where *ET* is the expression of *LE* as a quantity of vaporised/transpired water over a given time interval. As soil moisture content (θ) approaches zero, *LE* becomes minimal and a greater portion of available energy at the land surface is fed-back to the atmosphere as conductive heat with an increase in *H*. Hence θ regulates R_N partitioning into the major heat flux components (Reichle et al., 2002), thus influencing the Bowen ratio (Bowen, 1926):

$$\text{Bo} = \text{H/LE} \qquad \text{(Equation 1.13)}$$

1.2.3 Observation of Land surface quantities

The motor behind of much of the data assimilation research over the past couple of decades comes from the increasing availability of different spatially distributed data types related to land surface water and energy balance quantities, as observed from a range of satellite-based sensors—this aimed at improving LSM estimates. Therefore, it is also a motivator for the research in this thesis, where the assimilation of observation types that have yet to be widely tested in LSM assimilation studies i.e. LAI and SSM is examined.

Remotely sensed data assimilation for spatially distributed modelling, which is ultimately of most interest for applications such as vegetation and water resources monitoring

as well as catchment water balance studies, involves greater complexity and therefore greater uncertainty. The processing of raw remotely sensed observations to produce specific data products is done with algorithms/models which can be complex, imperfect and introduce errors. Also, varying degrees of landscape heterogeneity can occur within remotely sensed measurement footprints, where spatial disparity between in-situ validation data and remotely sensed data (and the relative sparsity of in-situ monitoring across the world) presents a challenge for properly characterising uncertainty (Glenn et al., 2007; Kalma et al., 2008), and which also limits the ability for robust validation of model/assimilation output.

The following sub-sections give an overview of observation methods relevant to the data that were used followed by a discussion of the remotely sensed data.

1.2.3.1 Soil moisture

Soil moisture is a crucial variable in hydrological processes (runoff, transpiration from the vegetation cover and evaporation from bare soil and). It impacts plant growth and carbon fluxes (Dirmeyer et al., 1999; Entekhabi et al., 1999). Ground based soil moisture content can be measured through gravimetric and in-situ dielectric based reflectometry techniques.

(i) Determining soil moisture via the gravimetric method involves weighing a field collected soil sample of known volume as soon as possible after collection and weighing the same sample after it has been oven dried at 105 °C for >24 hours. Thus, the total volume, the mass of water and mass of dry soil particles for a sample are all known and with some basic calculations the soil moisture content can be determined using Equation (2.1). This is a relatively accurate method of determining soil moisture if done carefully due to the direct use of an actual field sampled volume of soil and simplicity of the measurements and calculations involved. A drawback of the gravimetric method is the destructive sampling (at the point-scale) and the human effort required for it, which limits the temporal frequency and the spatial coverage that can be obtained.

(ii) Dielectric based techniques are used to measure soil moisture in-situ and are also limited to the point-scale, but can be set up for continuous measurement over time. They provide non-destructive measurements where probes of a known length are inserted in the soil and act as wave-guides for transmitted electromagnetic pulses (Topp et al., 1980). The propagation time of a pulse along the wave-guides is a function of the dielectric constant of soil surrounding them. Since liquid water has a high dielectric constant relative to dry soil the electromagnetic pulse travel time is a strong function of soil moisture content, thus time

measurements from these instruments can be converted to soil moisture content via a calibration equation.

(iii) The work of Ulaby, (1986, 1982) provides details on background theory and some practical aspects of remote sensing for soil moisture which is based on measuring microwave radiation. As presented by Wagner et al., 2007), key microwave bands in the electromagnetic spectrum that are relevant for soil moisture retrieval (with specific frequency (f) and wavelength (λ) ranges) are: L-band (f = 1-2GHz, λ = 30-15cm), C-band (f = 4-8GHz, λ = 7.5-3.8cm) and X-band (f = 8-12GHz, λ = 3.8-2.5cm). Microwave remote sensing can typically provide measurements for soil moisture estimation for the top few centimetres of soil, where the penetration depth into the soil is ~0.1-0.2 times the wavelength (Moran et al., 2004). Analogous to the basic principles behind the in-situ methods mentioned previously, microwave emissions from soil are sensitive to the soil dielectric constant which varies greatly with soil moisture content (Jackson et al., 1996; Moran et al., 2004). Passive and active microwave remote sensing are two distinct approaches relating to soil moisture retrieval.

Regarding the passive approach, a radiometer sensitive to natural microwave emissions from the land surface is used with the brightness temperature (T_B) being the actual quantity measured. T_B is a product of the emissivity of a surface and its physical temperature (Jackson et al., 1996). Independent measurement of physical temperature enables emissivity to be determined, which then provides the link to estimate soil moisture content. Some examples detailing soil moisture retrieval from T_B measurements can be found in works by Gao et al., (2006) and Owe et al., (2008) amongst others. Increased vegetation cover and surface roughness can hamper the ability to retrieve soil moisture from the measurements, but this becomes less of a problem with increased wavelength (Jackson et al., 1996; Moran et al., 2004). Active sensing techniques are radar based where microwave pulses are transmitted to the land surface and a backscattering coefficient (σ^o) is determined by comparing transmitted and received signals (Jackson et al., 1996). Soil moisture can be retrieved using σ^o which is related to emissivity and hence is sensitive to contrasts in dielectric properties between wet and dry soil (Jackson et al., 1996; Ulaby, 1986).

Application of active techniques is that they can provide higher spatial resolution data than passive techniques (Entekhabi et al., 2010). Therefore, algorithms for retrieving soil moisture from σ^o are more complicated than from passive radiometer data (Jackson et al., 1996), with issues of sensitivity to vegetation and surface roughness still needing to be fully overcome (Moran et al., 2004; Wagner et al., 2007). Change detection algorithms (e.g. Wagner et al.,

1999) are a promising approach for addressing the challenges of active sensor moisture retrieval. The basis of these is that noise in the measured signal is assumed to either be constant over time (bare ground roughness and topography) or have seasonal periodicity (vegetation). Therefore, the challenge is to adequately quantify and correct for the noise, and while some algorithms may do a reasonable job at this, vegetation may not always have the same seasonal variation over time in some regions. The recently-launched (early 2015) Soil Moisture Active Passive (SMAP) mission satellite combines both a passive radiometer and active radar that provide data with the best features of both sensing techniques – the greater overall certainty associated with passive microwave data retrieval and higher spatial resolution of active data (Entekhabi et al., 2010).

The C-band Advanced Microwave Scanning Radiometer (AMSR-E) on the NASA AQUA satellite (Njoku et al., 2003) is a prominent passive sensor which recently stopped operation (in October 2011). Observations represent ~1-2 cm soil depth and derived moisture products can have a spatial resolution down to ~25 km (Owe et al., 2008). Close to a 10-year observation series exists from AMSR-E and it has been replaced by its successor AMSR2 (Imaoka et al., 2010) which has similar measurement specifications. A prominent active sensor is the C-band Advanced Scatterometer (ASCAT; Wagner et al., 2013) on the Meteorological Operational satellite (MetOp). ASCAT soil moisture data represent the top ~1-2 cm with spatial resolution down to ~12.5 km (Wagner et al., 2013), and are typically produced as a scaled wetness index from 0-100% as opposed to explicit volumetric moisture content quantities.

Numerous validation studies have been carried out based on these soil moisture products (either from passive and active sensors) against in-situ moisture observations across different regions world-wide. For instance, Albergel et al., (2012) assessed both SMOS and ASCAT (together with a blended observation/model product), and Su et al., (2013) assessed SMOS, AMSR-E and ASCAT over Europe, the USA and Australia and for parts of Africa. From these studies, the overall error in the passive and active sensor products appear relatively comparable. While there is variation in the temporal repeat, spatial resolution and observation depths between them, they each contain information which can potentially contribute to improved model estimates via data assimilation.

However, incorporating the full range of moisture products available from the different sensors and based on various retrieval algorithms into data assimilation experiments was beyond the scope of this research.

1.2.3.2 Vegetation States

LAI is defined as half the developed area of photosynthetically active elements of the vegetation per unit horizontal ground area. It determines the size of the interface for exchange of energy (including radiation) and mass between the canopy and the atmosphere. This is an intrinsic canopy primary variable that should not depend on observation conditions.

Therefore, its estimation from remote sensing observations is scale dependent (Weiss et al., 2000; Garrigues et al., 2006). Note that vegetation LAI as estimated from remote sensing includes all the green contributors such as the understory when existing under forests canopies. However, except when using directional observations (Chen et al., 2005), LAI is not directly accessible from remote sensing observations due to the possible heterogeneity in leaf distribution within the canopy volume.

Therefore, remote sensing observations are rather sensitive to the 'effective' leaf area index, i.e. the value that provides the same diffuse gap fraction while assuming a random distribution of leaves. The difference between the actual LAI and the effective LAI may be quantified by the clumping index (Chen et al., 2005) that roughly varies between 0.5 (very clumped canopies) and 1.0 (randomly distributed leaves). Note that similarly to the other variables, the retrieved LAI is mainly corresponding to the green elements: the correct term to be used would be GAI (Green Area Index) although it is usually proposed to still use LAI for the sake of simplicity.

1.2.4 Land Surface Models (LSMs)

Important parameters such as soil moisture content, soil temperature, soil physical properties, vegetation cover, and physical and biological properties linked to specific vegetation categories control the partitioning of available net radiation energy at the land surface into latent and sensible heat feedbacks. These processes rely on different aspects. LSMs try to combine these factors in a mathematical framework, together with meteorological variables, for predicting water evaporation from soil and/or its transpiration through vegetation on a continuous time scale.

LSMs reveal several limitations since they attempt to represent highly fluctuating and complex physical mechanisms through empirically and/or simplified derived mathematical relationships. One more significant issue is that parameter values are often difficult to address because of the limited information on model soil and vegetation properties to precisely highlight the high temporal and spatial variation of these quantities (Franks and Beven, 1999; Yates et

al., 2003). While field measurements can assist in parameterizing models at the point scale with considerable effort (Mertens et al., 2005), this is more challenging when modelling across spatially heterogeneous regions without measurements especially the case of West Africa, (e.g. spatial remotely sensed soil moisture data is not of a depth that can provide direct information on root-zone soil hydraulic properties). Complexity of numerous models comes from the fact they often have several parameters for them all to be optimised with unique solution given a limited number of relevant types of field measured data (Franks and Beven, 1999). Inaccuracy in meteorological forcing data also affect the quality of model output. Overall, LSM predictions are intrinsically uncertain, with prediction uncertainty consistently rising with time.

Data assimilation is thus well appropriate to improve LSM predictions (e.g. Crosson et al., 2002; Reichle et al., 2008) since it allows to spatially and temporally integrates the observed information into LSMs in a consistent way to unobserved locations, time steps and variables. A major aspect of assimilation is consideration of estimates of uncertainty inherent in both model estimates and observed data, in a way to to adequately weight the degree of model state adjustment for improved predictions. Estimates of errors in different related model variables provide information to relate the updates made directly to one variable from an observation with updates to other related model variables. Global coverage and regular temporal repeat of emerging remote sensing data streams, related to land surface state and flux quantities, improves the prospects for routinely improving LSM predictions over different spatial scales via data assimilation.

In this thesis, the assumption put forward is that due to imperfect model architecture and parameter estimates, the major improvements to reanalyses of any particular LSM state coming from data assimilation would be from assimilating observations of the same variable or its most closely related one. Considering this hypothesis, model states would best be adjusted by the observation chosen to fit the variable of interest. In addition, this would not necessarily result in the most physically realistic values for all states. If the aim is to improve for instance LAI and SSM monitoring, then it seems natural to test the assimilation of LAI and SSM observations. Very little research has focused on the joint assimilation of remotely sensed instantaneous estimates of these quantities, perhaps partly due to the fact that these are emerging products. Therefore, the validation of such products within data assimilation systems are still major challenges, especially in data-sparse regions—which are already threatened by climate change—like West Africa.

It is well known that SSM and LAI share a link with weather and hydrology through regulating the partitioning of available energy at the land surface into LE and H (De Ridder, 2009; Koster et al., 2011, 2004; Pielke et al., 1998; Pitman, 2003). LSMs are designed to represent these state/flux processes, which relate to the energy and water balance components presented in section 2.1, in order to support tasks such as monitoring of land surface variables through data assimilation. Basically, a LSM is intended to represent the exchange of water and energy fluxes at the Earth surface–atmosphere interface via biophysical processes using physically-based equations. They include energy balance calculations for quantifying these fluxes, which factor in physical characteristics of the land such as vegetation cover and associated plant transpiration, along with formulations linking soil state dynamics (Ek et al., 2003; Overgaard et al., 2006).

Performing experiments of simulations through running LSMs requires time series meteorological forcing data inputs which provide values for water and energy supply to the land surface (as precipitation and radiation data) along with values for near surface atmospheric conditions with which calculations are made for evaporative demand. Model specific parameter data is required to quantify soil and vegetation properties which influence water and energy fluxes, and a list of inputs specific to the CO_2-responsive version of Interactions between Soil Biosphere Atmosphere i.e. the ISBA LSM (Calvet et al., 2004, 1998; Gibelin et al., 2006; Noilhan and Mahfouf, 1996). Uncoupled/stand-alone LSMs can be forced with meteorological variables which are usually routinely observed by national meteorological services or reanalysis data. This approach was used throughout this research in the experiments involved the ISBA model.

Another important characteristics within LSMs are soil parameters, especially those linked to the water retention/mobility properties of soils which impact on water availability to plants towards therefore available energy partitioning (main details are given in section 2.1). Key vegetation parameters can include time series of LAI from remote sensing and RZSM distribution, all of which being greatly impacted by hydrometeorological extremes such as floods and droughts. The spatial and/or temporally variation in soil and vegetation parameters enable the representation within LSMs of landscape heterogeneity and therefore the variability of energy and water balance components related to hydrometeorological extremes are better monitored and predicted.

Conversely to parameters, prognostic state variables require initial conditions to be prescribed and subsequent values are calculated as a function of previous model time step

values. Thus, they keep some memory relating to water and energy balances as they change with new forcing data at each time step. Key state variables in LSMs typically include soil moisture content and soil temperature (e.g. Dai et al., 2003).

Over the past few decades, LSMs evolution has been marked by a huge increase of the level of information detail attempting to improve their accuracy with more realistic representations of soil, vegetation and land-atmosphere interactions. In order to give a general overview, the following paragraphs provide a synthesis of the work of Pitman, (2003) and Sellers et al., (1997) who classified models as first, second or third generation in their reviews of LSM evolution.

First generation of LSMs are the most simplistic – the basic bucket model from Manabe, (1969) being a classic example. In this model, a single 15cm soil layer is used – it fills from precipitation, after filling any precipitation becomes surface runoff and water depletion from the soil occurs via ET. In order to derive ET, a potential value is calculated (applying the vapour pressure gradient form as described earlier) and then a simple linear soil moisture availability factor (β) based on the bucket water content (0 to 1 from completely dry to saturation) is used as a multiplier to determine actual ET. In this model, the major limitation is that an aerodynamic resistance term is used in ET calculations and vegetation canopy (stomatal) resistance is not included. This limitation is critical since plant stomatal control on transpiration in the presence of freely available water has an influence on ET (Milly and Shmakin, 2002). Stomatal resistance describes the regulation of water vapour transpiration through stomates in plant leaves. Further, Pitman, (2003) notes that only 1 or 2 soil layers are generally considered in first generation models and that soil temperature variations might also not be adequately represented from short term to multi-annual time scales.

Second generation (called also biophysical) models as described by Sellers et al., (1997) present further advanced vegetation representation than first generation ones which are described as representing vegetation as passive. This second generation of models aims to represent a soil-vegetation system interacting with the atmosphere. Among the advances in these models is they include canopy interception (and evaporation) with a more complex representation of soil moisture dynamics typically using Richard's equation (Pitman, 2003). Some examples of second generation models are the Biosphere-Atmosphere Transfer Scheme (BATS) by Dickinson, (1984), the Simple Biosphere Model (SiB) by Sellers et al., (1986) and the VB95 model (Viterbo and Beljaars, 1995) developed for ECMWF.

Conversely to first generation models, vegetation canopy resistance was incorporated more realistic biophysically based model structure (according to Sellers et al., 1997). Moreover, second generation models usually contain multiple soil layers with root distribution and improved soil temperature and moisture representation (Pitman, 2003).

Even though second generation models present a specific representation of vegetation, a limitation is noted on stomatal resistance (which is based is based on empirical relationships). Throughout the development of third generation (or physiological) models, more attention were considered on the mechanisms of plant stomatal functioning driven by photosynthesis. Thus, explicit representation of photosynthesis and the use of CO_2 by vegetation in relation to stomatal resistance and transpiration is a typical feature of them (Pitman, 2003; Sellers et al., 1997). The other processes considered in third generation models like soil hydrology and soil temperature are usually similar to representations used in second generation models (Pitman, 2003).

Although several improvements in recent years noted in the representation of some complex biophysical processes, incomplete model structure and errors within input data are still persistent, contributing to both error and uncertainty propagation. In terms of measurements accuracy and representation of spatial and temporal variability, uncertainty in initial state conditions, meteorological forcing data and parameter data are all sources of input error. Therefore, techniques such as data assimilation can play an important role in improving model representations of land surface states and their prediction through the combination of LSMs and available additional information from independent observations.

1.2.5 Data Assimilation

Data assimilation is defined by Holm, (2003) as an analysis (optimal state) resulting from the combination of a dynamic model of the physical system and a time series of distributed information from available observations. Data assimilation and the statistics describing it are thoroughly detailed by Evensen, (2009). In data assimilation, it makes more sense to consider the probability distribution function (*pdf*) for a model variable than single deterministic predictions since there are infinitely many equally likely solutions from a model's integration through time (due to the different sources of uncertainty mentioned in the preceding section). From a *pdf* information, it is easy to estimate the most likely value (the mean) along with the uncertainty (the variance) for a specific aimed variable.

Another definition of data assimilation is the estimation of the *pdf* of the model solution conditioned on measured observations Evensen, (2009). Basically, observed quantities which

can be on a variety of spatial and time scales and are related to model variables, are used to update model variables in a way which factors in the uncertainty of both observed and modelled quantities. In addition, Houser et al., (2010) defines land surface data assimilation as an approach which: "...aims to utilise both our knowledge of land surface processes as embodied in a LSM, and information that can be gained from observations, to produce an improved, continuous land surface state estimate in space and time". Model data fusion is sometimes used as an umbrella term for the different approaches to combining observed and modelled information for improving predictions, encompassing both parameter optimisation and state updating (e.g. Keenan et al., 2011; Wang and Liang, 2009). The term data assimilation is considered to be more specific based on much of the literature referenced throughout this thesis and its use here refers exclusively to model state updating.

1.2.5.1 Aim of Data Assimilation

The use of independently observed data to enhance model predictions is not recent. Numerous publications have been performed on model calibration especially for hydrological applications, where discussion of and information towards different approaches can be found in Vrugt et al., (2006). A typical strategy is to calibrate for a particular variable (or variables) by optimising model parameter values so that some objective function for differences between predictions and observations of the variable(s) of interest is minimised.

In contrast to optimisation with a focus limited to parameters, Vrugt et al., (2006) highlight that data assimilation gives specific value in sequentially updating model state variables through time whenever new measurements become available, to continuously improve predictions and estimate prediction uncertainty. The time step dependency of prognostic state variables enables the impact of updates to be carried forward to modelling time steps where observations are not available. Evensen, (2009) indicates there are differences in opinion between research communities about which approach – data assimilation or identifying parameters via optimisation – is best for providing proper scientific knowledge and improving modelled outcomes.

Furthermore, parameter optimisation may also be of value in the LDAS context, however for a remotely sensed product such as soil moisture, which represents only the top few centimetres of soil there is no direct comparison for finding optimal soil properties over the deeper rooting zones, which fluxes depend on. Robust data assimilation techniques require the factoring in of model uncertainty and therefore state updating can be beneficial where there is

sub-optimal input data. Data assimilation can also update other unobserved model variables (e.g. root-zone moisture states) based on their relationship with the observed model variable.

1.2.5.2 Data assimilation methods

Authors such as Walker et al., (2005) discriminate between dynamic observer and direct observer data assimilation techniques. The first technique i.e. dynamic observer assimilation is intended at finding the best fit between predicted model states and observations, forced by the only initial state uncertainty and the observation uncertainty. It is likened to a calibration approach where the initial state values for a given assimilation period are optimised based on the full series of observations over that entire period. Four-dimensional variational (4DVAR) assimilation is an example of a dynamic approach and a limitation is that no model error is assumed (Holm, 2003).

In addition, Walker et al., (2005) recapitulate direct observer assimilation as using the innovation – which is defined as the difference between an observation and a model prediction of the observation – to sequentially update model predicted state variables, whenever observations are available. The product of the innovation and a weighting factor – where the weighting represents the relative uncertainty in the observation and model predictions – is added to the predicted state variables in order to update them. (Holm, 2003) lists optimal interpolation (OI), three-dimensional variational assimilation (3DVAR) and the Kalman filter as common data assimilation algorithms, which are all direct observer approaches.

Predicted model states, with direct integration, are simply replaced with available observed information. Model or observation uncertainty is totally disregarded (the observation is treated as being perfect) and this approach is therefore very limited. Differences between most of the other aforementioned approaches relate largely to how their respective weighting factors are defined.

Firstly presented by Kalman (1960), the Kalman Filter (KF) is actually the basis of more modern versions such as the extended Kalman filter (EKF) and ensemble Kalman filter (EnKF). The weighting factor for KF approaches (called the Kalman gain) is based on estimates of observation error and on the model prediction error covariances being propagated forward in time along with the predictions themselves. With the standard KF a linearisation of non-linear models such as LSMs (through determining the tangent linear of the model) is used to estimate error covariances at each assimilation time (Bouttier & Courtier, 1999). By definition the EKF is where the model prediction is linearised using a Taylor's series expansion (Walker et al.,

2005). While error covariances can be propagated forward and estimated at assimilation times, actually defining the total model error in the first place – consisting of errors from initial conditions, forcing data, model physics and parameters – is extremely difficult (for any assimilation approach) (Bouttier & Courtier, 1999; Walker et al., 2005).

For computational reasons, the Simplified Extended KF (SEKF) was chosen as the technique to use for experiments in this thesis due to its robustness – it is easy too implement, efficient and has been shown previously to provide good results (Albergel et al., 2017; Barbu et al., 2014; Leroux et al., 2018). It has also been used in its own right for various published assimilation studies (with some of these referenced in following chapters). A description of the SEKF and its implementation for experiments in this thesis is presented in chapter 1, while the generic KF formulation on which it is based is as follows:

$$X_k^a = X_k^f + K(Z_k - Z_k^f) \qquad \text{(Equation 1.14)}$$

where subscript k refers to the assimilation time step, superscript f refers to a prediction and superscript a refers to an analysis (from an update). The model state vector is denoted by **X** and the observation is denoted by **Z**. The difference between an observed value and a model predicted value of the observation – i.e. the innovation ($\mathbf{Z}_k - \mathbf{Z}^f_k$) – is weighted by the Kalman gain (**K**) which determines the correction added to the predicted state vector. In addition to projecting from **Z** to **X** space, **K** is the weighting factor that represents the relative uncertainty of model predicted and observed values based on their covariances and is given by

$$K = P_k^f H^T (H P_k^f H^T + R_k)^{-1} \qquad \text{(Equation 1.15)}$$

where **P** represents the error covariance of the predicted model states and R is the error covariance of the observation. The matrix **H** is a nonlinear operator that relates the state vector **X** to the observation **Z**, with superscript **T** denoting the matrix transpose. Therefore, if **P** is large compared to **R** (i.e. observations more trustworthy than model prediction), then **K** will approximate to 1 when **X** and **Z** are the same scalar quantity (i.e. **H** = 1), and the innovation will be relied upon heavily to adjust the predicted states due to the small relative observation error. Alternatively, where **R** is large compared to **P**, **K** will approach 0 and the observation will not be trusted sufficiently leaving the final analysis vector X_k^a relatively unchanged, since the model's prediction is likely to be more reliable in this case.

Evensen, (2009) and Maybeck, (1988) present comprehensive detail on the KF including its statistical basis. It is discussed with reference to Bayes' theorem, given it is designed to determine the most likely value of a model state (the analysis) based on the pdf for an a priori model prediction conditioned on the pdf for some observed estimate of the modelled quantity. The pdf variances for predictions and observations are the quantities used for **P** and **R** respectively in Equation (2.26). As highlighted by Evensen, (2009) and Maybeck, (1988), amongst others, the statistical assumptions about the prediction and observation error distributions for an optimal KF are that they are zero mean (unbiased), independent of each other, represent random white noise, and are Gaussian. Errors may not be strictly Gaussian in reality, however it is often the case that only the mean and variance of error processes are known, and without clear knowledge of higher moment statistics a Gaussian distribution is the best assumption for the KF to minimise error in the analysis (Maybeck, 1988).

1.2.5.3 The bias issues

By definition, the KF is a linear combination of modelled and observed information, and based on the error distribution properties discussed in the previous section it deals specifically with correcting for random error in finding an optimal model prediction. Hence, systematic errors or biases between modelled and observed time series represent a challenge for data assimilation, which is an issue highlighted in several research article such as Reichle and Koster, (2004).

Regarding observations of a state variable like soil moisture from remote sensing or in-situ instrumentation, the dynamic range is a function of the measuring instrument(s) and algorithm along with associated uncertainties used to derive it. This range, together with the mean state over longer time periods (multi-annual, for instance) is likely to differ to that from a LSM which has its own inherent uncertainty issues arising from different sources, along with lack of information on soil parameters such as wilting point and field capacity (amongst others), which influence moisture dynamics (Koster and Milly, 1997).

Furthermore, the existing bias between LSM estimates and remotely sensed observations is recognized as a problem in data assimilation framework, which must be related to the relative contribution to total bias from the model and observation uncertainties. Though, the accurate identification and quantification of this bias remains a challenge (without independent information).

Therefore, a typical approach to treat the bias problem is to rescale observations prior to assimilation so that the observed time series matches the model climatology. This can be done via the use of a cumulative distribution function matching (*cdf-matching*) of the observed series to the simulated one (e.g. Barbu et al., 2014; Draper et al., 2009; Drusch et al., 2005; Reichle et al., 2007; Reichle and Koster, 2004). Another way to do so is to match the observed series mean and standard deviation to that one from the model – as done by Draper et al., (2009).

Despite the fact the previous approaches aimed at bias removal are relatively well documented they are not necessarily perfect. In fact, Reichle and Koster, (2004) established a relationship for rescaling remotely sensed soil moisture to model predictions over a one-year period, and when applied to longer-term (a nine-year) data series it reduced the bias but did not completely remove it. This shows the difficulty of thoroughly understanding bias relative to true climatology, particularly where only short data series are available.

Although the rescaling approach to deal with observation/model state bias having limitations, it is actually the best-known option when there is a lack of additional information independent of the assimilated observations and model state predictions. Therefore, rescaling was applied in this thesis for experiments which involved remotely sensed data assimilation and with clear bias between observed and modelled states over a one-year period (i.e. bias could be computed for a full cycle of seasons).

1.2.5.4 Summary of LSM Data Assimilation research

One of the early illustrations of fact-finding the ability of data assimilation to improve LSM estimates is a study by Entekhabi et al., (1994). This study demonstrated the potential for improving soil moisture and temperature predictions over a 1 m deep soil profile by assimilating data that is representative of remotely sensed skin temperature and soil moisture observations of only the first top centimetres of soil (this is considered as the typical layer/depth range of real remotely sensed soil moisture data).

Likewise, the work of Entekhabi et al., (1994), there are also several synthetic LSM data assimilation studies in the literature from over the years, including the work of Balsamo et al., (2007); Koster et al., (2009); Reichle et al., (2008), and Walker and Houser, (2004). Across these examples there is clear indication that assimilating near-surface soil moisture observations has potential for improving monitoring ability of soil moisture (including over the whole root-zone).

Testing LSM data assimilation with real observed data is essential towards developing and having confidence in real-world assimilation applications, although it entails certain challenges which are not encountered in synthetic studies. Specifically, in dealing with real data it is unlikely that the truth is perfectly known (hence the purpose of assimilation in the first place) where the best estimate of it relies on well-defined observational and model prediction errors. Therefore, in the absence of reliable data independent of the assimilated observations and model predictions, this is difficult to achieve – as is performing robust validation of assimilation results to assess the viability of particular assimilation strategies. This also relates to the difficulty in understanding the true source of any bias between observations and model predictions as discussed in the previous section.

Numerous investigations assimilating real one-dimensional point-scale data have been published, among them those by Heathman et al., (2003); Li and Islam, (1999) and Sabater et al., (2008) which involve soil moisture assimilation, and further demonstrate the potential for improving root-zone soil moisture prediction.

Finally, the intent of LSM assimilation in many hydrological applications is to use remotely sensed observations in order to provide improved spatially distributed modelling. Therefore, in progressing beyond synthetic studies and one-dimensional studies using point-scale field data to test the viability of particular LSM assimilation strategies, research into remotely sensed data assimilation is imperative despite the challenges. Many of the published remotely sensed data assimilation studies for LSMs have focused on assimilating microwave data, or the derived near-surface soil moisture products. These include (Draper et al., 2012; Liu et al., 2011; Margulis et al., 2002; Peters-Lidard et al., 2011; Reichle, 2005).

Most LSM assimilation studies in the literature appear to involve soil moisture or land surface temperature ervations. This can be seen to the number of example citations provided in the previous paragraphs. Considering the assimilation of other data types has also been tested in some studies, such as LAI (e.g. Sabater et al., 2008). Most recently, there is a large interest in using multivariate data assimilation system as a unifying context in which various type of observations from different sources are incorporated in a complex model. This approach is based from the theoretical point of view, the more the information a system gets, the better the obtained analysis.

And most lastly, Barbu et al., (2014) demonstrated that the joint assimilation of SSM and LAI shows a relevant positive impact on modelled soil moisture and LAI and a rather small

positive impact on evapotranspiration is observed for the correlations, as found in Albergel et al., (2017).

1.2.6 Climate change impacts over Africa

Climate change is undeniably occurring and poses new significant risks to a wide range of societies and natural systems. The latest report by the Intergovernmental Panel on Climate Change (IPCC) states global average surface air and ocean temperatures are increasing at rates unequivocal to any other period on record (IPCC, 2014). The resulting extreme conditions, expected to be exacerbated in the future, have already caused substantial flooding/drought and food shortage in Africa and constitute significant threats to water resource, agriculture, and public health management (Boko et al. 2007; Parry et al. 2007; Sylla et al. 2012). Africa is thus one of the most vulnerable continents to such changes, a situation aggravated by different interactions between population and ecosystems and low adaptive capacity (Lobell et al. 2011; Druyan 2011; Anyamba et al. 2014; IPCC 2014; Sylla et al. 2016). This is particularly true for West Africa, a region experiencing high water stress, lack of reliable obervation networks, and scarcity along with exponential population growth and facing recurrent and localized droughts and increased food shortage (Jenkins et al. 2005). While it is certain that climate change resulting from anthropogenic greenhouse gas (GHG) emissions will occur in West Africa including Burkina Faso via an increase in surface temperature and drought conditions (Sylla et al. 2010, 2015a; Diallo et al. 2012, 2016; Mariotti et al. 2014; Ibrahim et al. 2014), substantial uncertainty regarding the direction and magnitude on water resources and agriculture remains. In Burkina Faso, like most West African countries, water resources supply to satisfy population needs for domestic use and irrigated cropping is a key issue because of the high pressure on the resource. Climate change will thus affect future water resources availability through key LSVs such as soil moisture, surface runoff and evapotranspiration.

These above challenges are the main reasons of the scientific questions that have been raised in this study as detailed in the following section.

1.3 Research questions

In this thesis, the main research question is the following: How to address the challenges of assessing past and future hydroclimate information over Burkina Faso through an integrated modelling approach involving land surface modelling, data assimilation and climate change

projections?

The subsequent research questions have been investigated throughout this thesis:

- Does a land surface model such ISBA suitable for representing past hydroclimatic conditions over Burkina Faso?

The aim of this question is to better apprehend the reliability of the LSM ISBA in simulating past hydroclimatic surface states, which is highly dependant of the atmospheric forcing used i.e ERA-Interim and ERA5. The quality of the LSM passes through the validation of its atmospheric forcing.

- What is the impact of assimilating vegetation and soil moisture products into ISBA LSM output in providing improved long-term characterization of hydroclimate conditions across Burkina Faso?

In this above question, the added-value of data assimilation is investigated in order to see whether the improved/corrected data are able to represent correctly the land surface parameters over Burkina Faso. Additionally, it will be interested to see to what extent independent satellite datasets can be used to assess the quality of the reanalysis of LSVs.

- What are the projected changes of hydroclimatic indicators (precipitation, evapotranspiration, soil moisture, surface runoff and aridity conditions) over Burkina Faso?

In this third and last question, a focus is given to the annual mean changes of the above mentionned variables using high-resolution regional climate simulations in order to shed light on drought projections over Burkina Faso.

1.4 Thesis objectives

1.4.1. Main objective

The overall goal of this thesis is to assess the past and future hydroclimatic conditions over Burkina Faso through the integration of land surface modelling, coupled data assimilation and climate change projections.

1.4.2. Specific objectives

This broader objective was broken down into the components listed below:

- Evaluate the performance of the ISBA LSM to represent past hydroclimatic conditions over Burkina Faso;

- Assess the capacity of LDAS-Monde in providing improved long-term reanalysis of hydroclimate variables by jointly assimilating vegetation and moisture observations within the ISBA LSM;
- Analyze the impact on climate change on hydroclimatic variables such as evapotranspiration, surface runoff, soil moisture, and their potential impact on water resources availability.

1.5. Research hypothesis

To provide answers to the previous research questions, a series of hypotheses have been formulated:

- An accurate representation of surface state variables linked to hydrology, such as soil moisture and vegetation is critical in Western Africa especially for hydroclimatic and environmental monitoring.

In this first hypothesis, we assume that accurately representing land variables is highly important for climate change management e.g. in order to cope with droughts, floods and extreme events. This is in line with the fact that West Africa including Burkina Faso is among the regions where soil moisture coupling with atmosphere are among the strongest worldwide and also, where LSVs remain very difficult to model with accuracy.

- Coupled data assimilation of soil moisture and vegetation will improve the representation of hydroclimatic variables linked to water cycle in Sub-saharan Africa.

The possibility of integrating soil water and vegetation observations into complex land models is proven to be one of the most promising data assimilation methods towards the correction of estimates linked to water and carbon cycles. Its application in the sub-region is highly appreciated.

- Future hydroclimatic conditions will be highly affected by climate change

Burkina Faso is a region experiencing high water stress and scarcity along with increasing aridity and localized droughts. The country is also expected to be threatened by future climate change resulting from anthropogenic greenhouse gas (GHG).

1.6. Novelty

Several LSMS, LDASs and RCMs now exist, amongst them are the Global Land Data Assimilation System (GLDAS, Rodell et al., 2004), the Carbon Cycle Data Assimilation System (CCDAS, Kaminski et al., 2002), the Coupled Land Vegetation LDAS (CLVLDAS,

Sawada, 2018; Sawada et al., 2015; Sawada and Koike, 2014), the U.S. National Climate Assessment LDAS (NCA-LDAS, KUMAR et al., 2018) as well as LDAS-Monde (Albergel et al., 2017) to name a few. More recently, soil moisture (SM) data from the Soil Moisture Operational Product System (SMOPS) has been assimilated in the Noah model (Kumar et al., 2019). Those systems either optimize process parameters (e.g., CCDAS), state variables (e.g., GLDAS, NCA-LDAS, LDAS-Monde), or both (e.g., CLVLDAS). Only few studies have considered the integration of multiple remote sensing measurements (Albergel et al., 2017; Sawada, 2018) and even less have had a specific focus over West Africa (e.g., (Pinnington et al., 2018).

In addition, and considering Burkina Faso, any study (in our knowledge) has been addressed to provide high-resolution ensemble projections for water resources using a regional climate simulations ensemble under the resolution of 30 kms. Therefore, considering Sub-Saharan Africa, this study is among the first (if not the first to the best of our knowledge) aiming to produce and evaluate long-term reanalyses of LSVs by dynamically combing different sources of datasets in order to produce improved parameters linked to hydrological cycle as well as discussing future water availability due to anthropogenic climate change.

1.7. Scope of the thesis

The scope of this research was confined to the integration of land surface modelling, data assimilation and ultimately climate change projections for providing better prediction of hydroclimatic parameters over Burkina Faso. Using the objectives above as a guide, the primary focus was on assimilating different observation types (LAI and SSM) using reanalysis of land surface conditions and analyzing the impacts each had on predictions from that LSM already calibrated. This set of reanalysis derived from the experiments carried out throughout this thesis along with the projections in water resources availability will allow to better apprehend future water resources predictions planing and climate change monitoring.

1.8. Expected results

The main expectations from the studies conducted in this thesis are listed hereafter.

- From the use of ISBA land surface model, a historical representation of key hydroclimatic variables will be described. This will allow to present a “first-state” representation of the past hydroclimatology of Burkina Faso as well as, to advance scientific knowledge in the area of land surface modeling for hydrological purposes in

Burkina Faso.

- Improved (i.e bias-reduced) long-term reanalysis of historical hydroclimate variables will be provided by integrating soil moisture and vegetation observations in LDAS-Monde data assimilation platform. This will raise awareness on the impact of data assimilation in enhancing land surface variables represetation, especially in data-sparse areas like Burkina Faso.
- Finally, this thesis will yield information on the potential impacts of climate change on the hydroclimatology of Burkina Faso for a near (2041-2060) and far (2080-2099) future periods, thus supporting future planning efforts in water management sector as well as agriculture.

1.9. Outline of the thesis

This thesis is arranged into six chapters including this introduction chapter.

Chapter 1: Covers a review of literature and provides a synthesis of background information underpinning the work in this thesis. This includes summaries of: water interaction and energy between the land surface and atmosphere; remote sensing observations related to the data types used in modeling experiments in this thesis; characteristics of LSMs and how formulations have changed over time; and, data assimilation background along with different methods.

Chapter 2: covers presentation of the study area with description of Burkina Faso, including climate, vegetation, soil, hydrology, demography, environmental, social and economic activities.

Chapter 3: presents data, methods along with set of materials used to describe the study area. It is also described in this chapter the data origin, processing methods, modelling setup and experiments as well as the different assessement methods used.

Chapter 4: This chapter presents the validation of ISBA and LDAS-Monde over Burkina Faso. A primary task consisting of assessing the ability of atmospheric reanalysis to drive LDAS-Monde among previous ERA-Interim and ERA5 latest ECMWF reanalysis. This chapter concludes by using an independent validation of LDAS-Monde reanalysis using independent datasets such as evapotranspiration fluxes from the GLEAM (Global Land Evaporation Amsterdam Model).

Chapter 5: assesses the potential climate change impacts on water resources parameters, provides future aridity conditions and ultimately discusses future water resources availability over Burkina Faso.

Chapter 6: ends with a general conclusion highlighting the need of integrating land surface modelling and data assimilation as well as climate change modelling. The results of the three specific objectives are summarized and finally, recommendations and perspectives are provided.

Chapter 2: Presentation of the study area

This research is focused over Burkina Faso, a landlocked country in the Sahel region of West Africa. This chapter presents a comprehensive description of Burkina Faso which encloses its position, soil characteristics, land cover, climate, geology, topography, hydrography of the area, and population characteristics.

2.1. Geographic location

The area covered by Burkina Faso covers approximately 274000 km^2 for over 20 million people (in 2019). The country shares its limits with six nations (Figure 2.1c). It lies between the Sahara desert and the Gulf of Guinea, south of the Niger River, between latitudes 9° and 15°N, and longitudes 6°W and 3°E. Burkina Faso has water bodies such as lakes and river basins throughout its territory. However, the largest water network is located in the south of the country, which shows three main river basins: the Volta, the Comoé, and the Niger (Simonsson and Stockholm Environment Institute, 2005). In the rest of the country, rivers flow intermittently.

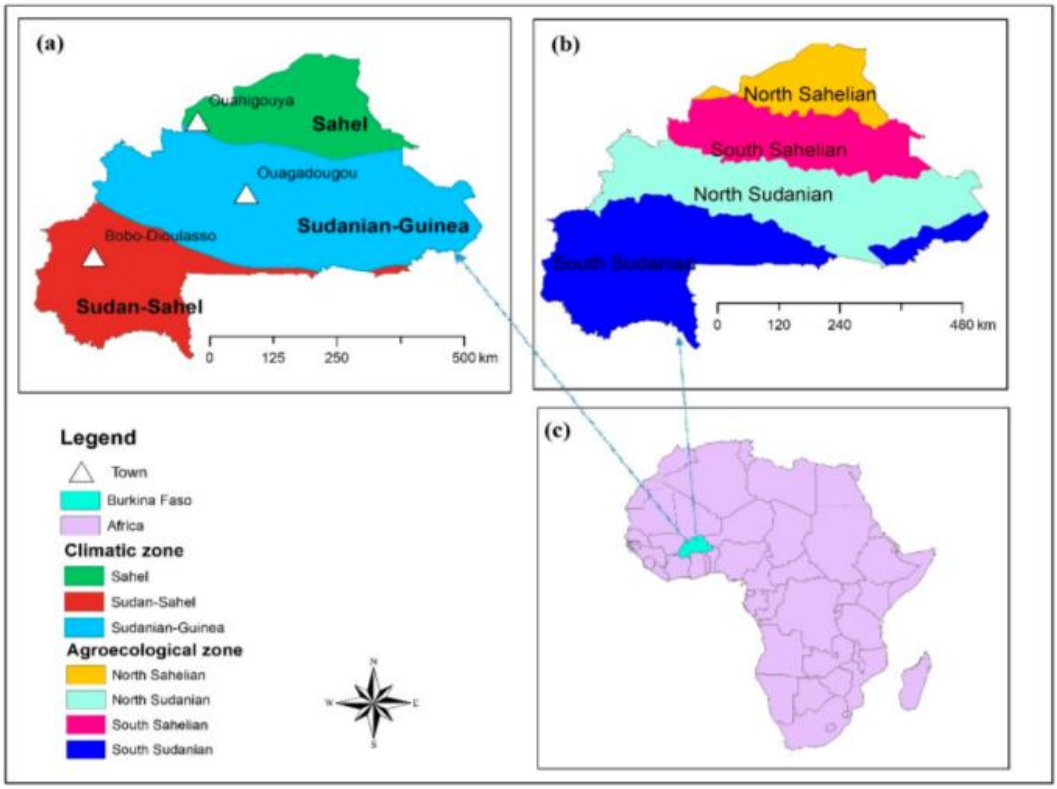

Figure 2.1: *(a) climatic zones, (b) agro-ecological zones, (c) Regional boundaries of Burkina Faso (MA, 2017)*

2.2. Relief and geology

The topography of Burkina Faso is formed by two major types of terrain. The major part of the country is covered by a peneplain, which shapes a gently undulating landscape with, in some areas, a few isolated hills, the last vestiges of a Precambrian massif. On the other hand, the southwest of the country, presents a sandstone massif, where the highest peak, Ténakrou, presents an elevation of 749 m. The massif is bordered by sheer cliffs up to 150 m high. The average altitude of Burkina Faso is 400 m and the difference between the highest and lowest terrain is no greater than 600 m. Thus, Burkina Faso is considered as a relatively flat country.

The geology of Burkina Faso is largely formed by Precambrian rocks of the Guinea Rise, a dome of Archaean rocks, composed largely of migmatites, gneisses and amphibolites, over which lie the greenstone belts of the early Proterozoic age. The latter are metasediments and metavolcanics assigned largely to the Birimian Supergroup, a series of rocks in which economically significant mineralization occurs. Pre-Birimian migmatites, gneisses, and amphibolites, located under the Birimian rocks, are the oldest rocks in the country. The Birimian deposits in the southwestern part of the country are typically divided between clastic and volcano-clastic formations.

2.3. Vegetation and fauna

Burkina Faso has a natural vegetation which is mainly driven by climatic conditions. The northern part of the country consists of savanna, with prickly shrubs and short trees that flourish during the rainy season. In the south, the prickly shrubs give way to scattered forests, which become denser along the banks of the perennial rivers. The karite (shea tree) and the baobab (hibiscus tree) are very common in this region. Animal life includes buffalo, antelope, lions, hippopotamuses, elephants, crocodiles, and monkeys. Bird and insect life is rich and varied, and there are many species of fish in the rivers. Burkina Faso’s national parks include Po in the south-centre of the country, Arly in the southeast, and “W” in the east, standing at both sides of the border with Benin and Niger.

2.4. Climate

Burkina Faso's climate is principally marked by a tropical climate with two different seasons (Figure 2.2). In the rainy season (four months, May/June to September), the country receives between 600 and 900 mm of rainfall; while the dry season is characterized by a hot and dry wind from the Sahara (Waongo et al., 2014). Three climatic zones (Figure 2.1a) can be

defined: the Sahel (SH), the Sudan-Sahel (SS), and the Sudan-Guinea (SG). The Sahel in the north typically receives less than 600 mm of rainfall per year and has high temperatures, up to 47 °C sometimes. Compared to the other parts of Burkina Faso, the SG zone receives more than 900 mm of rainfall each year and has lower average temperatures.

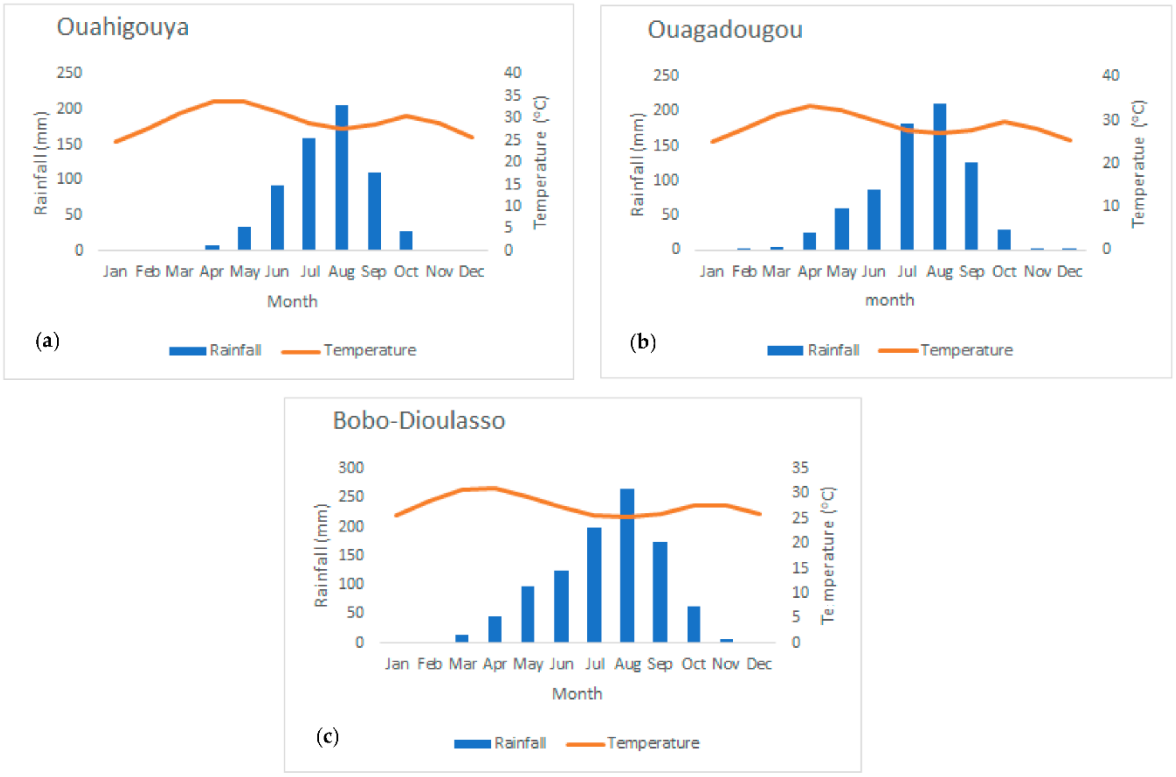

Figure 2.2: *Long-term (1980–2012) average rainfall (mm) and Temperature (°C) per month for the climatic zones of (a) SH, represented here with the city of Ouahigouya; (b) SG, represented here with the city of Ouagadougou; and (c) SS, represented here with the city of Bobo-Dioulasso (ANAM, 2018).*

2.5 Hydrography

The former name of Burkina Faso i.e. Upper Volta comes from its location with to three rivers which cross it: the Black Volta (or Mouhoun), the White Volta (Nakambé) and the Red Volta (Nazinon) (Figure 2.3). The Black Volta is one of the country's only two rivers which flow year-round, the other being the Komoé, which flows to the southwest. The basin of the Niger River also drains 27% of the country's surface. The Niger's tributaries – the Béli, the Gorouol, the Goudébo and the Dargol – are seasonal streams and flow for only four to six months a year. Therefore, they are often the source of important and large floods. The country also contains numerous lakes – the principal ones are Tingrela, Bam and Dem. The country contains large ponds, as well, such as Oursi, Béli, Yomboli and Markoye. Water shortages are often a problem, especially in the north of the country.

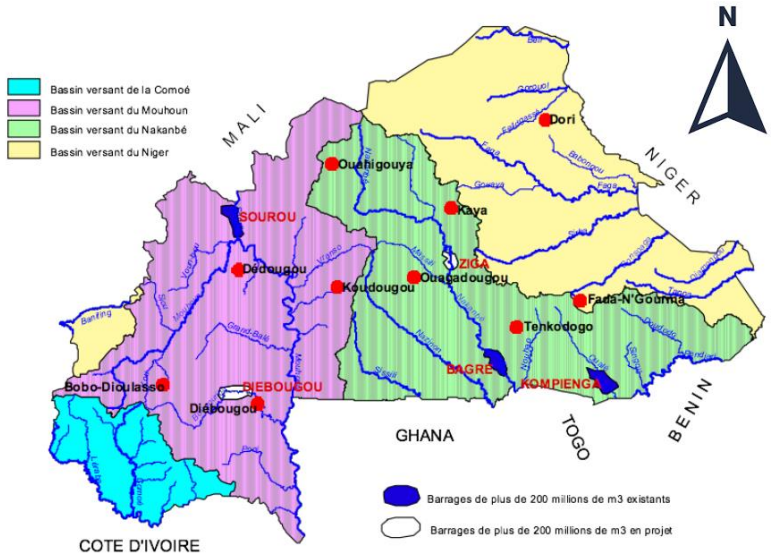

Figure 2.3: *Watershed map and hydrographic network of Burkina Faso (MEE, 1998).*

2.6. Soil and land use

Soil components play a primordial role in surface hydrology especially for infiltration and runoff processes (Kinnell, 2010). Topsoils in most parts of the country predominantly comprise an erodible texture such as sand-clay-loam, loam, and sandy-loam (Figure 2.4).

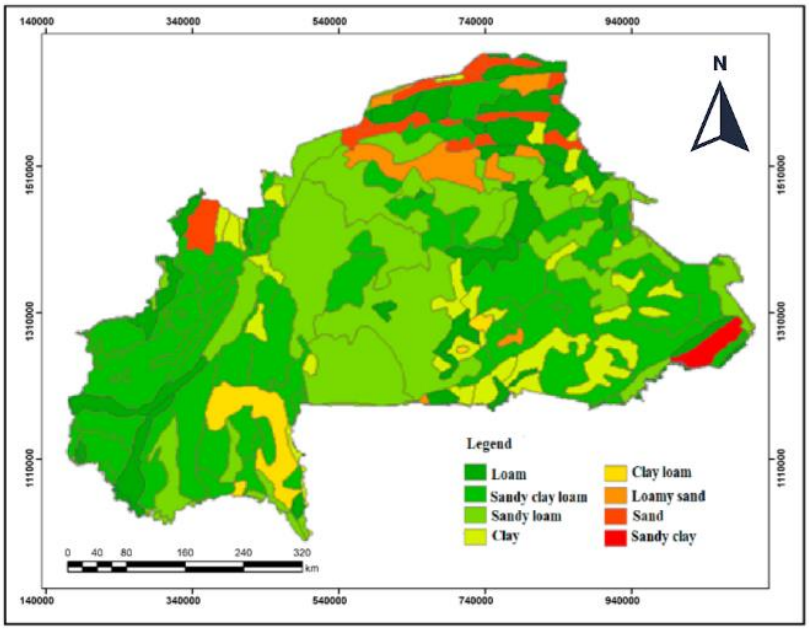

Figure 2.4: *Soil type classification across Burkina Faso (FAO, 2015).*

Land use and land cover in Burkina Faso are characterized mainly by savannah, bare soil, grasslands, woodlands and forests, croplands and pastures. The natural vegetation is

dominated by savannah (grassland sprinkled with shrubs and trees), forest (forest administrative park, mall dense and gallery forest). Cropland activities are among the most important in the country. However, Burkina Faso's land cover is constantly changing with different patterns and magnitudes. The conversion of grasslands, woodlands and forests into croplands and pastures has risen dramatically during the last few decades. Tropical dry forests, for instance, have been severely fragmented and disturbed and have tended to disappear (Cobo et al., 2010; Lal, 2001; Sivakumar, 200s7). The main drivers behind these changes combine population growth, rising demand for agricultural products, dietary changes, agricultural trade and adjustment, dependence on wood energy, recurrent bush fires, etc. (Toy et al., 2002; UNEP 2012; IRIN, 2009).

2.7. Demography, environmental, social and economic activities

The population of Burkina Faso is approximately 20 million of people (2020) consisting mostly by *Mossi's* ethny. They are largely concentrated in the South and Centre of the country. The country's experiencing an increase of rural population density (Figure 2.5) oftenly exceeding 48 inhabitants per km^2 (120 inhabitants per m^2).

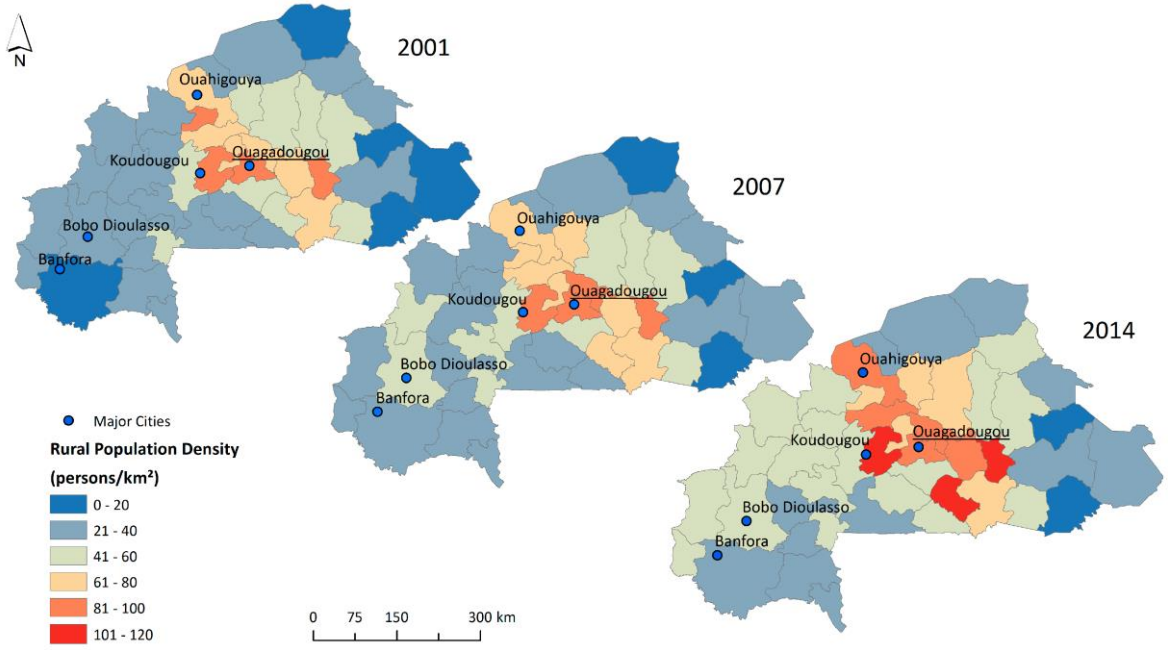

Figure 2.5: *Development of rural population density in the provinces of Burkina Faso between 2001 and 2014 (INSD, 2014).*

This population density causes annual migrations of hundreds of thousands of the population to Cote d'Ivoire and Ghana for seasonal agricultural work with important impacts

on the country's economy. The country experiences also recurring floods which are significant natural hazard. Current environmental issues include also: recent droughts and desertification severely affecting agricultural activities, population distribution, and the economy; overgrazing; soil degradation; desertification.

Economic activities are generally based on agriculture (substance farming and livestock raising). The country presents an average income purchasing-power-parity per capita of $1,900 and nominal per capita of $790 in 2014 (World Bank, 2019). More than 80% of the population relies on small-scale agriculture, with only a small fraction directly involved in industry and services. Many components among highly variable rainfall, poor soils, inadequate means of communications and low literacy rate make the country's economy very vulnerable.

2.8. Conclusion of the chapter

This chapter provided insights on Burkina Faso geographical location as a semi-arid country. Key aspects among its geography, terrain, climate, hydro-geology, soil properties have been provided. Socioeconomic information have been also addressed and the possible impacts they could have on geophysical characteristics as well as natural resources of the country.

Chapter 3: Data, materials and methods

In this thesis, numerous types of data, materials and methods are used. They have been derived from data collection and high-performance computations. The in-situ data were collected from National meteorological service level and the satellite products freely available from state-of-the-art online databases. All the materials and data have been treated following a concise methodology described throughout the present chapter and will serve as main datasets/materials for the upcoming chapters highlighting the thesis results.

3.1 Data

3.1.1 In Situ Measurements

- Precipitation and incoming solar radiation (SW_{in})

In this thesis, in situ data of precipitation for the 2010–2016 period were provided by the Agence Nationale de la Météorologie (ANAM) of Burkina Faso, as previously used by Waongo et al., (2014). This time-span was choosen after a quality-control check considering the whole network spanning over the study area. It consists of 134 stations, which are relatively well spread over the country except for less density in the north of Burkina Faso also called the Sahel zone (SH) and the eastern part of the Sudan-Sahel zone (SS) of the domain (Figure 3.1, lower panel). All stations include a daily time series of good quality (with few missing data) over the considered period. The in situ measurements of SW_{in} are also from the ANAM with data available every 15 min for 4 stations (Figure 3.1, upper panel). In the present study, 24h-mean values of these radiative fluxes are used.

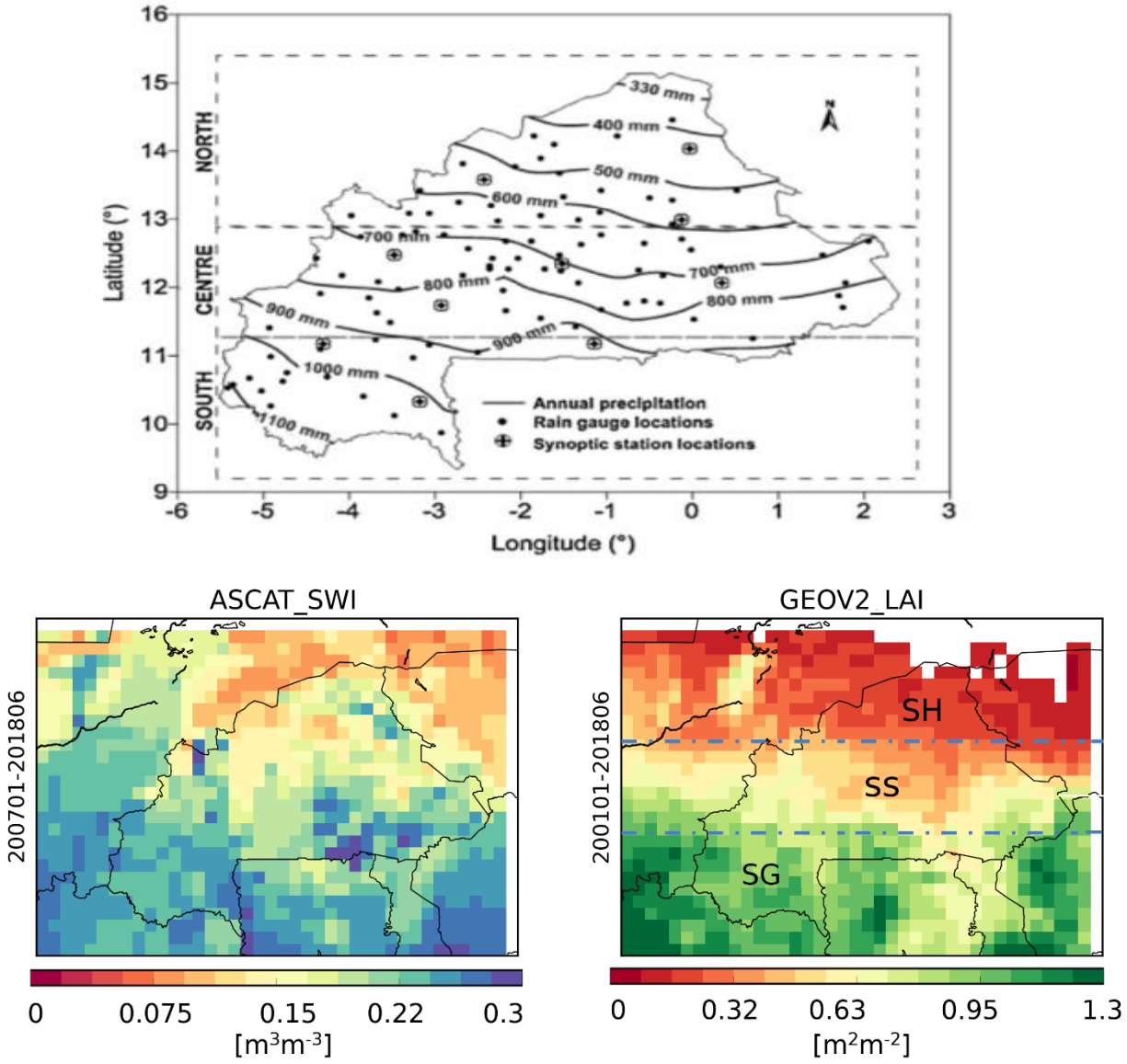

Figure 3.1: *Isohyets and dotted symbols represent annual precipitation (upper panel) and stations (rainfall and solar radiation). The three agroecological zones (SS, SS and SG) across Burkina Faso are highlighted in lower panels for soil moisture and vegetation products.*

3.1.2 Satellite-based datasets

- **ASCAT Soil Water Index and GEOV2 Leaf Area Index**

This thesis makes use of the ASCAT Soil Water Index (SWI) product distributed by the CGLS through its third version, i.e., SWI-001 Version 3.0. The SWI refers to the soil moisture content in relative units between 0 (dry) and 100 (saturated). It is computed based on a recursive exponential filtering method (Albergel et al., 2008) using the backscatter observations from the ASCAT C-band radar on board MetOP satellites (Bartalis et al., 2007; Reichle et al., 2004). The SWI retrieved from the exponential filter using a T-value (characteristic time length; the

higher the T-values, the smoother the SWI) of one day is used. It represents the SWI in the top soil layer (Albergel et al., 2008). It is used in the present study as a proxy for SSM. During the period considered in the experiment, the amount of soil moisture data increases in 2015 because the data from MetOP-B (launched in 2012) are used in addition to those from MetOP-A (launched in 2006).

For the purpose of assimilating the SSM product, a rescaling of observations into model climatology space is needed in order to avoid introducing any artificial bias in the system caused, for example, by a possible mis-specification of physiographic parameters related to soil texture types (Drusch et al., 2005; Reichle et al., 2004). To that end, the SWI product is transformed into model-equivalent SSM (from the model second layer of soil, 1–4 cm), based on the first two statistical moments (the mean and the variance) through a linear transformation (Scipal et al., 2008). The relevance of performing a seasonal rescaling was emphasized by several studies (e.g., Barbu et al., 2014; Draper et al., 2011). In this study, the matching of SSM statistical distributions was made on a monthly basis by using a 3-month moving window over the January 2007–June 2018 period after screening for the presence of urban areas (>15%) and complex terrains (1500 m a.s.l.). Finally, the SWI observations are interpolated by an arithmetic average to the 0.25° model grid points (from their original 12.5 km spatial resolution).

The GEOV2 LAI observations are also distributed by the CGLS. They are retrieved from the SPOT-VGT and PROBA-V satellite data using the methodology prescribed in Verger et al. 2014. The 1 km × 1 km resolution observations are interpolated to 0.25° model grid points through an arithmetic average as in Albergel et al., (2017), so that at least 75% of the grid points are observed. In terms of temporal resolution, LAI observations are available with a 10-day frequency (at best). Figure 3.1 (lower right) illustrates the averaged LAI (January 2001–June 2018).

It is worth emphasizing that these satellite observations have been validated in previous studies over Western Africa through the ALMIP experiment with quite good consistencies with in situ data of soil moisture in Burkina Faso (Albergel et al. 2012, Fatras et al. 2014; Louvet et al. 2015) - making them reliable in terms of use for our study domain.

3.1.3. Reanalyses: ERA-Interim, ERA5 atmospheric reanalyses and ERA5-Land reanalyses.

- **ERA-Interim**

ERA-Interim is a global atmospheric reanalysis produced by the ECMWF (Dee et al., 2011). Reanalyses provide a numerical description of the recent climate by combining models with observations using data assimilation systems. ERA-Interim overlays the period from 1 January 1979 onward and continues to be extended forward in near-real time. It is based on the integrated forecast system (IFS) version 31r1 (more information at https://www.ecmwf.int/en/forecasts/documentation-and-support/, last access: November 2018) using approximately an 80 km (T255) spatial resolution and with analyses available for 00:00, 06:00, 12:00, and 18:00 UTC. A detailed explanation of the ERA-Interim product archive is provided in Berrisford et al., (2009); Dee et al., (2011).

- **ERA5**

Recently, ERA5 (Hersbach and Dee, 2016), the latest version of ECMWF reanalyses, was released as the fifth generation produced. It is envisioned that ERA5 will replace the release of the current ERA-Interim reanalysis, from 1979 to the near real time period (on a regular basis). Regarding climate information, ERA5 has numerous improved characteristics compared to ERA-Interim reanalysis. It presents one of the most updated versions of the Earth System Model and data assimilation techniques used at ECMWF, which enables the use of more sophisticated parametrization of geophysical processes in comparison to the previous versions used in ERA-Interim. Moreover, ERA5 has two other important features, which are the improved temporal sampling and spatial resolution: From 6-hourly in ERA-Interim to hourly in ERA5, and from 79 km in the horizontal dimension and 60 vertical levels to 31 km and 137 levels in ERA5. Eight variables from ERA5 and ERA-Interim have been used to constrain LDAS-Monde, including the lowest model level (about 10-m above ground level), air temperature, wind speed, specific humidity and pressure, and the downwelling fluxes of shortwave and longwave radiation as well as precipitation partitioned in the liquid and solid phases (the latter being null over the considered domain).

At the time of this research thesis, ERA5 is a new product and to the best of our knowledge, only three other studies compared the performance of ERA5 and ERA-Interim. In Albergel et al., (2018), the authors assessed the two reanalysis ERA5 and ERA-Interim using them to force the ISBA LSM over North America. Better performances in the representation of evaporation, snow depth, soil moisture, and river discharge estimates were observed in the simulations forced by ERA5. They were attributed by the authors to the improved precipitation estimates. Urraca et al., (2018) compared SW_{in} estimates from ERA5 and ERA-interim at a global scale, and observed a better performance with ERA5. Finally, Beck et al., (2018)

highlighted the good performance of ERA5 precipitation with respect to 26 gridded subdaily precipitation datasets using Stage-IV gauge-radar data for the evaluation over the continental United States of America.

3.1.4. Evapotranspiration, Gross Primary Production, and Sun-Induced Fluorescence

This thesis makes use also of independent datasets of evapotranspiration and the CO_2 uptake from photosynthesis defined as gross primary production (GPP) as well as in order to evaluate the quality of the surface reanalysis generated in this study. These previous datatsets are useful evaluation tools since they are very difficult to measure, thus valuable for Sub-saharan context. Note that only a limited flux towers are available across Africa, which are insufficient for systematic evaluation of remote sensing fluxes such as evapotranspiration (for example).

- **Evapotranspiration**

Terrestrial evapotranspiration estimates are from the GLEAM (Global Land Evaporation Amsterdam Model) v3.1. product (Martens et al., 2017). They cover the period of 1980–2016 and are available at a spatial resolution of 0.25° × 0.25°. The GLEAM dataset is widely used for investigating both trend and spatial variability in the terrestrial water cycle as well as for evaluation purposes (e.g., Greve et al., 2014; Miralles et al., 2014; Zhang et al., 2016) as well as land atmosphere interactions (e.g., Guillod et al., 2015; Miralles et al., 2014). In short, the model computes the terrestrial evaporation and root-zone soil moisture (Owe et al., 2008) and is mainly driven by microwave remote sensing observations, the potential evaporation amount being constrained by satellite-derived soil moisture. GLEAM datasets have already been comprehensively validated against FLUXNET (Fluxnet Networks) observations and used for multiple hydro-meteorological applications over Sub-saharan Africa including Burkina Faso (Trambauer et al., 2014; Forzieri et al., 2017; Lian et al., 2018; Richard et al., 2018; Vicente-Serrano et al., 2018; Zhan et al., 2019).

- **Gross Primary Production**

For the evaluation of the carbon uptake related to photosynthesis i.e GPP, we use estimates derived from meteorological parameters through the use of machine learning algorithms within the FLUXCOM project (Jung et al., 2017). These algorithms are trained using a combination of land cover data, observed meteorological data and remotely sensed vegetation

properties (fraction of absorbed photosynthetic active radiation). A model tree ensembles are also used to provide estimates of carbon fluxes at FLUXNET sites (including Burkina Faso) with available quality-filtered flux data, after which the trained model can be implemented globally using grids of the input data. This set of observations can be found at the Max Planck Institute for Biogeo-chemistry data portal (https://www.bgc-jena.mpg.de/geodb/projects/Home.php, last access: December 2019) and is available at a 0.5° x 0.5° spatial resolution with a monthly temporal frequency over the 1982-2013 period. In this study, GPP products were used over the 2001–2013 time (time span available at the time of completion of the thesis).

- **Sun-induced fluorescence**

We also use estimates of sun-induced fluorescence (SIF) from the GOME-2 (Global Ozone Monitoring Experiment-2) scanning spectrometer (Joiner et al., 2016; Munro et al. 2006) evaluate GPP. Leroux et al., 2018 has shown that observations of SIF can be used as a proxy to evaluate the influence of data assimilation on simulated GPP using correlations. We use in this study the Level-3 v27 SIF product, giving a daily-averaged SIF at 0.5° × 0.5° resolution over the 2010–2016 period. Observations are rescaled to match the spatial resolution of the two atmospheric forcing data-sets, 0.25° × 0.25° and 0.50° × 0.50° for ERA5 and ERA-Interim, respectively.

3.2 Materials

3.2.1 The SURFEX modeling platform and ISBA model evolution

The ISBA model is a component of the modeling platform called SURFEX “Surface Externalisée” in French (Martin et al., 2007, Le Moigne, 2009), developed at Météo-France at the CNRM (Figure 3.2). This platform describes the surface in four major categories called “tiles”: oceans or seas, lakes, nature (soil and vegetation) and urban areas. The physical parameters and fractions of each of the “tiles” are retrieved from the ECOCLIMAP database (Masson et al., 2003) which is a global database of land surface parameters at 1-km resolution**.** SURFEX can be coupled with an atmospheric model (Sarrat et al., 2009), it is the online version of the platform. It can also be used uncoupled from the atmosphere. In this case, SURFEX is forced with observations or atmospheric reanalyses, this version is referred as “offline”.

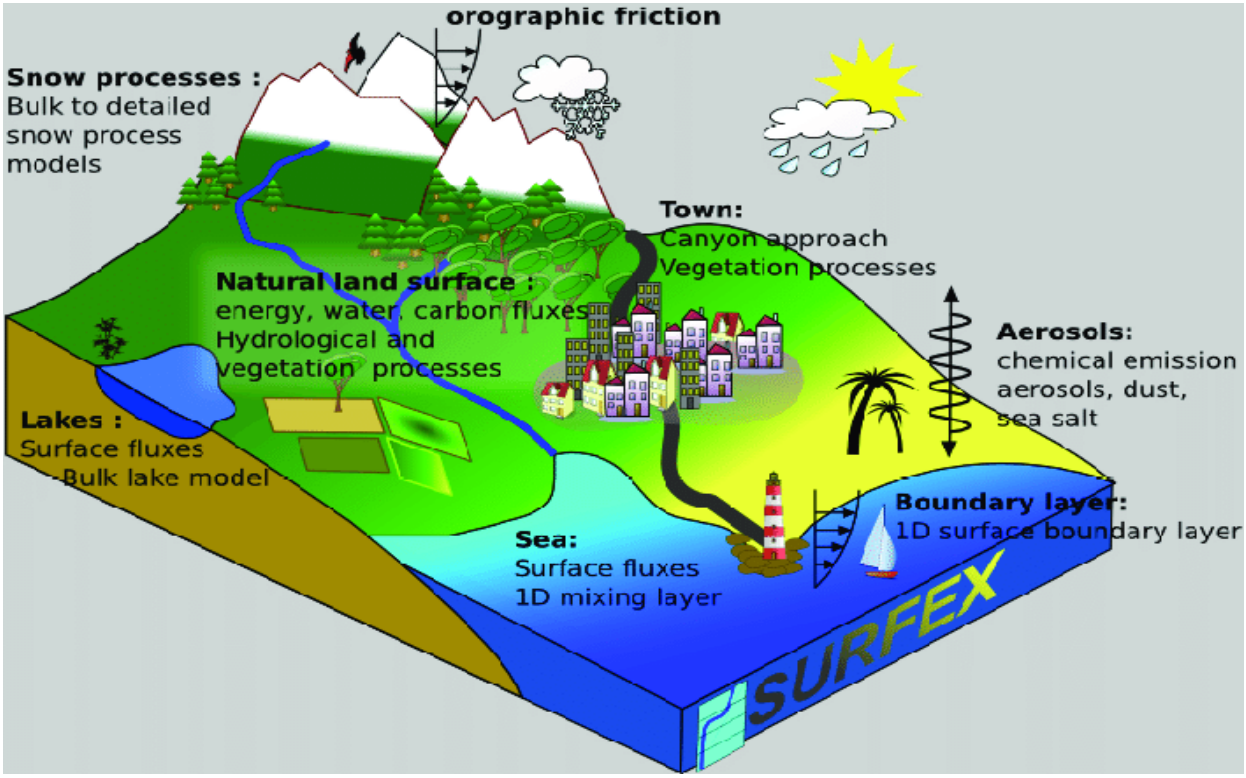

(Source: https://www.umr-cnrm.fr/surfex/)
Figure 3.2: *SURFEX modeling platform*

ISBA model (Noilhan and Planton, 1989 and Noilhan and Mahfouf, 1996) is therefore capable to simulate mass and energy balances in the soil-vegetation-atmosphere system of the nature "tile". The first version of ISBA i.e. ISBA-standard, is a "bucket" model (Manabe, 1969). It was improved to represent soil surface humidity and evaporation at the soil surface using the "force-restore" method. In this configuration, the soil is characterized in two layers, one superficial layer with a thickness of one centimeter and a deep layer including the root zone. The thickness d_2 of the latter varies according to the soil type and vegetation type. Both surface and deep ground temperatures T_g and T_2 are simulated, as well as the surface and deep volumetric water contents w_g and w_2. In this initial version, the vegetation is described as a homogeneous layer and the surface is characterized by 8 parameters: the root depth d_2, the minimum stomatal resistance SR_{min} and the contribution of the vegetation at the surface thermal inertia coefficient C_v, which are constants over time, then the vegetation proportion *veg*, LAI, roughness length *z0*, albedo α and emissivity ε which depend on the seasonal cycle. The stomatal resistance *SR*, i.e. the regulation of gas exchanges (CO_2 and water vapour) between the leaf and its environment, is calculated according to the formalism of Jarvis, (1976). It takes into account the impact of environmental factors (soil water, air humidity, solar radiation and

air temperature) on the opening of stomata and thus on photosynthesis. A coefficient allows to represent the effect of soil drying, water stress, on the vegetation response. This coefficient varies from 0 to 1 depending on the humidity conditions of the root zone, from the wilting point to the field capacity. The evolution of this coefficient over time depends on the soil available water storage capacity.

This basic version has been upgraded with new options and modules to simulate water and heat transfers at the surface along with more details. To the two-layer ("2L") representation of the soil in the "force-restore" version has been added a third layer to create ISBA-3L (Boone et al., 2009). A multi-layer version which is more complex, allowing to represent the processes of water and heat diffusion in soil was developed in parallel (Boone et al., 2000). Surface hydrology has been improved by taking into account the heterogeneity under the rainfall grid (Decharme and Douville, 2006) as well as mesh processes such as drainage and runoff (Etchevers et al., 2001; Habets et al., 1999).

3.2.2 ISBA-A-gs

The ISBA-A-gs model (Calvet et al., 1998) based on the ISBA-standard model was developed to assess climate change impacts on vegetation while taking into account the induced effect of CO_2 concentration increase in the atmosphere on vegetation (Figure 3.3). Apart from being able to simulate biomass and LAI (which is no longer considered as a model parameter but as a prognostic variable), it allows to represent the vegetation response facing water stress, temperature increase and increase of CO_2 concentration, and thus to meet the requirements of resulting problems at parcel level (Garrigues et al., 2015; Gibelin et al., 2008; Rivalland et al., 2005), at regional level (Brut et al., 2009; Calvet et al., 2012; Canal et al., 2014) and on global scale (Gibelin et al., 2008).

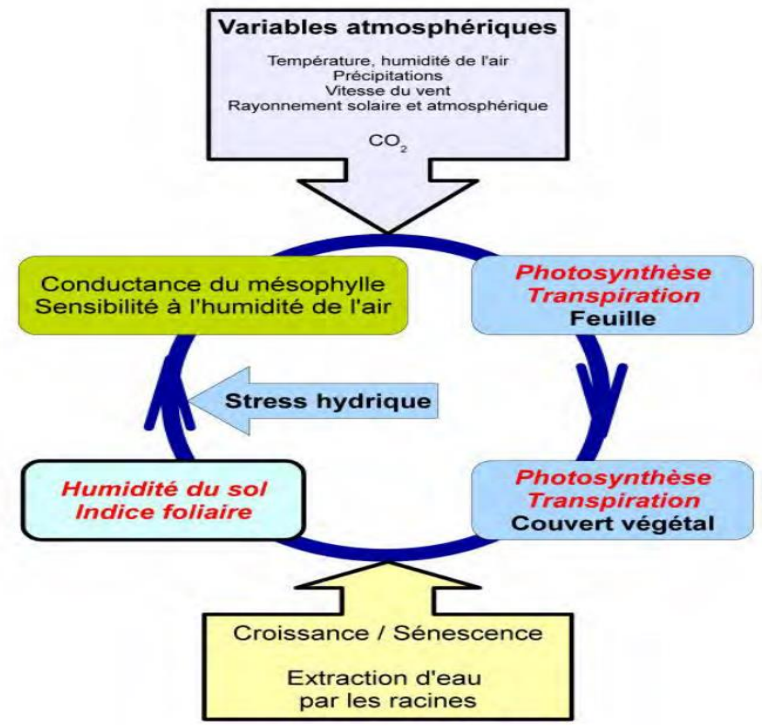

(Source: https://www.umr-cnrm.fr/spip.php?article146&lang=fr)
Figure 3.3: *ISBA-A-gs Land SurfaceModel main components*

The model used to describe the photosynthesis processes is the one from the Jacobs et al., (1996) which used the approach developed by Goudriaan et al., (1985). This latter allows to compute the canopy conductance from the net rate of assimilated carbon by the vegetation which have essentially three limiting factors:

- the atmsopheric concentration of CO_2;
- the temperature;
- the photosynthetically active radiation (PAR);
- the air humidity.

This parameterization is derived from a set of equations that take into account the type of vegetation, C3 (Farquhar et al., 1980) or C4 (Collatz et al., 1992). ISBA-A-gs is able to link the stomatal conductance gs of a vegetation type to its net assimilated carbon through photosynthesis, A_n. In order to compute A_n (in mg CO_2 m^{-2} of leaf s^{-1}) and g_s (in mm s^{-1}), several variables computed by the model are required such as the leaf temperature T_s (in °C) as well as the soil water content.

These processes at the leaf scale (photosynthesis and transpiration) are extrapolated at the scale of the canopy thanks to a radiative transfer scheme that take into account the

attenuation of global radiation within the canopy (Calvet et al., 1998 and Carrer et al., 2013). Thus, the net assimilated carbon together with the stomatal conductance at the canopy scale are obtained by integrating A_n and g_s calculated at different levels within the vegetation canopy.

An important parameter is used to initiate this LAI calculation when atmospheric conditions allow the plant to perform the photosynthesis: the minimum LAI (LAI_{min}). The values of this defined parameter at the global scale have been fixed at 0.3 m^2m^{-2} for C3 and C4 crops and grasslands and deciduous trees, and 1 m^2m^{-2} for evergreen trees. These LAI values arbitrarily chosen allow therefore to represent a possible interannual variability of the LAI values simulated by the model (Gibelin et al., 2006).

ISBA-A-gs allows vegetation growth to be reproduced under water limited conditions by a parameterization of water stress which affects key parameters of photosynthesis in the model. It is the soil moisture that is estimated taking by into account the physical properties of the soil (the proportion of clay and sand, the wilting point, the field capacity and the amount of water at saturation) that will control the response of the vegetation to a soil dryness (stress function of ISBA-standard).

For this thesis work, ISBA parameters are prescribed for 12 generic land surface types, which consist of (i) nine plant functional types (needle leaf trees, evergreen broadleaf trees, deciduous broadleef trees, C3 crops, C4 crops, C4 irrigated crops, herbaceous, tropical herbaceous and wetlands), (ii) bare soil, (iii) rocks, and (iv) permanent snow and ice surfaces. Those parameters are derived from the ECOCLIMAP land cover database (Faroux et al., 2013).

ISBA also provides estimates of soil moisture in the whole root i.e root zone soil moisture (RZSM). In fact, the model initializes the surface soil moisture at the surface level and propagates the information up to 1m of depth through the model's physics.

3.2.3 LDAS-Monde

LDAS-Monde routinely uses a simplified extended Kalman filter (SEKF, Mahfouf et al., 2009) to assimilate observations of SSM and LAI. This is a sequential approach with a forecast step followed by an analysis step (see Figure 3.4 for schematic diagram describing how it works).

- The forecast step propagates the initial state over a 24-h assimilation window with the ISBA LSM. Then, the analysis step corrects the forecast by assimilating observations. This step involves an observation operator defined as the product of the model

propagation of control variables over the 24-h assimilation window with the projection of those variables to observation equivalents.

- In this study, the analysis step updates the modeled LAI and soil moisture from layer 2 (1–4 cm) to layer 7 (60–80 cm). The approach is fully detailed in Albergel et al., (2017).

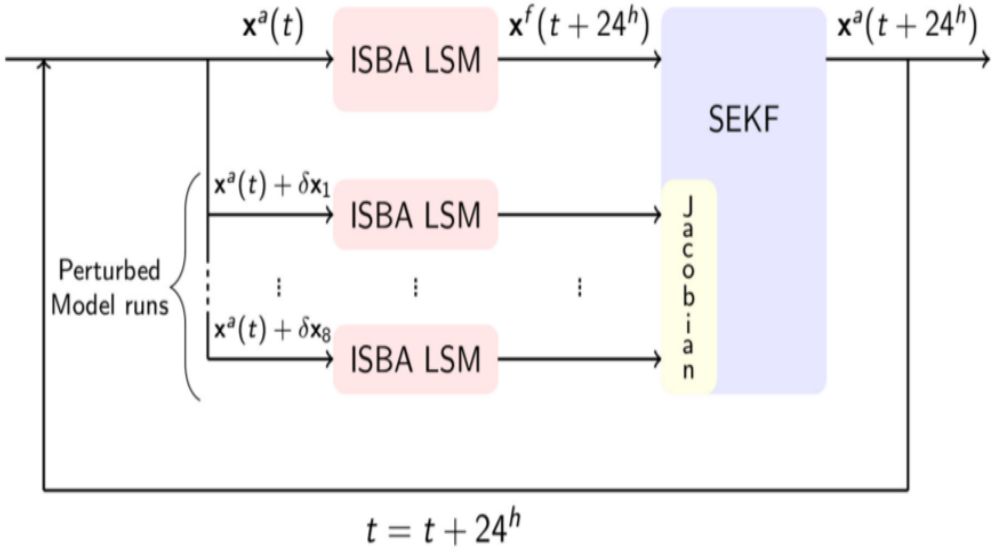

Figure 3.4: *Diagram depicting the sequential cycle of LDAS-Monde using a Simplified Ensemble Kalman Filter (SEKF).*

A mean volumetric standard deviation error of 0.04 $m^3 \cdot m^{-3}$ was affected to soil moisture in the second layer of soil (i.e., the model equivalent of the SSM observations). Then, for deeper layers, the mean volumetric standard deviation error of 0.02 $m^3 \cdot m^{-3}$ was used, as suggested by several authors for RZSM (Barbu et al., 2014, 2011; Draper et al., 2011; Mahfouf et al., 2009). The observational SSM error is set to 0.05 $m^3 \cdot m^{-3}$ as in Barbu et al., (2014). This value is consistent with errors typically expected for remotely sensed soil moisture (e.g., De Jeu et al., 2008; Draper et al., 2011; Gruber et al., 2016). Soil moisture observational and background errors are assumed to be proportional to the soil moisture range (the difference between the volumetric field capacity (w_{fc}) and the wilting point (w_{wilt}), calculated as a function of the soil type, as given by Noilhan and Mahfouf, (1996). The standard deviation of errors of GEOV2 LAI is assumed to be 20 % of GEOV2 LAI. The same assumption is made for the standard deviation of errors of the modelled LAI (20% of modelled LAI) for modelled LAI values higher than 2 $m^2 \cdot m^{-2}$. For modelled LAI values lower than 2 $m^2 \cdot m^{-2}$, a constant error of 0.4 $m^2 \cdot m^{-2}$ is assumed, according to Barbu et al., (2011).

3.2.4 RegCM4 (Regional Climate Model) description

In order to investigate the future climate change impacts on hydrcolimatic parameters over Burkina Faso, we build a multi model ensemble based on RegCM4 regional climate model. The RegCM4 (Giorgi et al. 2012) is the latest version of a series of RCMs developed and maintained at the Abdus Salam ICTP (International Centre for Theoretical Physics) to study and understand, among other topics, climate change and its impact on hydrology, especially over developing countries. RegCM4 is a primitive equation, sigma vertical coordinate limited-area model based on the hydrostatic dynamical core of the National Centre for Atmospheric Research/Pennsylvania State University's Mesoscale Meteorological Model version 5 (NCAR/PSU's MM5; Grell et al. 1994). In the experiments presented here, interactions between the land surface and the atmosphere are described using the Community Land Model version 3.5 (CLM3.5; Oleson et al. 2008) while convective precipitation is calculated with the Massachusetts Institute of Technology (MIT) scheme of Emanuel (Emanuel 1991; Emanuel and Rothman 1999).

RegCM4 is used to dynamically downscale at 25 km of horizontal resolution and 18 vertical levels two ESMs participating in the Coupled Model Intercomparison Project Phase 5 (CMIP5) (Taylor et al. 2012): Hadley Centre Global Environment Model version 2—Earth System configuration (HADGEM2-ES; Jones et al. 2011), Geophysical Fluid Dynamics Laboratory Earth System Model version 2M (GFDL-ESM-2M; Dunne et al. 2013). These ESMs are described in detail by (Taylor et al. 2012). Note also that these two ESMs were the only available at the time of completion of these simulations and are used to build a multi-model-ensemble (MME). For each ESM forcing, five 20-year downscaling experiments over the whole West African domain including Burkina Faso, as defined by Browne and Sylla (2012), were completed: one historical forced by observed natural and anthropogenic atmospheric composition (2001–2018) and four future (2041–2060 and 2080–2099) under two Representative Concentration Pathway (namely, RCP4.5 and RCP8.5; Moss et al. 2010; Van Vuuren et al. 2011) GHG forcing scenarios from the IPCC. These two periods have been choosen thanks to the AR5 IPCC (2014) recommendations for hydroclimatic changes assessment and are referred as near future (NF) and far future (FF) as in Sylla et al. (2018) – keeping in mind that changes in different GHGs in all the RCP scenarios start from the 2040s. RCP4.5 emission scenario represents a medium-level GHG concentration forcing scenario (Thomson et al. 2011), while RCP8.5 is a high forcing scenario (Riahi et al. 2011). For each period and each forcing, multimodel ensemble means are performed. The historical simulations

performed in this thesis have been validated previously for the whole West Africa domain by Sylla et al. (2018).

3.3 Methods

3.3.1 Evaluation of ISBA land surface model

In this thesis, the performance of ISBA LSM is investigated indirectly i.e. through assessing the quality of its atmospheric forcings (ERA5 and ERA-Interim here). This will ultimately (in the second specifc objective of the thesis) allow to evaluate the ability of LDAS-Monde to provide improved land surface states. To this end, we will focus on precipitation and radiation variables, which are among the most important variables controlling the ISBA model quality as atmospheric forcings (Albergel et al. 2017).

Firstly, both precipitation and incoming shortwave radiation (SW_{in}) variables from ERA-Interim and ERA5 reanalyses will be assessed against in situ measurements. Then, ISBA is driven by both ERA5 and ERA-Interim reanalyses, with all atmospheric variables interpolated at a spatial resolution of 0.25° × 0.25° and 0.5° × 0.5°, respectively. In order to drive the model to the equilibrium state, the first year (2001) is spun-up 20 times for both the ERA5 and ERA-Interim configurations. It is the same framework as used in Albergel et al., (2017). The experiment covers the period of 2001–June 2018.

A 10,000 samples bootstrapping is used to determine the 95% confidence interval of the median from the precipitation reanalyses. For the evaluation of both precipitation and SW_{in} from ERA5 and ERA-Interim reanalyses, the 2010–2016 period and the year of 2017 are considered, respectively.

Note that the same evaluation techniques are used for both the ISBA simulations (called openloop) and the estimates from LDAS-Monde (called analysis) against satellite datasets.

3.3.2 Evaluation strategies

3.3.2.1 Scores

Performance metrics are used in order to assess the performance of the assimilation system to better improve the representation of LSVs. They are used as in the following:

- (i) to evaluate ERA-Interim and ERA5 reanalyses against ground-based data.
- (ii) to assess the quality and ability of LDAS-Monde to represent the land surface

conditions. For that, four metrics were used to compare the satellite products (sat) with the model simulations or analyses (mod):

- Correlation Coefficient (CC)
- Bias
- Standard Deviation of Differences (SDD)
- unbiased Root Mean Square Difference RMSD (ubRMSD)

These quantities are defined as:

$$CC = \frac{\sum_{k=1}^{N}(sat_k - \overline{sat})(\mathrm{mod}_k - \overline{\mathrm{mod}})}{\sqrt{\sum_{k=1}^{N}(sat_k - \overline{sat})^2 \sum_{k=1}^{N}(\mathrm{mod}_k - \overline{\mathrm{mod}})^2}} \quad \text{(Equation 4.1)}$$

$$\text{With } \overline{sat} = \frac{1}{N}\sum_{k=1}^{N} sat_k \text{ and } \overline{\mathrm{mod}} = \frac{1}{N}\sum_{k=1}^{N} \mathrm{mod}_k$$

$$Bias = \frac{1}{N}\sum_{k=1}^{N}(\mathrm{mod}_k - sat_k) \quad \text{(Equation 4.2)}$$

$$SDD = \sqrt{\frac{1}{N}\sum_{k=1}^{N}(\mathrm{mod}_k - sat_k - Bias)^2} \quad \text{(Equation 4.3)}$$

$$RMSD = \sqrt{\frac{1}{N}\sum_{k=1}^{N}(\mathrm{mod}_k - sat_k)^2} \quad \text{(Equation 4.4)}$$

N represents the number of gridded observations, equal to the number of different gridded model estimates) used in the calculation of the scores at several dates.

It is also worhtnoting that the ubRMSD means RMSD with biases being removed.

4.3.2.2 Increments and sensitivity analysis of the assimilation

Increments are defined by Equation (2) in Barbu et al. (2014). They correspond to the difference between the analyzed variables (i.e. after the assimilation of satellite observations) and the model prediction (prior the assimilation):

$$\Delta x = \mathrm{K}[y^0 - \mathrm{H}(x)] \quad \text{(Equation 4.5)}$$

where x is the state vector (RZSM and LAI), y^0 the observation vector (SSM and LAI), H is the linearized observation operator, and **K** is the Kalman gain. The $y = H(x)$ term represents the model counterpart (SSM and LAI) of the observations.

The increments on the state variables impact several key variables such as the carbon (photosynthesis through Gross Primary Production (GPP), and water (evapotranspiration (ET), drainage) fluxes.

In order to assess the sensitivity of the the analysis to the observations, it is required to compute the Jacobian of the observation operator. It is calculated using finite differences obtained by perturbed model runs over 24-h assimilation windows. For a given grid point and vegetation patch, each control variable requires a perturbed model run obtained by initializing ISBA with the initial state perturbed for the selected control variable (0.1% typically, see Albergel et al., (2017).

3.3.3 Climate change projections

In order to address future water availability issues for Burkina Faso under climate change, we investigate to what extent anthropogenic climate change modifies the hydroclimatology of the country. This will be done using signal change method (future – present). Specifically, we examine how different RCP forcings impact evapotranspiration, atmospheric water demand, surface runoff, and ultimately, the aridity of the region for the near future (2041–2060) and by the end of the twenty first century (2080–2099). The atmospheric water demand is calculated as potential evapotranspiration (PE) using the method developed by Hamon (1963) through this formula:

$$\mathrm{PE} = 715.5\Omega \frac{e^*(\mathrm{T_m})}{(\mathrm{T_m}+273.2)} \qquad \text{(Equation 4.6)}$$

where Ω is daylength (fraction of day), Tm is the mean monthly temperature (°C). $e^*(\mathrm{T_m})$ is the saturation vapor pressure (kPa) at the temperature T(°C) and is given by:

$$e^*(\mathrm{T_m}) = 0.611 * \ln \frac{17.67/\mathrm{T_m}}{(\mathrm{T_m}+243.5)} \qquad \text{(Equation 4.7)}$$

The aridity index used in this thesis is based on the one devised in Thornthwaite and Mather (1955) and modified by Willmott and Feddema (1992). The aridity index (Im) is described as follows:

$$\mathrm{I_m} = \frac{\mathrm{P}}{\mathrm{PE}} - 1 \text{ for } \mathrm{P} < \mathrm{PE} \qquad \text{(Equation 4.8)}$$

$$I_m = 1 - \frac{PE}{P} \text{ for } P > PE \quad \text{(Equation 4.9)}$$

$$I_m = 0 \text{ for } P = PE \quad \text{(Equation 4.10)}$$

where P is the total annual precipitation and PE is the total annual potential evapotranspiration. The Im values range from −1 to +1 (see Table 3.1), where a value of 0 indicates that the annual moisture supply (P) is equal to the annual moisture demand (PE).

Table 3.1: Description of moisture index and the corresponding aridity types from Feddema (2005).

Aridity Classification	
Aridity Type	**Moisture Index**
Saturated	0.66 – 1.00
Wet	0.33 – 0.66
Moist	0.00 – 0.33
Dry	-0.33 – 0.00
Semi-arid	-0.66 – -0.33
Arid	-1.00 – -0.66

3.3.4. Conclusion of the chapter

This chapter presented the different datasets in this thesis: the in-situ data, the remote sensing data of vegetation and soil moisture, the atmospheric reanalysis ERA-Interim and ERA5 as well as the LSM ISBA and the land data assimilation system LDAS-Monde implemented to improve the representation of LSVs. It is further highlighted the RCM simulations used to assess future climate change impacts on key water-related parameters. Methodological tools include the data assimilation technique used, evaluation stratetgies and finally hydroclimatic change signals assessment. All of these materials and methods are used throughout the next chapters.

Chapter 4. Evaluation of ISBA model and assessment of LDAS-Monde reanalysis*

**Present results published in Tall et al. (2019):*

Tall, M.; Albergel, C.; Bonan, B.; Zheng, Y.; Guichard, F.; Dramé, M.S.; Gaye, A.T.; Sintondji, L.O.; Hountondji, F.C.C.; Nikiema, P.M.; Calvet, J. Towards a Long-Term Reanalysis of Land Surface Variables over Western Africa: LDAS-Monde Applied over Burkina Faso from 2001 to 2018. Remote Sens. *2019,* 11*, 735.*

The objective of this Chapter is to provide results largely based on the implementation of ISBA LSM and LDAS-Monde system over Burkina Faso. It first assesses the validation of the atmospheric reanalysis, which is considered as an indirect evaluation of ISBA model capability to yield past conditions of LSVs. Then, results about the performance of LDAS-Monde are provided. More specifically, this meant to:

- assess the quality of the forcing datasets i.e. ERA5 and ERA-Interim reanalyses using in situ observations spanning over Burkina Faso;
- set up ISBA model over Burkina Faso;
- evaluate LDAS-Monde simulated LAI and soil moisture against their observed satellite products through the application of relevant statistical metrics;
- and evaluate LDAS-Monde against independent datasets for fluxes like evapotranspiration and gross primary production.

4.1. Validation of ISBA: Performance evaluation of the latest ECMWF atmospheric forcings

4.1.1. ERA5 and ERA-Interim reanalyses validation

- **Precipitation**

In the preliminary tasks i.e. before running ISBA model, we assesssed the quality of ECMWF reanalysis (ERA5 and ERA-Interim) that are used to force the land data assimilation system. To that end, we used in situ data of precipitation and incoming solar radiation (Sw_{in}) as explained in Section 3.1 for the validation.

Statistical metrics for 2010–2016 daily precipitation from ERA5 and ERA-Interim compared to 134 gauge stations spanning all over Burkina Faso are presented in Table 4.1. The Median R, ubRMSD, bias, and RMSD values for the total monthly precipitation time series considered their 95% confidence level are 0.82 ± 0.009, 52.02 ± 1.390 mm/month, − 15.00 ± 3.270 mm/month, and 56.15 ± 3.600 mm/month for ERA5, and 0.77 ± 0.010, 58.44 ± 1.420 mm/month, − 19.85 ± 3.770 mm/month, and 63.89 ± 3.250 mm/month for ERA-Interim. These previous findings have indicated a better performance with ERA5 reanalysis in representing precipitation variability than ERA-Interim. ERA5 performs better than ERA-Interim for 84% of the precipitation gauging stations for R values, 89% for ubRMSD values, 83% for bias values, and 86% for RMSD values. Same conclusions have been illustrated by the maps in Figure 4.1, where triangle (circle) symbols indicate stations where ERA5 performs better (worse) than ERA-Interim in terms of R (Figure 4.1a) and ubRMSD (Figure 4.1b). In the two maps of Figure 4.1, triangle symbols dominate indicating that ERA5 precipitation reanalyses demonstrate a better quality i.e. are in better agreement with in situ observations than ERA-Interim over Burkina Faso. Overall, the better performance of ERA5 with regard to ERA-Interim is likely due to an improved representation of convective precipitation in the tropical region (Bechtold, 2016) and to the larger number of assimilated data; it is also possibly related to its higher spatial resolution.

Table 4.1: *Comparison of precipitation (P) and incoming solar radiation (SWin) forcing with in situ observations for ERA5 and ERA-Interim over the period of 2010–2016 (based on monthly sum). Scores are given for significant correlations with p-values < 0.05.*

.	Median R[1], 95 % confidence interval[2] (% of stations for which this configuration is the best)	Median ubRMSD[1] on precipitation time series (in mm/month) and incoming solar radiation (in W/m^2), 95 % confidence interval[2] (% of stations for which this configuration is the best)	Median Bias[1] on precipitation time series (in mm/month) and incoming solar radiation (in W/m^2), 95% confidence interval[2] (% of stations for which this configuration is better)	Median RMSD[1] on precipitation time series (in mm/month) and incoming solar radiation (in W/m^2), 95% confidence interval[2] (% of stations for which this configuration is better)
ERA5 (P)	0.82 ± 0.009 (84 %)	52.02 ± 1.39 (89 %)	-15.00 ± 3.27 (83%)	56.15 ± 3.60 (86%)
ERA-Interim (P)	0.77 ± 0.010 (16 %)	58.44 ± 1.42 (11 %)	-19.85 ± 3.77 (17%)	63.89 ± 3.25 (14%)
ERA5 (SWin)	0.59 ± 0.07 (100%)	36.23 ± 6.48 (100%)	19.40 ± 32.43 (100%)	42.24 ± 21.76 (100%)
ERAI (SWin)	0.46 ± 0.15 (0%)	41.03 ± 4.22 (0%)	28.12 ± 29.80 (0%)	50.72 ± 18.63 (0%)

[1]Only for stations presenting significant R values on precipitation time series (p-value < 0.05): 134 stations; sample bootstrapping.

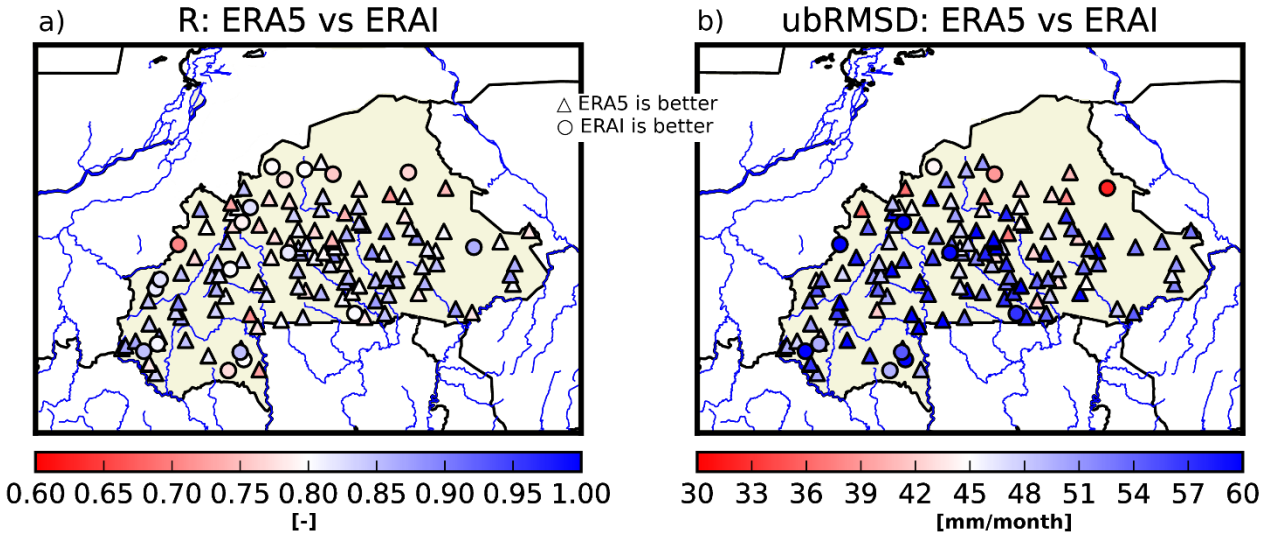

Figure 4.1: *Maps of correlation (R) on precipitation time series (a) and ubRMSD (mm/month) on precipitation time of series (b) between in precipitation situ measurements and both ERA-Interim and ERA5. For each station presenting significant R (p-value < 0.05), the simulation that presents the better R values is presented. Triangle symbols indicate when ERA5 presents the best value and circles when it is ERA-interim.*

- **Incoming solar radiation validation**

The statistical scores for the 2017 daily mean surface SW_{in} from ERA5 and ERA-Interim with respect to four stations (see Figure 4.2) are shown in Table 4.1. Median R, ubRMSD, bias, and RMSD values along with their 95% confidence interval are 0.59 ± 0.070, 36.23 ± 6.480 W/ m^2, 19.40 ± 32.430 W/m^2, and 42.24 ± 21.760 W/m^2 for ERA5, and 0.46 ± 0.150, 41.03 ± 4.220 W/m^2, 28.12 ± 29.800 W/m^2, and 50.72 ± 18.630 W/m^2 for ERA-Interim.

It is highlighted in Figure 4.2 maps of R and ubRMSD values between ERA5 daily mean surface SW_{in} and in situ measurements at four stations (Figure 4.2a,b) as well as their differences against R and ubRMSD values from ERA-Interim (Figure 4.2c,d) over 2017. We can clearly observe from Figure 4.2 higher correlations and lower ubRMSD values for ERA5 with regard to ERA-Interim for the considered four stations. This is consistent with the observed positive correlation differences (ERA5—ERA-Interim, Figure 4.2c) and negative ubRMSD differences (ERA5—ERA-Interim, Figure 4.2).

Figure 4.3 presents the 2017 time series of the daily SW_{in} for ERA-Interim (blue), ERA5 (green), and the in situ observations (red) for Bobo (Figure 4.3a; 11.16°N, 4.30°W) and Dori (Figure 4.3b; 14.03°N, 0.03°W) stations belonging to the SG and SS zones, respectively. At these subtropical sites, the temporal structure of the annual cycle of SW_{in} is strongly shaped by the top-of-the atmosphere incoming radiation, which drives the two well defined maxima of SW_{in} (Guichard et al., 2009; Slingo et al., 2009). At Bobo, they occur in April and October while further North in Dori, the second maximum is less pronounced. Both reanalyses broadly capture these features, even though they tend to overestimate SW_{in} (in particular during the monsoon, when clouds induce sharp drops which can reach more than 100 W/m^2)—a similar bias also noted by Agustí-Panareda et al., (2010) at the relatively close Sahelian site of Niamey. However, this bias is slightly reduced in ERA5. This implies that ERA5 performs better in representing SW_{in} variations than ERA-Interim over Burkina Faso. This better performance of ERA5 can also be probably linked to the implementation of an improved radiation scheme (see Hogan and Bozzo, 2018 for more details).

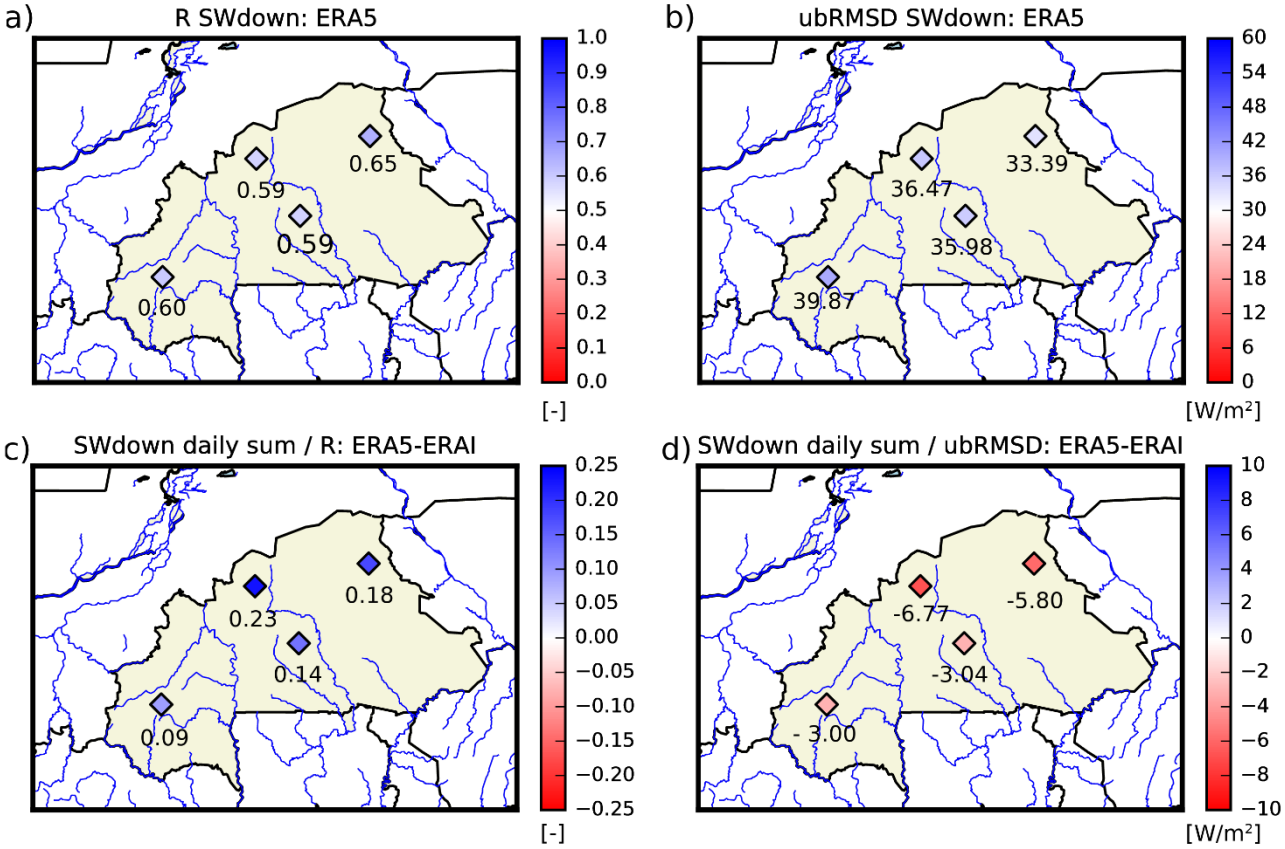

Figure 4.2: *Maps of correlation R (a) and ubRMSD (b) between incoming solar radiation time series from ERA5 and in situ measurements. (c,d) represent the difference between ERA5 and ERA-Interim in correlation and ubRMSD for 2017, respectively. For each station presenting significant R (p values < 0.05), the simulation that presents the better R values is represented.*

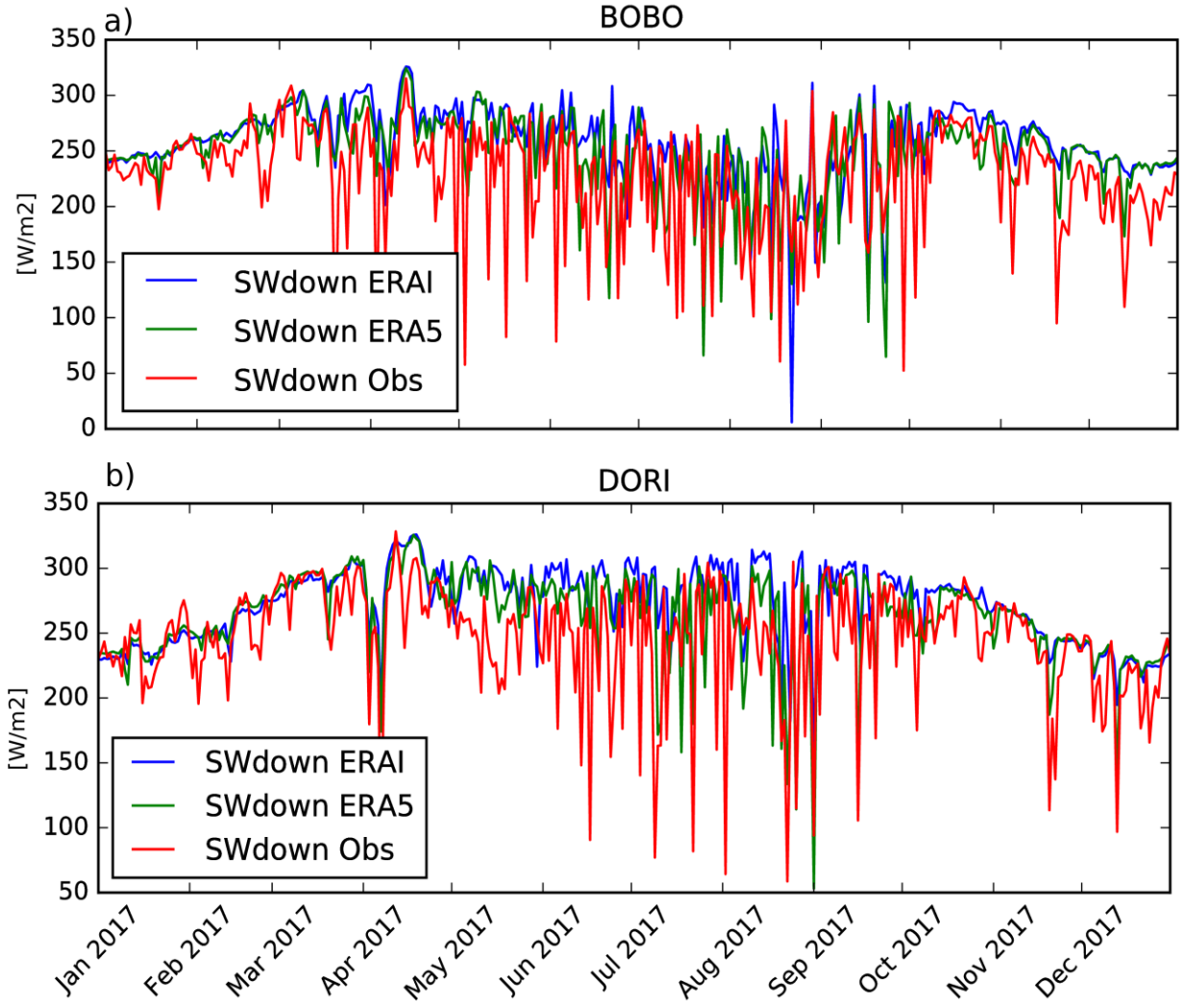

Figure 4.3: *Incoming solar radiation temporal evolution for ERA-Interim, ERA5, and in situ measurements for (a) Dori and (b) Bobo stations for 2017.*

4.2. LDAS-Monde performance evaluation:

In order to obtain the land surface analysis, satellite derived observations are combined with the model simulations through the above-mentioned data assimilation technique. In doing that, the resulting analysis is expected to be closer to the assimilated observations (LAI and SSM) than the open-loop (i.e., model with no assimilation).

4.2.1 LDAS-Monde performance evaluation:

- **Results for LAI**

From the joint assimilation of LAI and SSM, a largest impact is observed for LAI. Figure 4.4 shows maps of the monthly average values of precipitation from ERA5 as well as

LAI from the LDAS-ERA5 openloop, the observations, LDAS-ERA5 analysis, and the difference between the analysis and the openloop. Observations indicate a sharp jump of LAI in April, very likely in response to the increase of soil moisture availability due to the start of the rainy season. However, an increase in LAI is also observed earlier in the SG region (southern part of the domain) from February to May; i.e., before the first rains. Interestingly, this peculiar behaviour would be consistent with findings from in situ studies from Shackleton et al. 1999; Seghieri et al. 2009; Awessou et al. 2017; which point to some tree species that put on leaves before the first rains of the season. This functioning does not appear to be linked to soil moisture (Peugeot, C.;, 2018). It could involve rises of the air temperature or humidity, though the precise mechanisms at play are still unknown. In any case, this process is not represented in the ISBA LSM, leading to a temporal shift of two to three months in the leaf onset and an underestimation of the observed LAI.

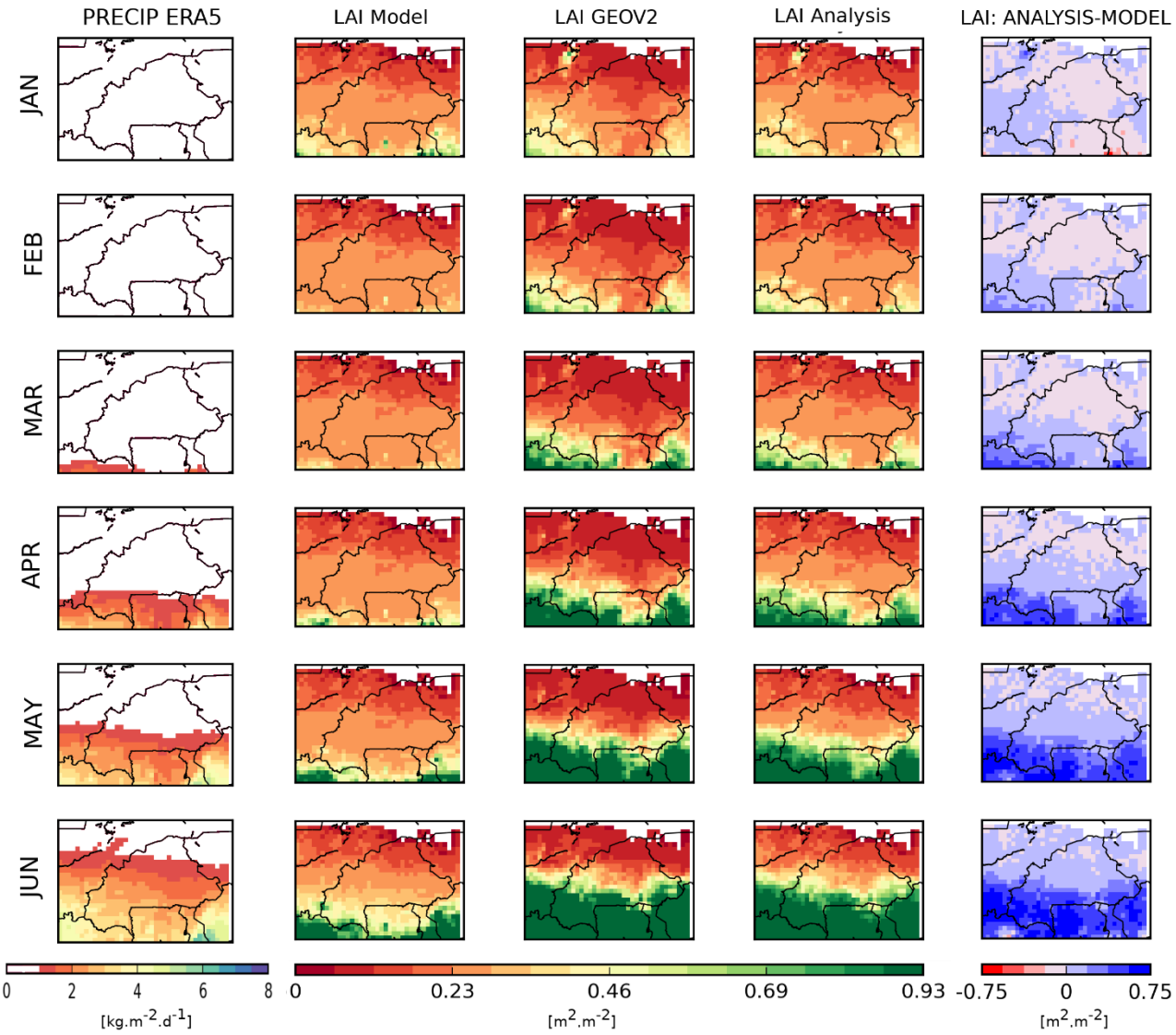

Figure 4.4: *Seasonal average (from January to June) maps of precipitation [kg·m^{-2}·d^{-1}] and LAI [m^2·m^{-2}] over January 2001 to June 2018. From left to right: precipitation, LAI model, LAI analysis, LAI analysis-model difference. The latter column shows the impact of assimilating LAI and SWI on the simulated LAI. LDAS-ERA5 configuration is used.*

Figure 4.4 also shows little impact of the assimilation on the estimated LAI where observations are below 0.4 $m^2 \cdot m^{-2}$. This is due to a limitation of the ISBA LSM. As mentioned in section 3.2.2 of chapter 3, a minimum LAI threshold is prescribed to 0.3 $m^2 \cdot m^{-2}$ for every vegetation type (except coniferous forests) in ISBA. To satisfy that threshold, we force the SEKF to reset every LAI estimate below 0.3 $m^2 \cdot m^{-2}$ to that value, thus limiting the impact of assimilation.

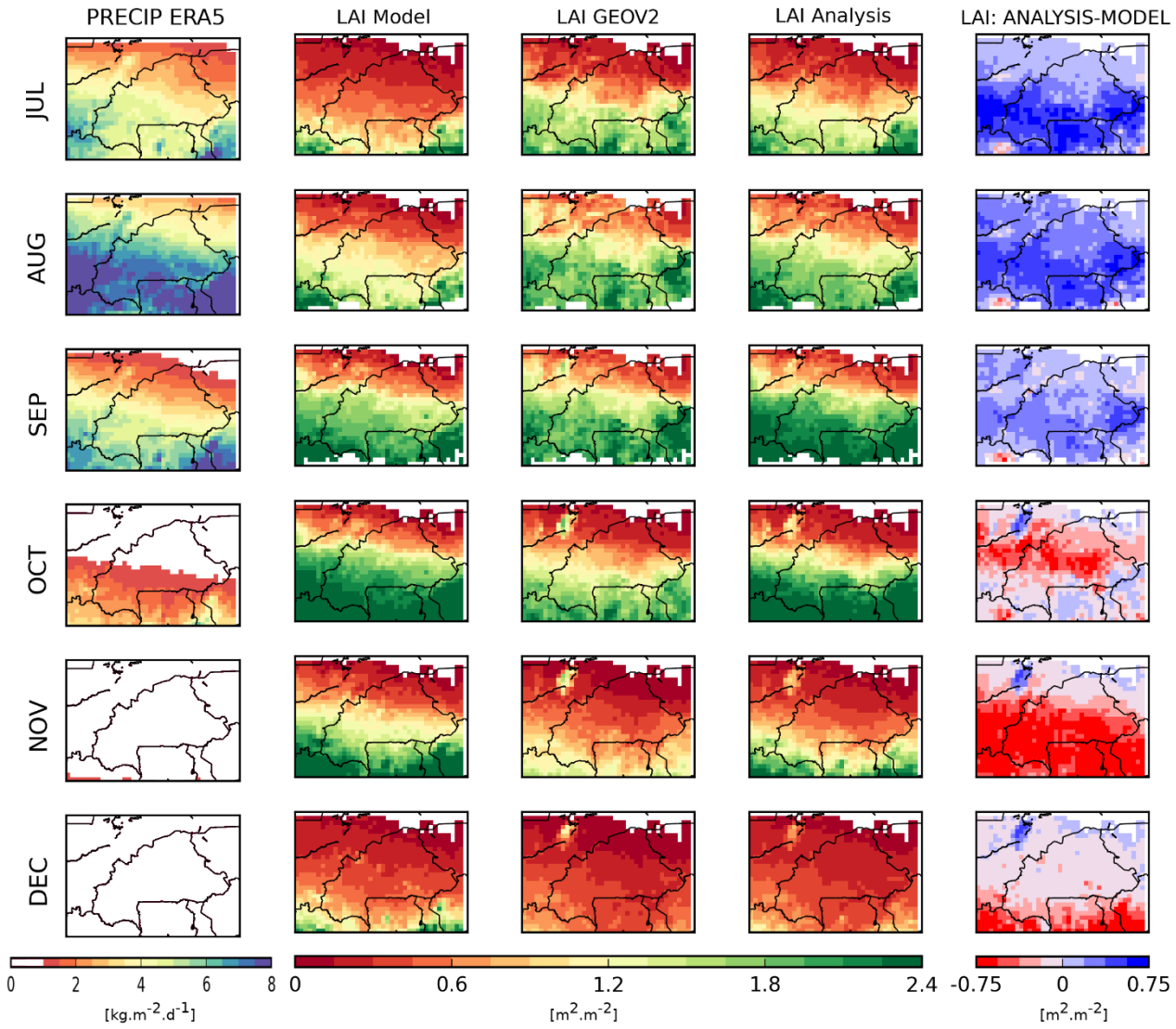

Figure 4.5: *Seasonal average (from July to December) maps of precipitation [kg·m^{-2}·d^{-1}] and LAI [m^2·m^{-2}] over January 2001 to June 2018. From left to right: precipitation, LAI model, LAI analysis, LAI analysis-model difference. The latter column shows the impact of assimilating LAI and SWI on the simulated LAI. LDAS-ERA5 configuration is used.*

The analysis is efficient at compensating for these two model caveats, as shown in Figure 4.4 and Figure 4.5. This is also clear in Figure 4.6, which shows the LDAS-ERA5 configuration LAI monthly mean time series averaged values over the whole domain for January 2001 to June 2018. Observations indicate interannual fluctuations in the yearly maximum of LAI, with, for instance, higher values in 2003, 2010, and 2012 (see Figure A.1 and A.2 in Annexes) and lower values (see Figure A.1, A.2 and A.3 in Annexes) in 2002, 2011, and 2017 (consistent with Kergoat et al., 2017; Pierre et al., 2016). Beyond differences in the structure of their annual cycles, the model and the analysis both capture part of this interannual variability, which is quite interesting to note.

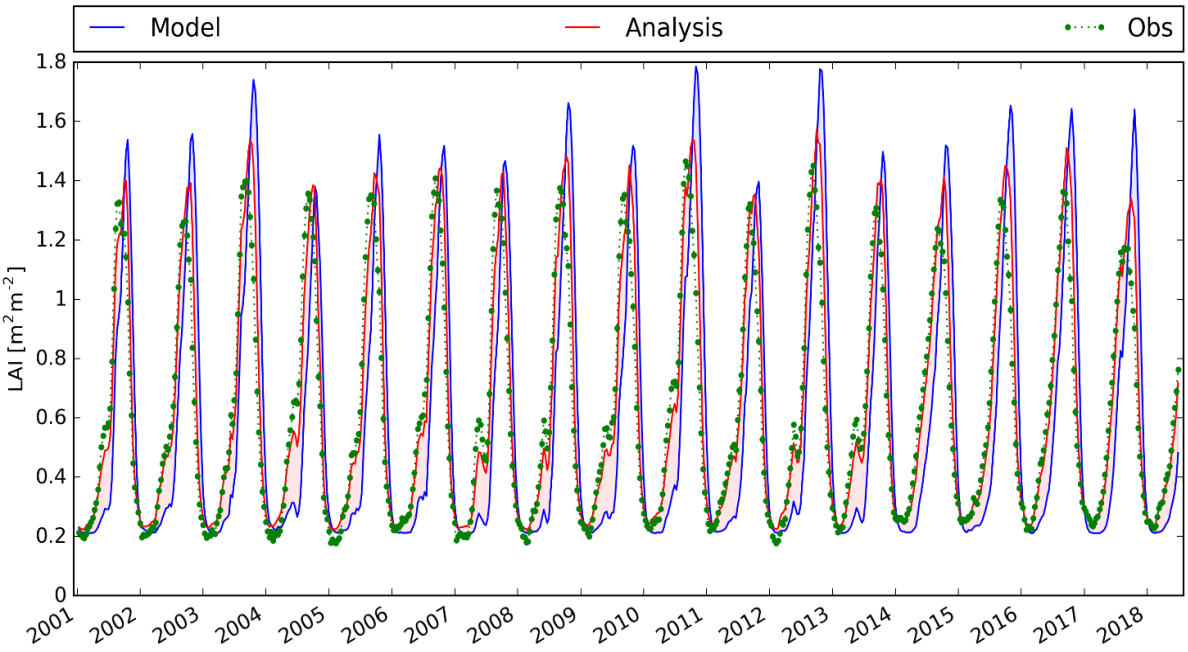

Figure 4.6: *Monthly average values of LAI from 1 January 2001 to June 2018: model (blue line), satellite product (green circles), analysis (red line) in the LDAS-ERA5 configuration.*

The improved annual cycle of LAI provided by the analysis is associated with a higher correlation and a positive impact on the SDD, Bias, and RMSD scores over the study region in all months (as seen on Figure 4.7; Table 4.2). It is also visible that the analyses add skill to both configurations, LDAS-ERA5 and LDAS-ERAI, which indicates the healthy behavior from the land data assimilation system.

Table 4.2: *LAI Seasonal scores (SDD; Correlation; bias; RMSD) for the model and the analysis over January 2001 to June 2018.*

Period	Version	Bias	Correlation	RMSD	SDD
JAN	Model	0.014	0.670	0.112	0.111
JAN	Analysis	0.017	0.929	0.051	0.048
FEB	Model	-0.009	0.665	0.118	0.117
FEB	Analysis	0.018	0.913	0.070	0.067
MAR	Model	-0.053	0.647	0.208	0.202
MAR	Analysis	0.004	0.928	0.104	0.104
APR	Model	-0.135	0.717	0.337	0.309
APR	Analysis	-0.025	0.952	0.152	0.150
MAY	Model	-0.233	0.765	0.458	0.395
MAY	Analysis	-0.057	0.964	0.193	0.184
JUN	Model	-0.272	0.771	0.483	0.399
JUN	Analysis	-0.065	0.963	0.190	0.178
JUL	Model	-0.370	0.795	0.543	0.398
JUL	Analysis	-0.103	0.947	0.233	0.209
AUG	Model	-0.428	0.841	0.556	0.356
AUG	Analysis	-0.124	0.934	0.270	0.240
SEP	Model	-0.096	0.882	0.370	0.357
SEP	Analysis	0.076	0.951	0.269	0.258
OCT	Model	0.479	0.897	0.658	0.451
OCT	Analysis	0.296	0.972	0.451	0.340
NOV	Model	0.601	0.886	0.846	0.596
NOV	Analysis	0.167	0.955	0.352	0.310
DEC	Model	0.193	0.756	0.452	0.409
DEC	Analysis	0.028	0.930	0.093	0.088

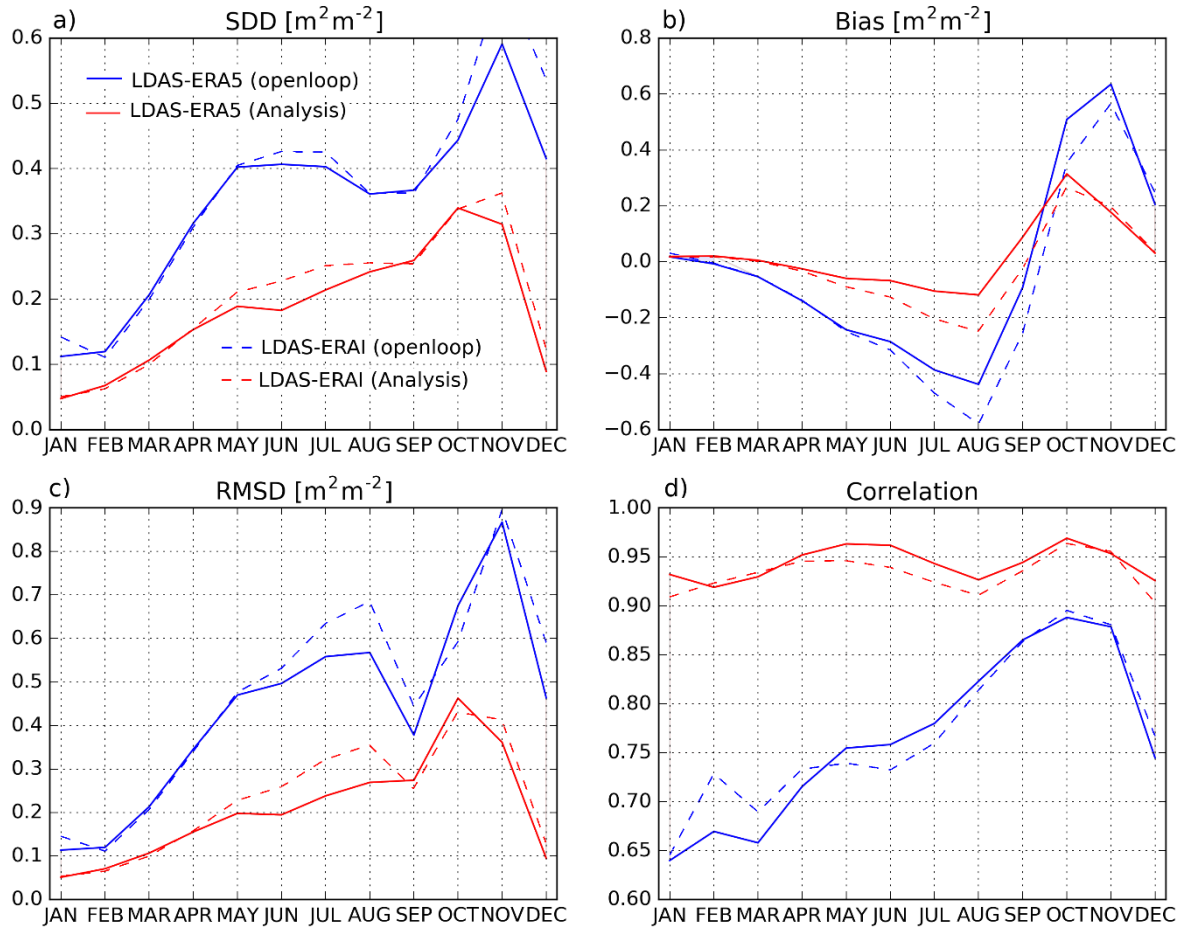

Figure 4.7: *Seasonal (a) SDD (b) bias (c) RMSD and (d) correlation between LAI from either LDAS-ERA5 (solid lines) or LDAS-ERAI (dashed lines) model (blue) and analysis (red) and observed LAI over January 2001 to June 2018.*

Considering now the three climatic regions of Burkina Faso, it appears that the correlation between the analyzed and observed LAI is lower during the rainy season in the SG region while it is higher in the SS and SH regions (see analysis in Figure 4.8; Figure 4.9b for the LDAS-ERA5 configuration).

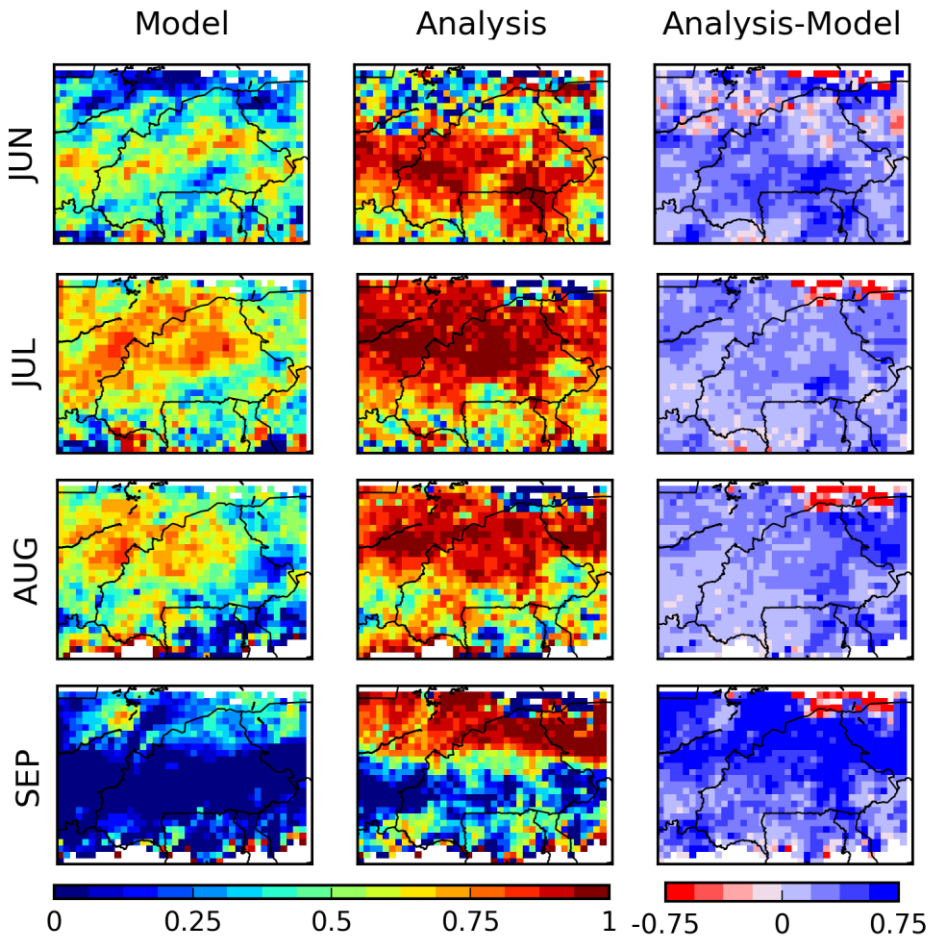

Figure 4.8: *JJAS Seasonal correlation of LAI (model, analysis and their difference) over January 2001 to June 2018 for the LDAS-ERA5 configuration.*

This reduction of R values in the analysis during the rainy season in the SG region could be related to a decrease in the number of the observed LAI linked to cloud cover (see Table 4.3). Overall, the assimilation corrects the model seasonal responses by increasing the LAI during the rainy season and decreasing (Figure 4.10) the LAI after the rainy season, especially in the Sudanian region (SS and SG regions).

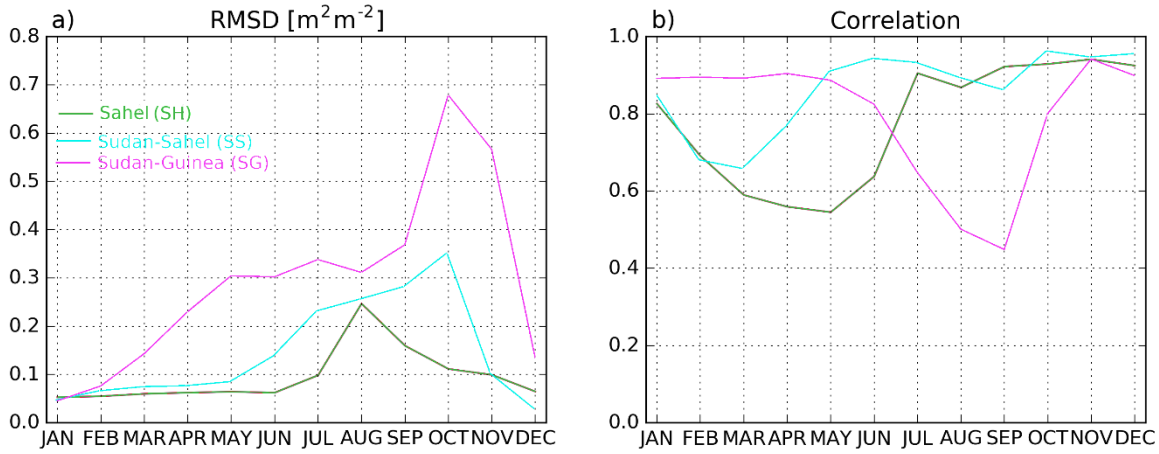

Figure 4.9: *Seasonal (a) RMSD and (b) correlation of LAI analysis when compared to the observations considering the three climatic regions (SH, SS, and SG) over January 2001 to June 2018 for the LDAS-ERA5 configuration.*

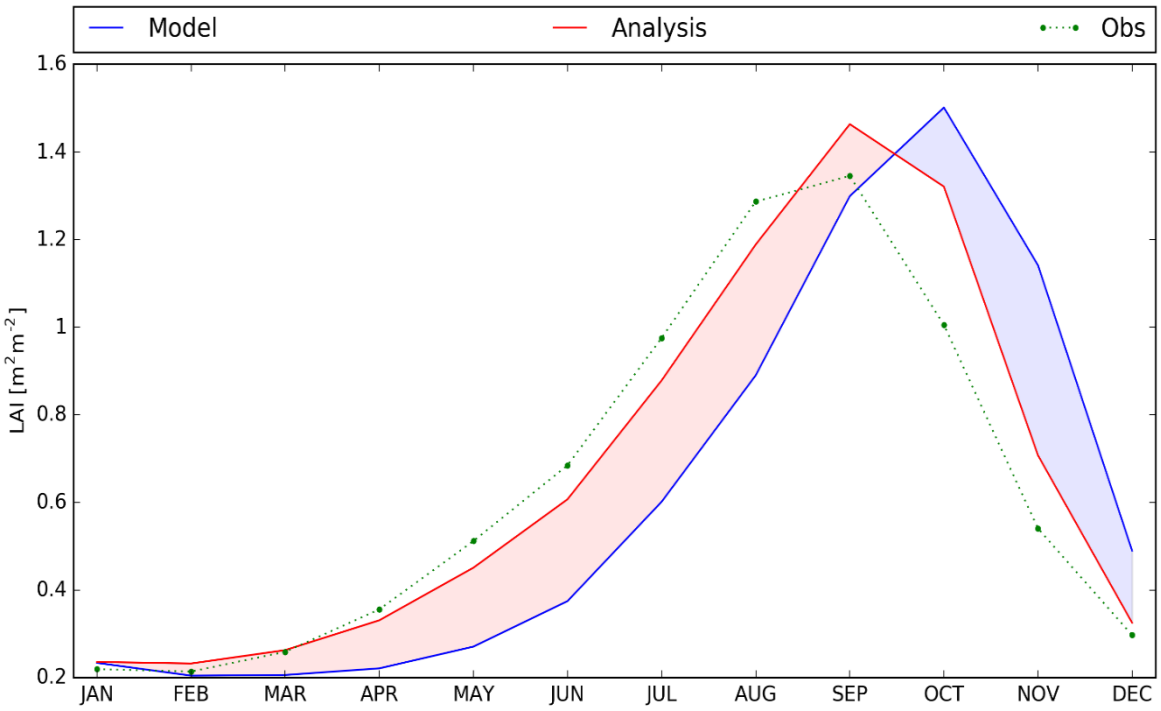

Figure 4.10: *Seasonal values of LAI for the observations (green), the model (blue) and the analysis (red).*

Table 4.3: Seasonal number of LAI values (N) from 1 January 2001 to 30 June 2018 for the LDAS-ERA5 configuration.

	Jan	Feb	Mar	Apr	May	Jun	Jul	Aug	Sep	Oct	Nov	Dec
Burkina Faso	59724	59723	59724	59715	58914	53840	48140	48006	46022	54265	56406	56406
SH	18684	18683	18684	18679	18674	18678	17638	17644	17646	17646	17646	17646
SS	19440	19440	19440	19440	19440	19440	18334	18357	18319	18360	18360	18360
SD	21600	21600	21600	21596	20800	15722	12168	12005	10057	18259	20400	20400

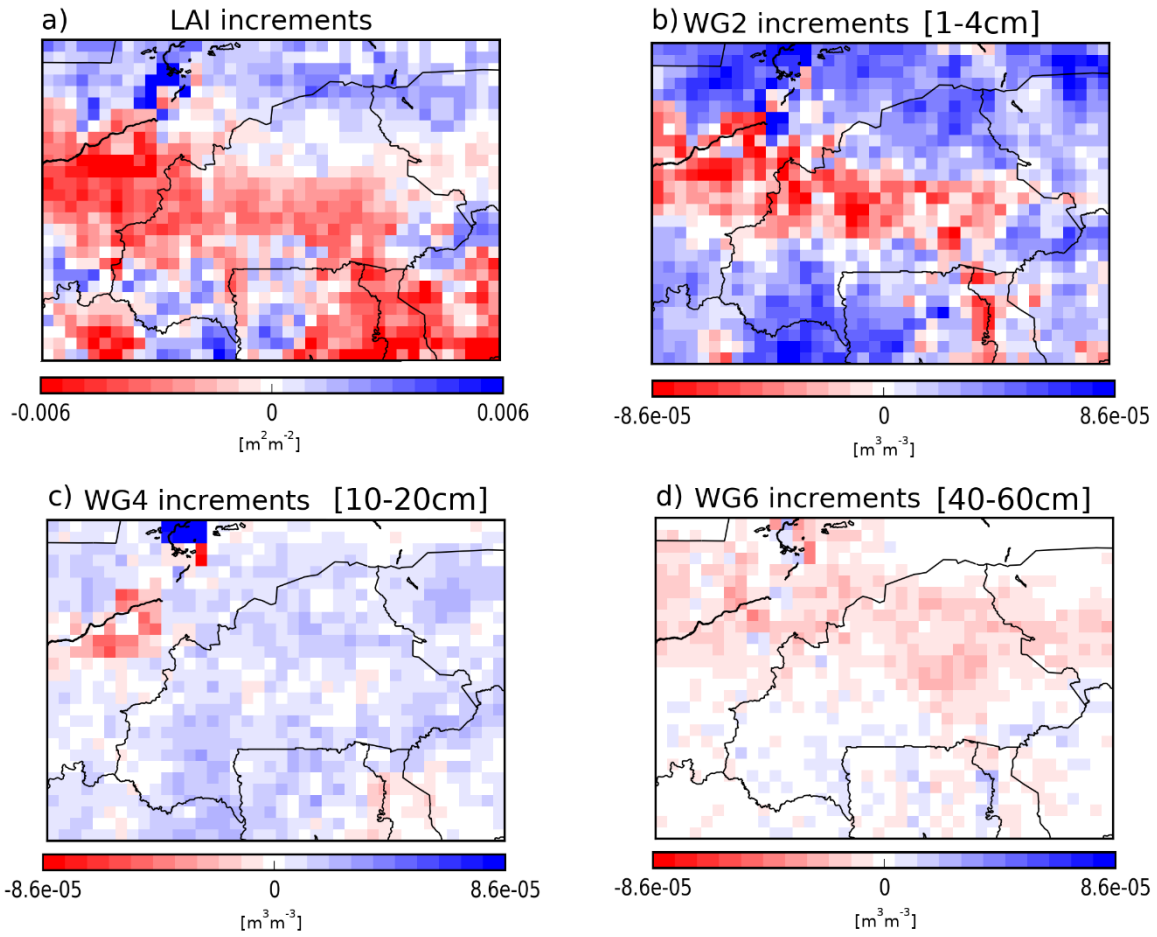

Figure 4.11: *Averaged analysis increments for January 2001 to June 2018. Four control variables are illustrated: (a) leaf area index and soil moisture in (b) the second (WG2, 1–4 cm), (c) fourth (WG4, 10–20 cm), and (d) sixth (WG6, 40–60 cm) layer of soil for the LDAS-ERA5 configuration.*

- **Results for soil Moisture**

Comparatively to the assimilation impact on LAI, simulated SSM present lower improvements after assimilation. As mentioned above, the impact of assimilation on SSM is relatively weaker than on LAI. In fact, the assimilation does not appear to importantly impact the openloop (see seasonal cycle of SSM for the model and the LDAS-ERA5; Figure 4.12).

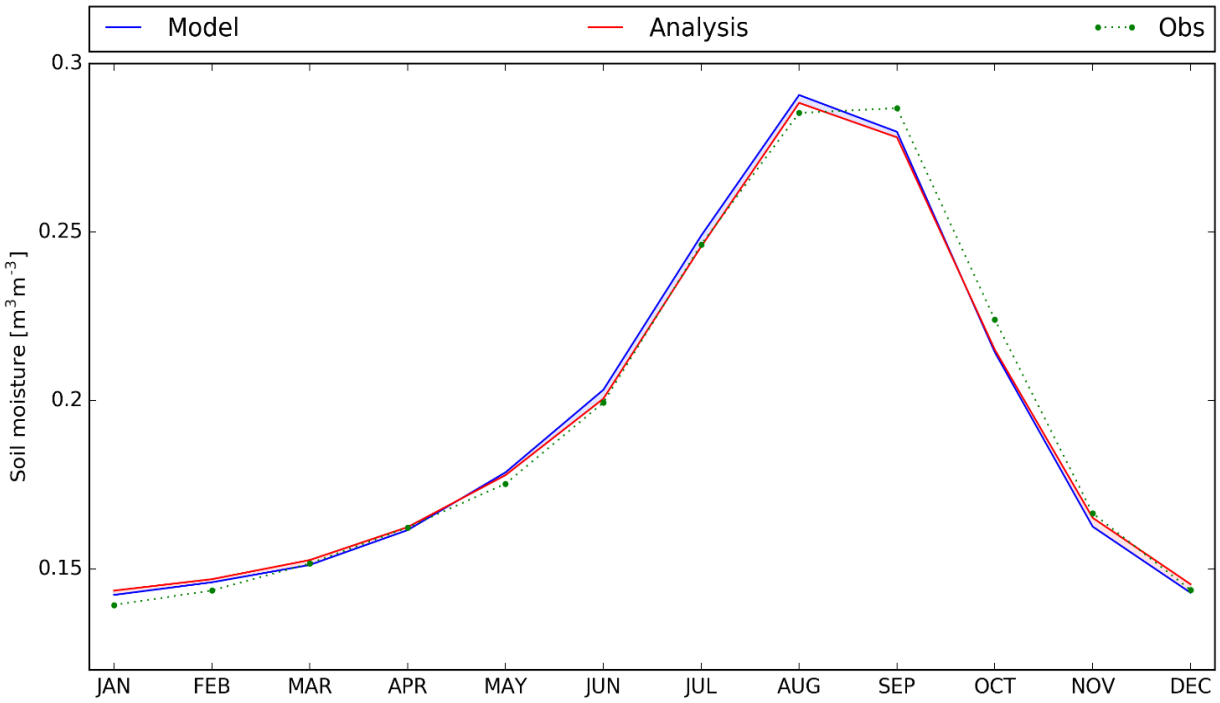

Figure 4.12: *Seasonal values of SSM for the CGLS observations (green), the model (blue) and the LDAS-ERA5 analysis (red).*

This has a consequence on statistical metrics, for instance, in Figure 4.13a, which shows the correlation values between SSM from the openloop and the analysis (for both LDAS-ERA5 and LDAS-ERAI configurations) and the SSM estimates from CGLS. Note that the seasonality effect has been removed through the use of the anomaly time series in order to assess the shorter-term variability of soil moisture. Figure 4.13a indicates a positive impact of the assimilation especially from January to May and from October to December regarding the model, emphasizing the improvement in SSM values. The impact of the assimilation on the representation of the shorter-term soil moisture variability is further presented using maps of the anomaly correlations between soil moisture before and after assimilation against ASCAT SSM estimates (Figure 4.13b,c); as well as using their correlation differences (Figure 4.13d) for the LDAS-ERA5 configuration. It is evident from Figure 4.13c that the analysis improves soil moisture simulations (see Table 4.4) over the whole domain with a more pronounced impact over the Sudanian region, i.e., SH and SG (Figure 4.13c).

Table 4.4: *SSM Seasonal scores (Bias, Correlation, RMSD, SDD) for the model and the analysis over January 2001 to June 2018.*

Period	Version	Bias	Correlation	RMSD	SDD
JAN	Model	0.001	0.967	0.011	0.011
JAN	Analysis	0.003	0.980	0.009	0.009
FEB	Model	0.001	0.951	0.015	0.015
FEB	Analysis	0.002	0.965	0.013	0.013
MAR	Model	-0.001	0.923	0.021	0.021
MAR	Analysis	0.001	0.941	0.018	0.018
APR	Model	0.001	0.914	0.026	0.026
APR	Analysis	0.002	0.926	0.024	0.024
MAY	Model	0.002	0.894	0.033	0.033
MAY	Analysis	0.002	0.900	0.032	0.031
JUN	Model	0.006	0.912	0.035	0.035
JUN	Analysis	0.004	0.912	0.035	0.034
JUL	Model	0.003	0.908	0.037	0.037
JUL	Analysis	0.000	0.905	0.037	0.037
AUG	Model	0.006	0.919	0.033	0.033
AUG	Analysis	0.004	0.919	0.033	0.033
SEP	Model	-0.009	0.936	0.032	0.031
SEP	Analysis	-0.010	0.939	0.032	0.030
OCT	Model	-0.012	0.949	0.028	0.025
OCT	Analysis	-0.010	0.959	0.025	0.023
NOV	Model	-0.004	0.947	0.017	0.017
NOV	Analysis	-0.001	0.962	0.014	0.014
DEC	Model	-0.002	0.966	0.011	0.010
DEC	Analysis	0.001	0.982	0.008	0.008

Looking at the correlation differences based on the anomaly time series (Figure 4.13d), it is evident that positive values dominate, especially in the SH and SS regions, along with a rather neutral effect in the southern part of the domain.

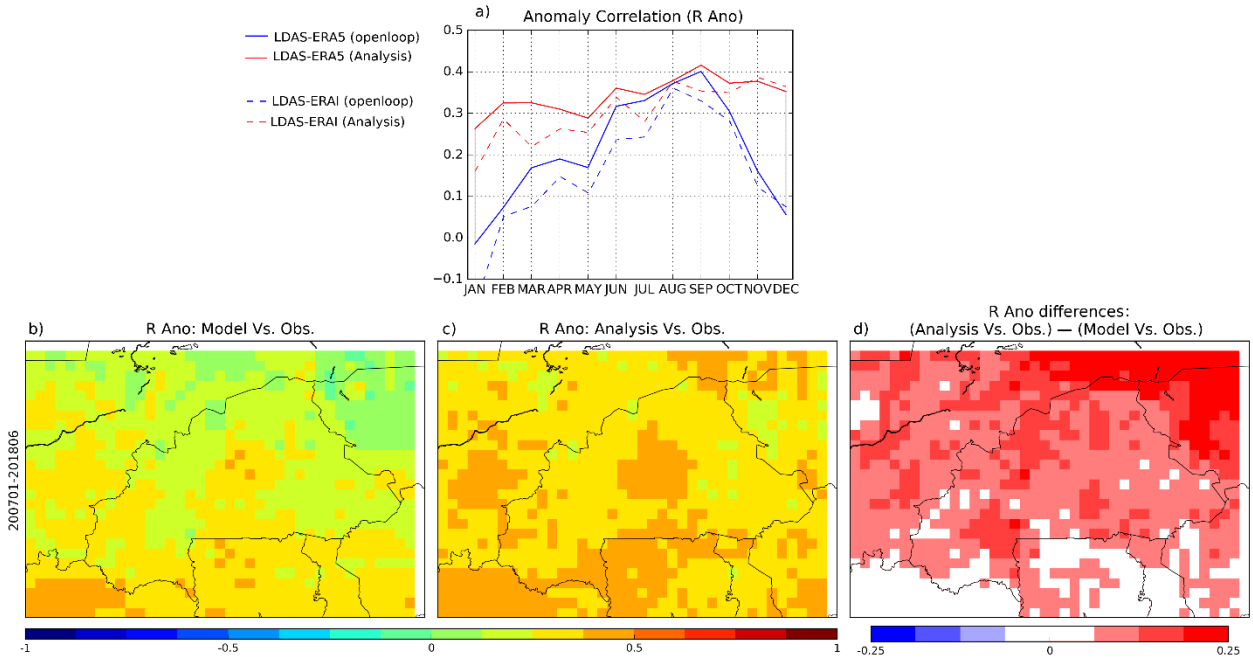

Figure 4.13: *Seasonal correlations for (a) anomaly time series between SSM estimates from the CGLS project and SSM from the second layer of soil of ISBA LSM (in blue) and the assimilation (in red) over the period of 2007–06/2018 for both the LDAS-ERA5 and LDAS-ERAI configurations. (b,c) Maps of the anomaly correlation between SSM of the model, the analysis, and the SSM estimates from CGLS, respectively, (d) map of the correlation differences. (a–c) are for the LDAS-ERA5 configuration.*

4.2.3. LDAS-Monde Impact

- **Model sensitivity to the observations**

Jacobian operators are used to assess model sensitivity to the observations used. In fact, Jacobians are governed by the physics of the model and their examination is crucial to understand the data assimilation system performances (Albergel et al., 2017; Barbu et al., 2011; Fairbairn et al., 2017; Rüdiger, C., Albergel, C., Mahfouf, J.-F., Calvet, J.-C., and Walker, J. P., 2010). Mean Jacobians values over January 2010 to June 2018 for the whole domain of Burkina-Faso are presented in Table 4.5.

Table 4.5: *Mean Jacobians values for the eight control variables considered in this study over the whole spatial domain for January 2001 to June 2018.*

Jan. 2001-Jun. 2018	$\frac{\partial SSM}{\partial LAI}$	$\frac{\partial SSM}{\partial w_2}$ 1-4 cm	$\frac{\partial SSM}{\partial w_3}$ 4-10 cm	$\frac{\partial SSM}{\partial w_4}$ 10-20 cm	$\frac{\partial SSM}{\partial w_5}$ 20-40 cm	$\frac{\partial SSM}{\partial w_6}$ 40-60 cm	$\frac{\partial SSM}{\partial w_7}$ 60-80 cm	$\frac{\partial SSM}{\partial w_8}$ 80-100 cm
Mean	-0.0006	**0.5372**	**0.2033**	0.0818	0.0441	0.0142	0.0049	0.0020
	$\frac{\partial LAI}{\partial LAI}$	$\frac{\partial LAI}{\partial w_2}$ 1-4 cm	$\frac{\partial LAI}{\partial w_3}$ 4-10 cm	$\frac{\partial LAI}{\partial w_4}$ 10-20 cm	$\frac{\partial LAI}{\partial w_5}$ 20-40 cm	$\frac{\partial LAI}{\partial w_6}$ 40-60 cm	$\frac{\partial LAI}{\partial w_7}$ 60-80 cm	$\frac{\partial LAI}{\partial w_8}$ 80-100 cm
Mean	**0.2578**	0.0134	0.0223	**0.0432**	**0.0911**	**0.0522**	0.0318	0.0188

Table 4.5 top row represents the impact of perturbating individually each control variables of LDAS-Monde (LAI, soil moisture from layers 2 to 8), by a (positive) small amount at the beginning of an assimilation window, on the model equivalent of SSM at the end of the assimilation window (i.e. 24 hours later). The model equivalent of SSM being the second layer of soil (w_2 between 1 and 4 cm depth), it is expected that the sensitivity of SSM to changes in soil moisture of that layer ($\frac{\partial SSM}{\partial w_2}$) will be higher compared to those of the other layers of soil ($\frac{\partial SSM}{\partial w_3}$ to $\frac{\partial SSM}{\partial w_8}$). As seen on Table 4.5, the mean Jacobian value is clearly higher for w_2 than for any other layers. The model sensitivity to SSM decreases with depth suggesting that the assimilation of SSM will be more effective in modifying soil moisture from the first layers than the deeper layers. Over Burkina Faso, mean Jacobian values with respect to SSM observations (Table 4.5, top rows) range from 0.5372 to 0.0020 for layers w_2 to w_8, respectively and is –0.0006 for LAI ($\frac{\partial SSM}{\partial LAI}$). This negative value indicates that a small positive increments of LAI will generally lead to a decrease of SSM (w_2).

Table 4.5, bottom row, show the same for LAI: sensitivity of LAI to changes in LAI ($\frac{\partial LAI}{\partial LAI}$) and in soil moisture ($\frac{\partial LAI}{\partial w_2}$ to $\frac{\partial LAI}{\partial w_8}$), from left to right, respectively. Sensitivity of LAI and in soil moisture suggests that control variables related to soil moisture will also be impacted by the assimilation of LAI. Table 4.5 also illustrates that the assimilation of LAI will be more effective in modifying soil moisture from layers 4 to 6 than from the surface layers.

Figure 4.14 illustrates the seasonal cycles of the Jacobians averaged over January 2001 to June 2018. For sake of clarity, only $\frac{\partial LAI}{\partial LAI}$, $\frac{\partial SSM}{\partial w_2}$, $\frac{\partial SSM}{\partial w_4}$, $\frac{\partial SSM}{\partial w_6}$ and $\frac{\partial SSM}{\partial w_8}$ are presented. Looking at the SSM Jacobians, the depth impact already highlighted by Table 4.5 is visible (i.e, less sensitivity to surface soil moisture at deeper layers than at upper layers). From Figure 4.14, a seasonal impact is also visible, $\frac{\partial SSM}{\partial w_2}$ are higher in winter months than in summer months, suggesting that LDAS-Monde will be more efficient assimilating SSM during winter months. Similarly, from $\frac{\partial LAI}{\partial LAI}$ one may notice a dual seasonal cycle, LDAS-Monde will be more efficient assimilating LAI during April to June, October to November.

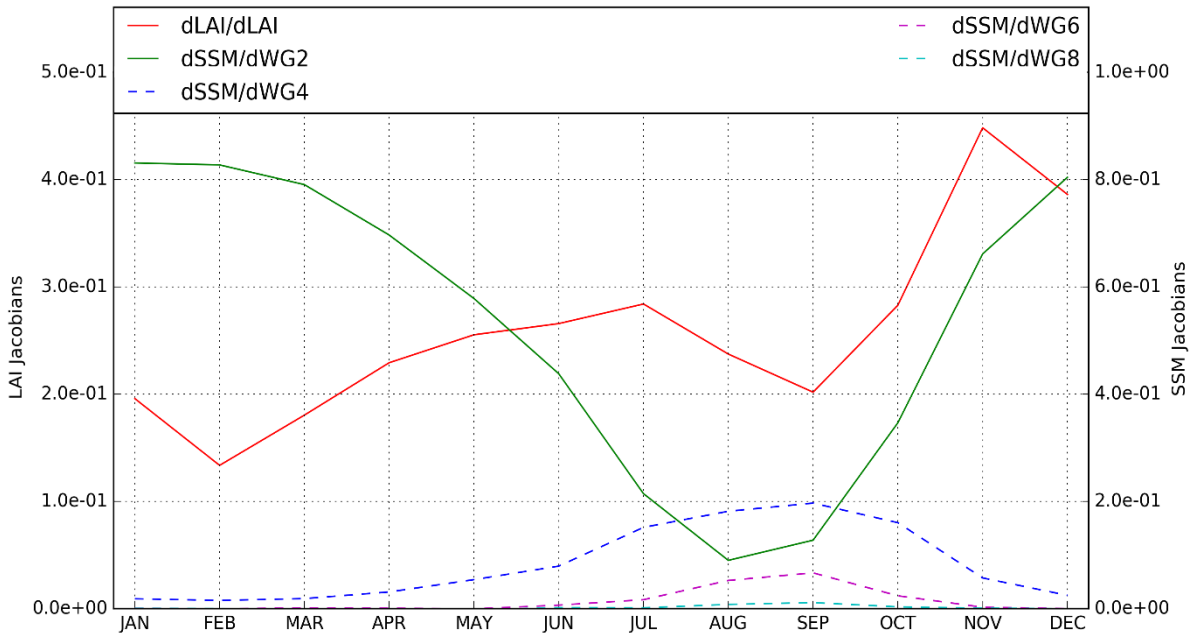

Figure 4.14: *Seasonal evolution of LDAS-ERA5 Jacobians averaged over January 2001 to June 2018.*

It is worth mentioning that the configuration where ERA5 is used to force LDAS-Monde was considered to present the Jacobians evaluation.

4.2.4 LDAS-Monde performance: evaluation using Independent datasets

For evapotranspiration and Gross Primary Production (GPP), seasonal scores (RMSD and R values in Figure 4.15) are computed for the model and for the analysis in both the LDAS-ERA5 and LDAS-ERAI configurations. Only vegetated grid points (>90%) are considered. After the joint assimilation of SSM and LAI, a small positive impact on evapotranspiration is observed for the correlations, as found in Barbu et al., (2011), and it is interesting to note a small degradation of the RMSD values in the second part of the year (August to December).

However, there is a clear improvement in GPP in terms of the RMSD and R scores, especially from January to August (Figure 4.15c,d). While the impact on R values of the analysis is equally distributed over the domain for both evapotranspiration and GPP, a larger (positive) impact on RMSD values is found on the southern part of the domain (not shown). This is in agreement with the analysis impact on LAI described above. LDAS-ERA5 generally performs better than LDAS-ERAI for both the openloop and the analysis. It is particularly true when considering RMSD values for evapotranspiration (Figure 4.15a).

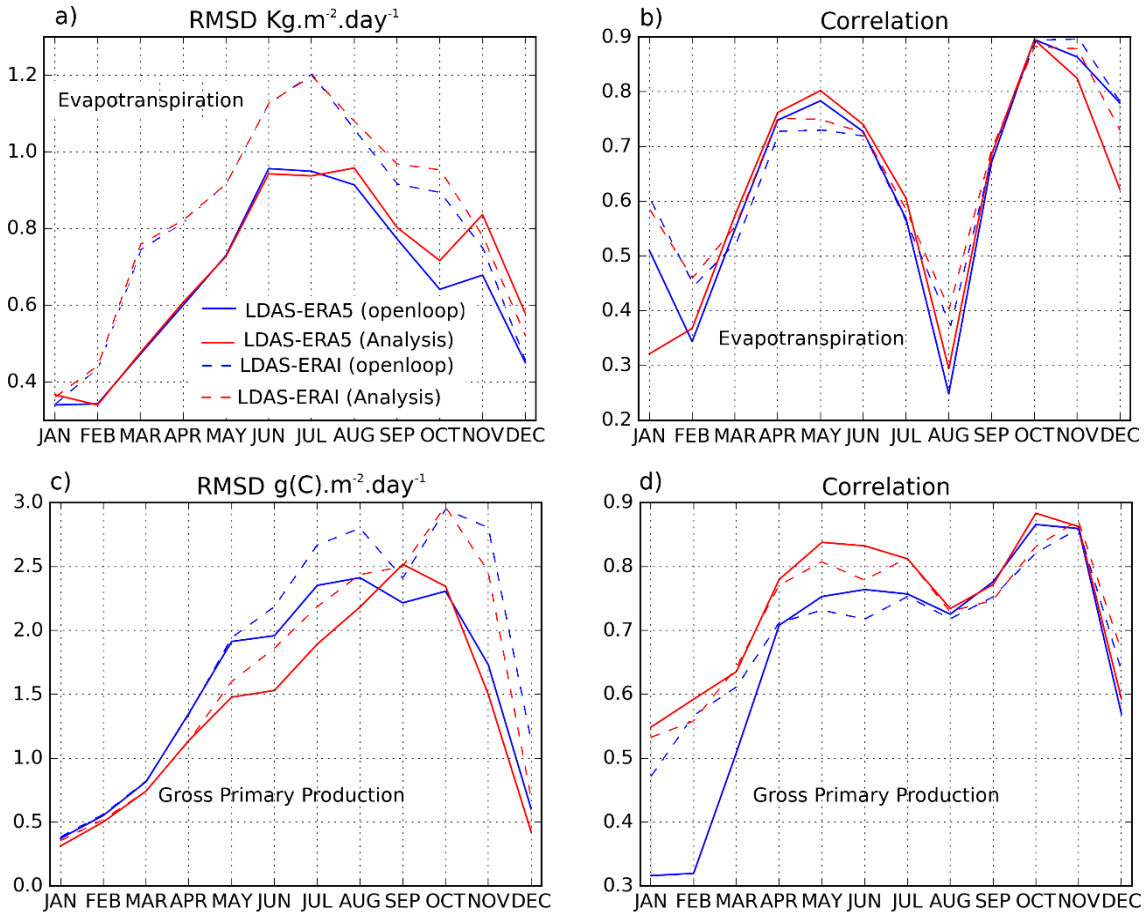

Figure 4.15: *Seasonal evapotranspiration (a,b) and gross primary production (GPP) (c,d) scores when compared to the observations over January 2001 to June 2018.*

Figure 4.15a indicates, however, the degradation of the evapotranspitation estimation by LDAS-ERA5 and LDAS-ERAI when compared to the GLEAM dataset. It is worth noting that the GLEAM dataset is not a direct remotely sensed observation, but rather a remote sensing-based evaporation retrieved model with its own uncertainties. For instance, Pagán et al., (2019) have recently assessed the potential of satellite observations of solar-induced chlorophyll fluorescence (SIF), normalized by photosynthetically-active radiation (PAR), to

diagnose the ratio of transpiration to potential evaporation ("transpiration efficiency") from several state-of-the-art models, including SURFEX and GLEAM. They obtained better results with SURFEX than with GLEAM, in particular during the vegetation decaying phase.

Looking at the seasonal time series of the analysis increments (Figure 4.16 for the LDAS-ERA5 configuration), it is very interesting to notice that the degradation from the analysis over the open-loop (from August in both the LDAS-ERA5 and LDAS-ERAI configuration) corresponds to a sign inversion in the LAI increments (from positive to negative) as well as a sharp positive increase in soil moisture increments (analysis increments of soil moisture from the second (WG2) and fourth (WG4) layer of soil are presented). This situation in the vegetation decaying period seems conflictual and may suggest a lack of consistency between the two observation types (LAI and SSM), leading to the observed degradation in RMSD values.

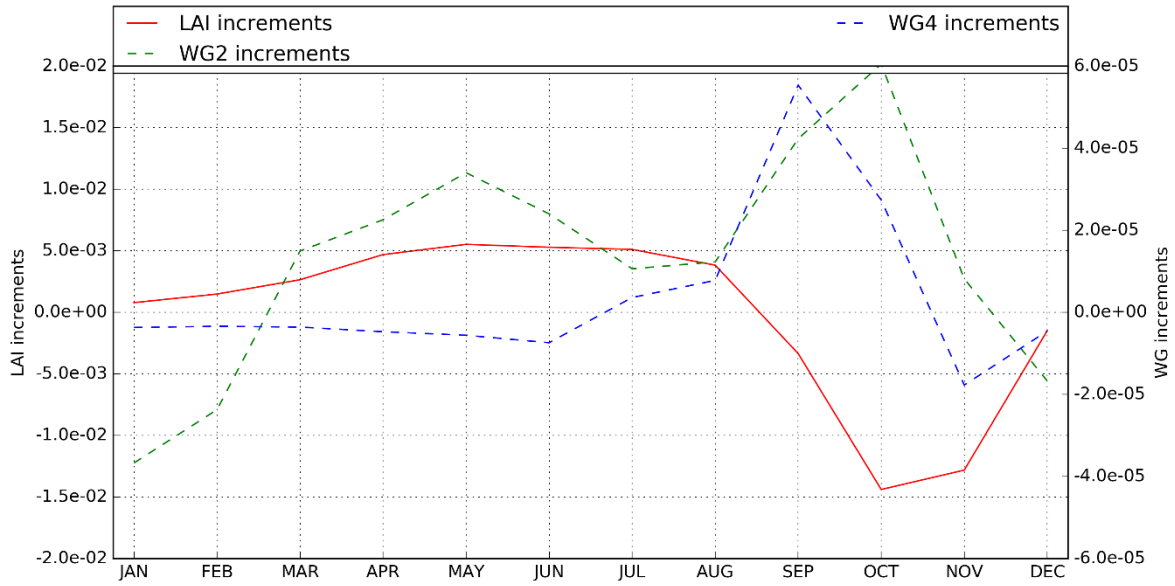

Figure 4.16: *Seasonal evolution of LDAS-ERA5 analysis increments averaged over January 2001 to June 2018 for three control variables: LAI, and soil moisture from the second (WG2) and fourth (WG4) layer of soil.*

For SIF, seasonal scores (R values in Figure 4.17) comparing the observed SIF and simulated GPP for vegetated grid points are computed for model and analysis estimates in both the LDAS-ERA5 and LDAS-ERAI configurations. A positive impact of data assimilation on R can be seen from January to August with an averaged improvement of 0.1 on R for both configurations. For the rest of the year, the impact is rather neutral. Using ERA5 or ERA-Interim as atmospheric forcing does not have much influence on R. This was also the case for

FLUXCOM GPP in Figure 4.15. This is due to a diminished impact of atmospheric forcing on the modelled GPP. The positive impact is of the same scale for the three agroclimatic areas covering Burkina Faso (not shown). This is consistent with what was observed for correlations between simulated GPP and the FLUXCOM dataset.

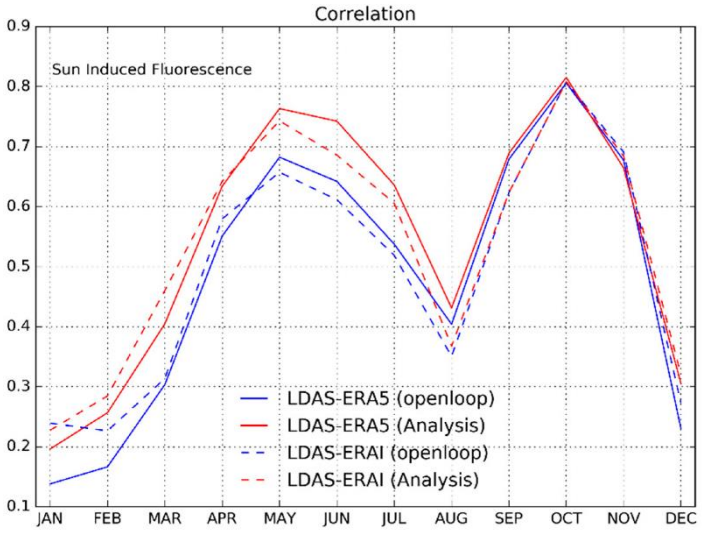

Figure 4.17: *Seasonal correlation between GOME-2 sun-induced fluorescence and simulated GPP covering the period of 2010–2016.*

4.3 Partial conclusion

This chapter focused on the evaluation of ISBA and the capacity of LDAS-Monde to provide an improved reanalysis of historical land surface conditions through the joint assimilation of satellite-derived soil moisture and vegetation products over Burkina Faso in western Africa. The ISBA LDAS-Monde offline system was forced by both ERA5 new atmospheric reanalysis and ERA-Interim former atmospheric reanalysis, leading to a 0.25° × 0.25° and a 0.5° × 0.5° spatial resolution reanalyses. The quality of ERA5 with respect to the former ERA-Interim reanalysis was evaluated using (i) in situ measurements of precipitation and incoming solar radiation (Sw_{in}) as well as (ii) the output of LDAS-Monde. The comparison of the two atmospheric forcing yields two key results: ERA5 provides substantial improvements compared to ERA-interim for precipitation (over 2010–2016), and also for the SW_{in} variable (over 2017). Using ERA5 and ERA-Interim to force the ISBA LSM (open-loop) provides a good model first guess, e.g., on the LAI variable with an advantage to ERA5. However, comparing the open-loop with the observed LAI has highlighted the missing processes in the representation of vegetation phenology. The assimilation is able to improve the simulation of both SSM and LAI when using either ERA5 or ERA-Interim, showing that the analyses add

skill to both configurations and indicating the healthy behavior of LDAS-Monde. From the analysis, important improvements in the representation of the LAI, SSM, and GPP variables were obtained with better scores for the analysis than for the model equivalent (open-loop simulation). In particular, the LAI analysis is very good at compensating for caveats, such as the model's failure in capturing leaf onset prior to the first rains for particular plant species.

Chapter 5: Projected changes in the hydroclimatology of Burkina Faso

Burkina Faso is among the sahelian countries, which are well known to be experiencing high water stress and scarcity along with exponential population growth and facing recurrent and localized droughts and increased food shortage (Jenkins et al. 2005). While it is certain that climate change resulting from anthropogenic greenhouse gas (GHG) emissions will occur in Western Sahel and Burkina Faso via an increase in surface temperature and drought conditions (Sylla et al. 2010, 2015a; Diallo et al. 2012, 2016; Mariotti et al. 2014; Mbaye et al. 2015), substantial uncertainty regarding the direction and magnitude on water resources and agriculture remains.

In order to investigate the impact of different anthropogenic climate changes on the hydroclimatology of Burkina Faso, we thus make use of a multimodel ensemble generated from the ICTP Regional Climate Model (RegCM4) simulations. Regional climate models (RCMs) are proven to be particularly valuable in the representation of fine-scale forcing and land surface heterogeneity such as complex topography, coastlines, and land surface variations (Paeth et al. 2005; Rummukainen 2010; Diallo et al. 2014; Sylla et al. 2015b, Torma et al.2015), which are unresolved by the low-resolution earth system models (ESMs) (Sylla et al. 2015a; Diallo et al. 2015). We focus, in particular, on the changes of water-related parameters such as precipitation, evapotranspiration, soil moisture, surface runoff, and aridity to finally discuss potential future water availability and agricultural activities in Burkina Faso.

5.1 Hydroclimatic changes

5.1.1 Temperature

Projected temperature changes over Burkina Faso for the near future and the late twenty-first century for both RCP4.5 and RCP8.5 are presented in Figure 5.1**.** For the near future (Figure 5.1a and Figure 5.1b), the different anthropogenic GHG forcings lead to temperature changes ranging between 1 and 2.5 °C. The magnitudes of the changes are almost uniform for the whole study domain except in the eastern part where the highest values are found in both RCPs and over the Northwestern regions close to Southern Mali where RCP8.5 shows values of around 2.5 °C. The hottest temperatures are however, projected by the end of the twenty-first century where the GHG forcings are maximum. In fact, RCP4.5 results in a temperature rise of

2.5 °C along the southern part of Burkina Faso and 3 °C in the interior of the country while RCP8.5 leads to a substantial increasce in temperature of about 4 to 6.5 °C following a south-north gradient with maximum changes in the north. Therefore, the northern regions of Burkina Faso appear to be more sensitive to global warming. These temperature changes will substantially affect the future atmospheric water demand for the region.

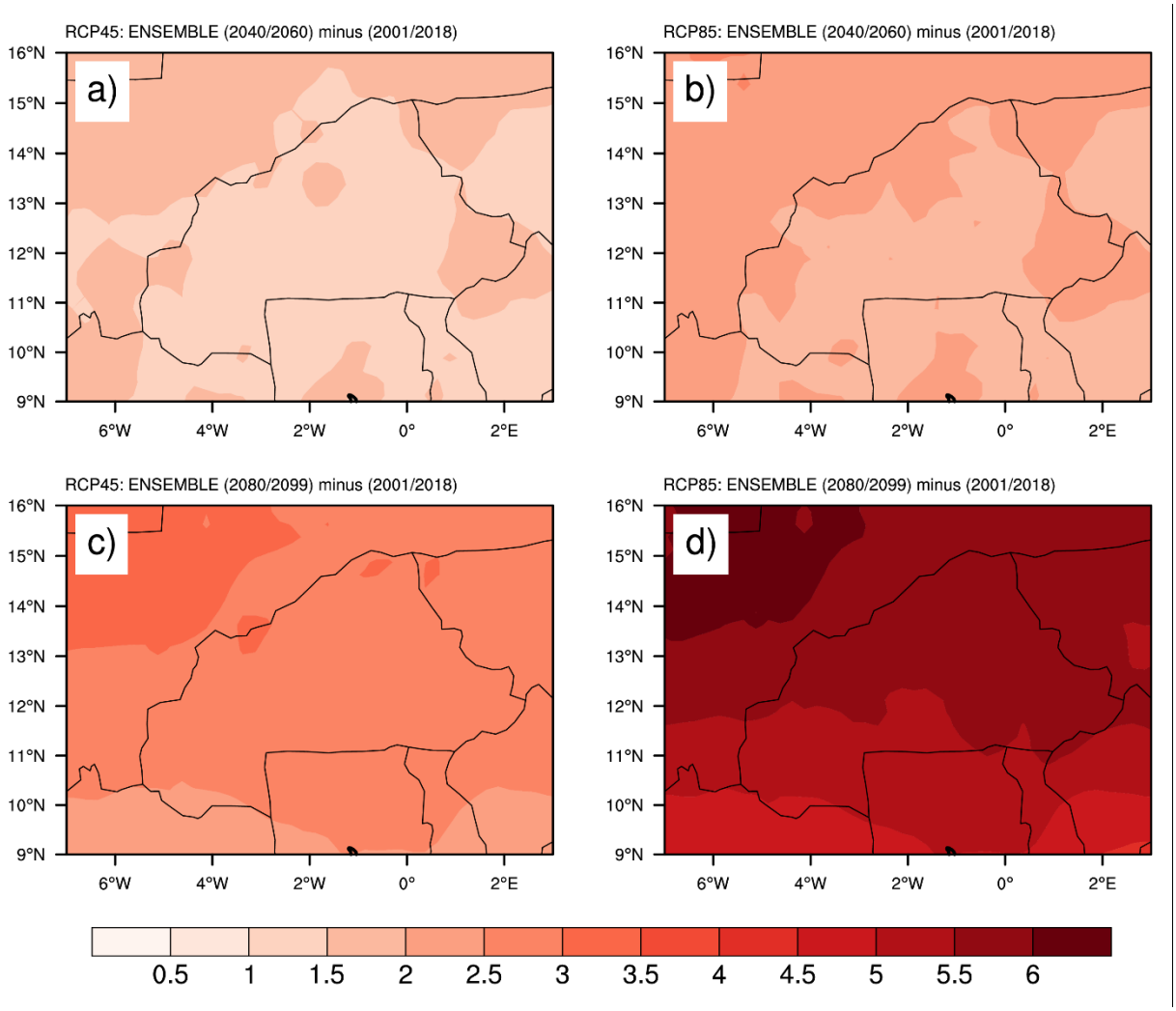

Figure 5.1: *Changes (related to the reference period) in annual mean temperature (in °C) for the near future (2041–2060, upper panels) and the far future (2080–2099, lower panels) and for both RCP4.5 (left panels) and RCP8.5 (right panels).*

5.1.2 Precipitation

Figure 5.2 shows the precipitation changes for the two periods and for both scenarios. The near-future changes reveal an increase ranging between 10 and 50 % in precipitation in most regions of Burkina Faso. The two scenarios almost exhibit the same signal changes, with higher increases in southern part when considering the scenario RCP4.5. The end of the twenty-first century, in turn, experiences precipitation decreases for both scenarios. While in the

RCP4.5, precipitation decrease is quite uniform (more than 20 %) in central and northern regions and smallest (less than 10 %) in the southeast region and with some intermediate magnitudes (between 5 and 10 %) in the central regions, RCP8.5 yields more dryness (up 30 %) generalized all over the western country as a result of stronger long-term GHG forcing. It is thus clear that climate change causes increased precipitation in the near future and decreases in the late twenty-first century, indicating that during the 2050s, the natural variability is predominant while in the 2090s when the GHG forcing is highest, anthropogenic climate change prevails.

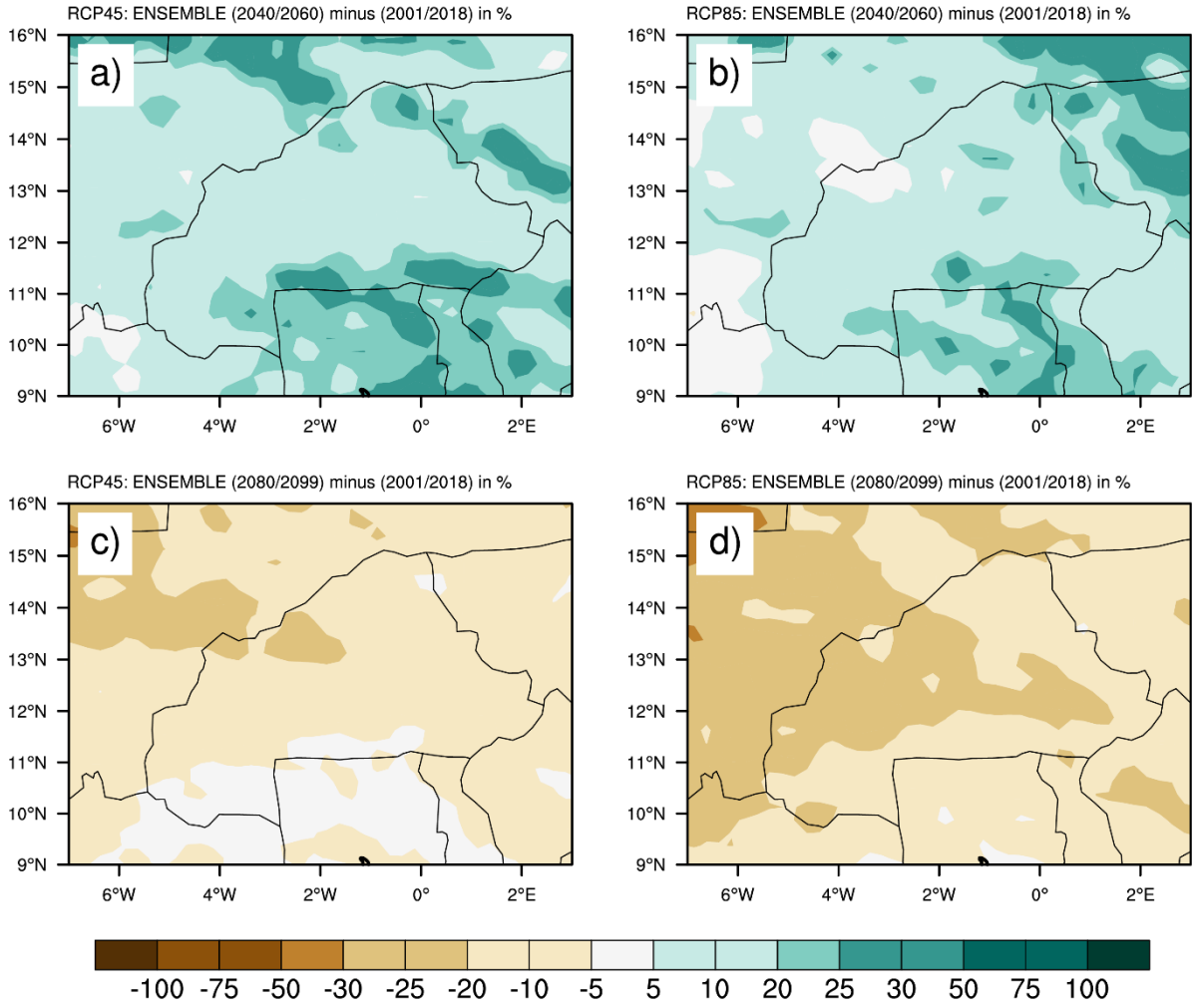

Figure 5.2: *Changes (related to the reference period) in annual mean precipitation (in %) for the near future (2041–2060, upper panels) and the far future (2080–2099, lower panels) and for both RCP4.5 (left panels) and RCP8.5 (right panels).*

5.1.4 Soil Moisture

Mean precipitation changes influence in general those from the soil moisture (Figure 5.3). In fact, for the near future and both RCPs (Figure 5.3a and Figure 5.3b), soil moisture has

a tendency to increase in south-central and eastern regions of Burkina Faso, where projected precipitations are more important, with rather neutral trend in the western country where little increases or dryness occur. For the late twenty-first century (Figure 5.3c and Figure 5.3d), as precipitation decreases, soil moisture also decreases up to maxima of 25 % in the western region of Burkina Faso for RCP4.5. In RCP8.5, as for precipitation, these decreases are more extensive and cover almost the whole Burkina Faso. It is worth mentioning that all simulations use same land use map i.e. not considering the dynamics of vegetation from the historical to the future periods. Therefore, land use changes may affect soil moisture projections in contrasting ways. For example, El-khoury et al. (2015) found that land use changes might control the same water quantity/quality in the same direction as climate change over a Canadian river basin, while Wilson and Weng (2011) found that climate change would have a greater impact that land use changes in the Des Plaines River watershed, Chicago Metropolitan Area, Illinois.

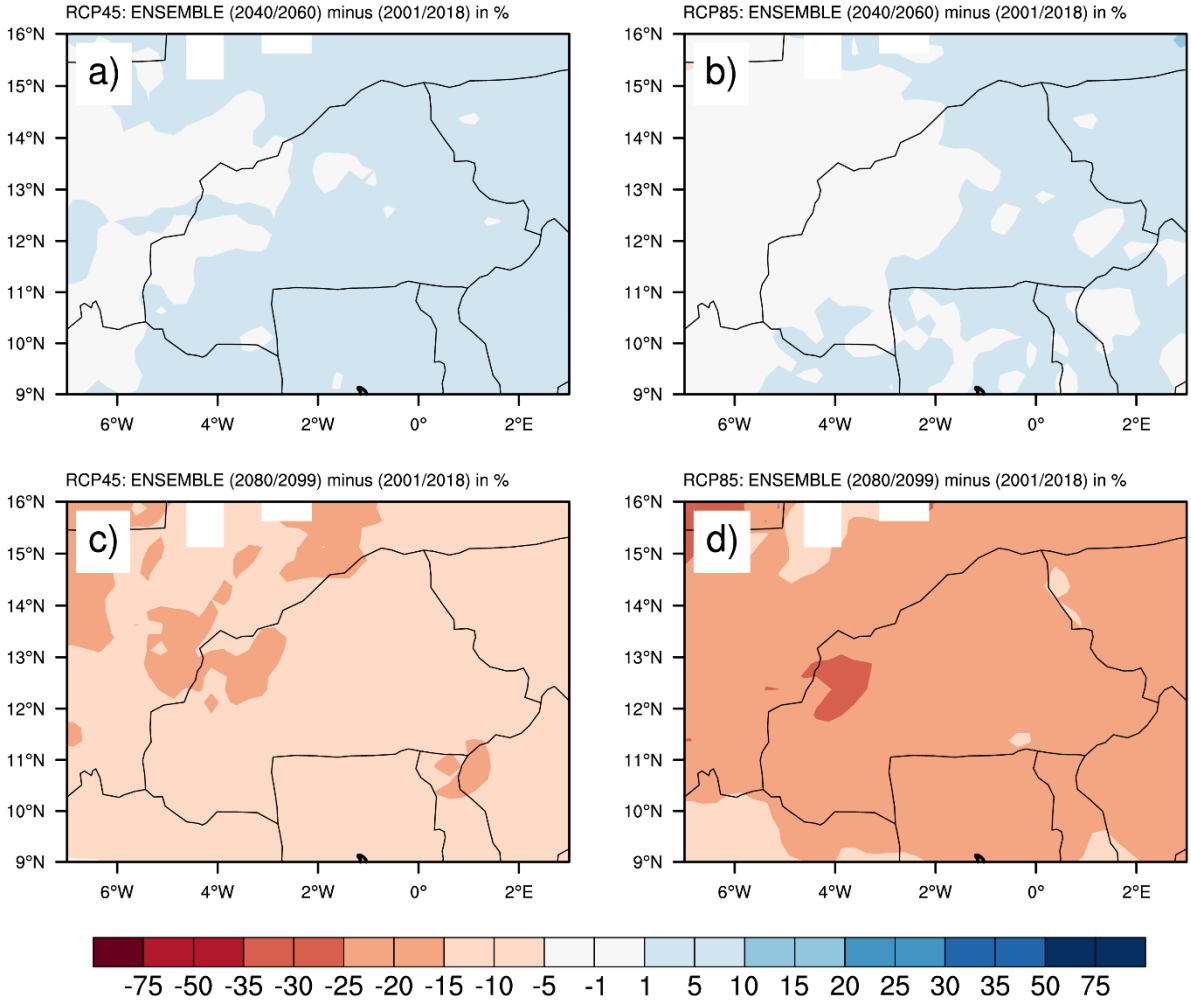

Figure 5.3: Changes (related to the reference period) in annual mean soil moisture (in %) for the near future (2041–2060, upper panels) and the far future (2080–2099, lower panels) and for both RCP4.5 (left panels) and RCP8.5 (right panels).

5.1.5 Evapotranspiration

The changes in evapotranspiration (Figure 5.4) essentially follow those from the mean precipitation and soil moisture with more evapotranspiration during the near future and generalized decrease/increase via a south/north gradient in the late twenty-first century as a result of combined water availability (precipitation and soil moisture) and temperature increases. It should be noted that in the southern Burkina Faso and for both scenarios during the late twenty-first century (Figure 5.4c and Figure 5.4d) evapotranspiration tends to decrease probably because of the lesser projected temperatures in the southern Burkina Faso. In fact, soil moisture and surface temperature are among the two most important factors affecting evapotranspiration. Hence, for the late twenty-first century, these evapotranspiration changes are primarily the result of increased temperature over the study domain.

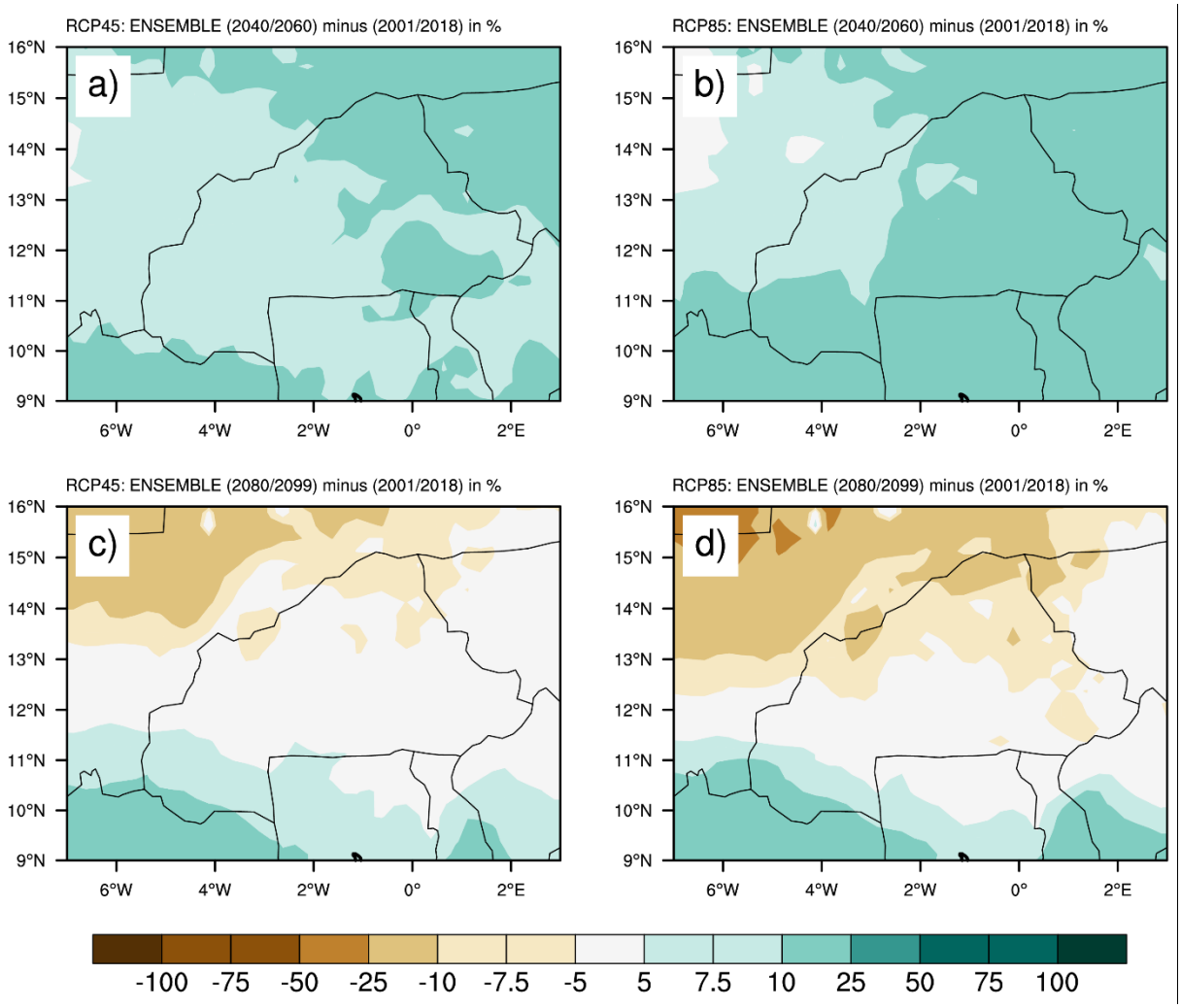

Figure 5.4: Changes (related to the reference period) in annual mean evapotranspiration (in %) for the near future (2041–2060, upper panels) and the far future (2080–2099, lower panels) and for both RCP4.5 (left panels) and RCP8.5 (right panels).

5.1.6 Surface runoff

The surface runoff (Figure 5.5) exhibits different patterns of changes than do precipitation and soil moisture. In fact, both increases and decreases of surface runoff are projected over short distances regardless of whether the region receives more or less precipitation in future climate. This suggests that precipitation in future climate is subject to stronger spatial gradients making it difficult to follow the mean precipitation changes. This also indicates that the heavy precipitation may be more intense under future climate change over Burkina Faso. It should be emphasized that in the near future, the northern and southern parts of Burkina Faso almost undergo an increase of surface runoff while a decrease is projected for the eastern region (more obvious in the RCP4.5 scenario). In the late twenty-first century, the central-western part experiences substantial decreases in surface runoff, tending thus, in some extent, to depress irrigated agricultural activities. However, in the near future, the southern part of the study domain could probably favor irrigated agriculture as the surface runoff increases. However, other important factors such as topography and land use changes may play also decisive roles for agricultural activites.

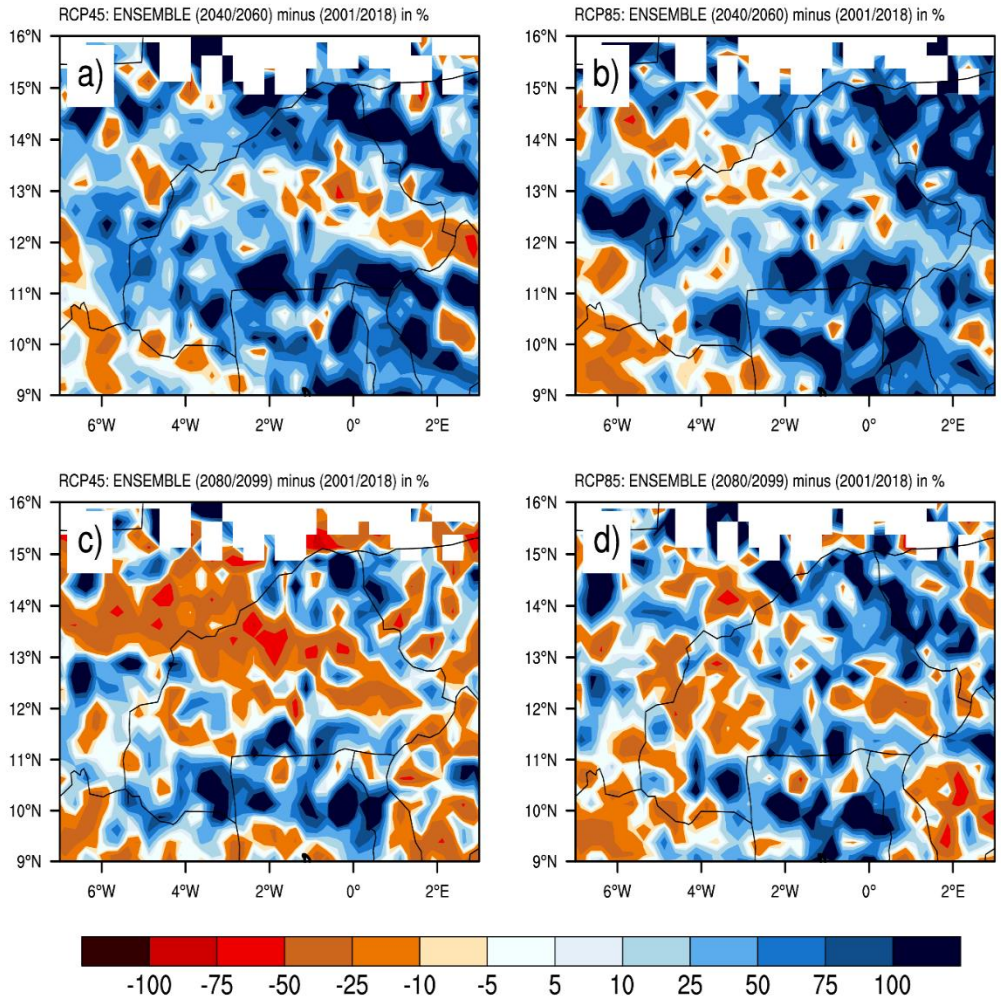

Figure 5.5: Changes (future minus reference period) in annual mean surface runoff (in %) for the near future (2041–2060, upper panels) and the far future (2080–2099, lower panels) and for both RCP4.5 (left panels) and RCP8.5 (right panels).

5.2 Future aridity conditions

To examine how these combined changes will affect the moisture conditions of Burkina Faso, a multivariate approach has been used, for instance the revised Thornthwaite moisture classification, and derive an aridity index for the country following Feddema (2005). The aridity index is shown in Figure 5.6 for the historical, near future, and late twenty-first century and for both RCP4.5 and RCP8.5. The historical period shows that Burkina Faso is essentially a semi-arid country (Figure 5.6a). For the near future, this semi-aridity is less extensive where some dry and, to a lesser extent, moist conditions emerge in the Southern regions. However, for the late twenty-first century and for both scenarios, the centre and northen regions of the country shift toward arid conditions.

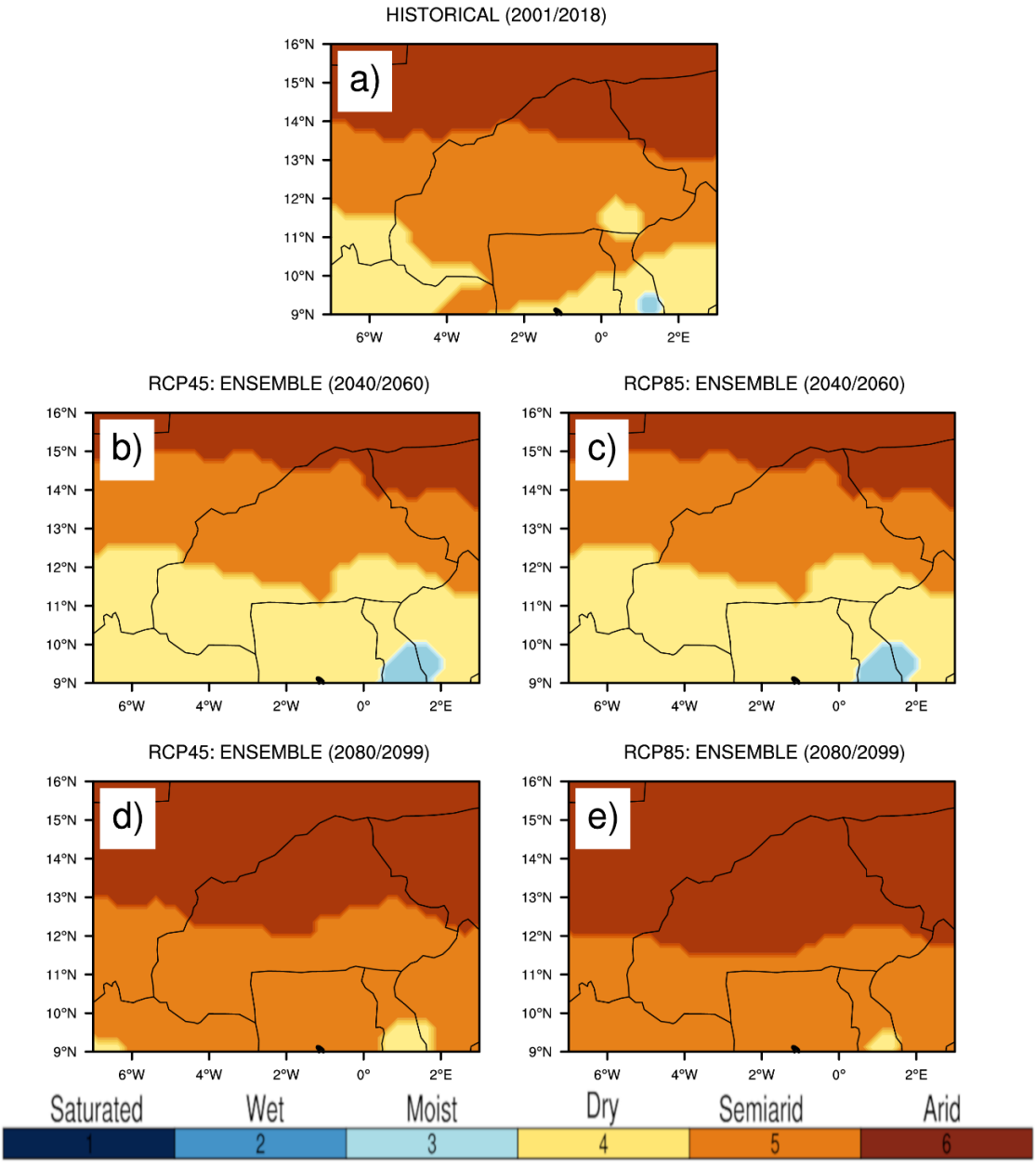

Figure 5.6: Distribution of the aridity index for the historical (2001–2018, upper panel), the near future (2041–2060, middle panels), and the far future (2080–2099, lower panels) and for RCP4.5 (left panels) and RCP8.5 (right panels)

5.3 Partial conclusion

With regards to these results, it is clear that climate change will substantially affect the hydroclimatology of Burkina Faso during the near future toward a lesser surface water amount and a generalized decrease of water availability during the late twenty-first century (decrease of surface runoff and increase of evapotranspiration). Such changes will add more stress to irrigated agricultural activities over the country at a period where the crops need more water due to the increases in aridity (more pronounced in the North). Hence, reliable adaptation, water

management policies and mitigation measures. Important mitigation practices include land-use change and management, cropland management, reforestoration and wastewater treatement and the use of hydropower energy for surface waters and would allow to reduce the increases in GHGs.

Chapter 6: General conclusion, recommendations and perspectives

6.1 Conclusions

This thesis is devoted to assessing past and future hydroclimatic conditions by integrating land surface modelling, data assimilation and climate change over Burkina Faso. This is performed thanks mainly to the use of the CO_2-responsive version of ISBA, the global land data assimilation system LDAS-Monde and the last version of the regional climate model RegCM4. ISBA estimates have been indirectly validated through assessing the quality of its forcings (i.e. ERA5 and ERA-Interim), this determine generally the quality of LSVs simulated by the model. Then, reliable earth observation data such as SSM and LAI from the CGLS have been integrated into the land data assimilation system LDAS-Monde in order to produce improved land surface reanalysis. These land reanalyses are critical for climate science and hydrology as well as environmental monitoring and prediction, especially in data sparse area, like Burkina Faso.

Prior to any assimilation experiment, atmospheric forcings which are used to tune up the land surface model ISBA have been evaluated. In fact, ERA5 and ERA-Interim reanalyses have been assessed with regard to ground-truth measurements of relevant calibration parameters such as precipitation and incoming radiation parameters. At the same time, ERA5's quality with regard to the former reanalysis ERA-Interim was also highlighted. All of these tasks have been performed using stastical metrics. These scores have shown that both ERA5 and ERA-Interim presented good performance in representing precipitation variability and solar radiation (with better agreement for precipitation). The better improvement for precipitation was likely linked with an improvement of its parametrization in tropical Africa. Therefore, it was concluded that ISBA LSM had the potential to produce good quality of land surface parameters such as LAI, SSM, evapotranspiration etc.; and hence, can be used as model estimates (open-loop) within a land data assimilation fraemework.

The assimilation experiment design has been carried out by integrating satellite-derived soil moisture and vegetation products (SSM and LAI) into the ISBA model using a simplified Kalman Filter (SEKF). This configuration has led to long-term characterization and representation of surface hydroclimatic variables (soil moisture, evapotranspiration etc.); which

have been evaluated with regard to their observed counterparts as well as using relevant/proxy independent datasets.

Overall, main results demonstrated a good quality of LDAS-Monde reanalysis to monitor land surface conditions at different time scales (monthly, yearly, seasonal etc.) over Burkina Faso with adequate range of uncertainties. Then, a comparative performance assessment has been addressed using the two previous atmospheric forcings ERA5 and ERA-Interim driving the ISBA LSM (open-loop) i.e. LDAS-ERA5 and LDAS-ERAI. The two configurations have provided a good model first guess, for instance, on the LAI variable along with an asset utilizing ERA5. Nevertheless, the comparison done between the open-loop (ISBA without assimilation) and the observed LAI has highlighted the lacking processes in the representation of vegetation phenology. The assimilation was able to improve the simulation of both surface soil moisture and LAI when using either ERA5 or ERA-Interim. This pointed out that the assimilation add skill to both configurations and proved the healthy behaviour of LDAS-Monde system. Furthermore, important improvements in the representation of the LAI, SSM, and GPP variables were obtained with better scores for the analysis than for the model equivalent (open-loop simulation). In particular, the LAI analysis was very good at compensating for caveats, such as the model's failure in capturing leaf onset prior to the first rains for particular plant species.

We used an integrated assimilation platform to represent and monitor key LSVs relevant to hydrological cycle over Burkina Faso and evaluated the associated representation uncertainty, thus providing a range of possible estimates of LSVs (soil moisture, for instance) on a specific period of time and space. Importantly, the assimilation system used in this thesis can be coupled with a physically based hydrological model and has the advantage to accommodate to variations in time, climate and environment. Therefore, it can be used to address some water resources issues such as monitoring and forecasting of streamflow by updating input data over a catchment-scale or for larger areas. These types of information will help build reliable information regarding water resources management and planning especially over data-scarce regions as well as in the evaluation of current and future hydroclimatic changes towards the development of more appropriate adaptation measures and mitigation strategies to cope with global changes. Trustworthy information on water resources availability in data-scarce areas like West Africa can also boost the development of irrigation. This is especially relevant in a future climate change context, where rain-fed agriculture being mostly threatened.

For these previous reasons, we developed an ensemble-based simulation from RegCM4 model to investigate to what extent climate change will affect future water availability over Burkina Faso. This was done by assessing changes in hydroclimatic variables such as precipitation, soil moisture, evapotranspiration and surface runoff along with an assessment of future aridity conditions.

The results indicated that the different GHG forcings produce different magnitudes of temperature changes ranging from 1 °C in the RCP4.5 and for the near future to 6.5 °C for RCP8.5 and for the late twenty-first century. The impact of such warming on the regional water demand is substantial. In addition, the mean precipitation change exhibits interesting features. In fact, mean precipitation in the near future shows a tendency to increase in both scenarios; however, for the late twenty-first century, drier conditions occur, with RCP8.5 projecting the highest decrease. This indicates that natural variability plays an important role when the GHG forcing is low (i.e., the near future). Evapotranspiration and soil moisture essentially follow changes of mean precipitation – along with other factors such as vegetation dynamics, which are not taken into account by most of the regional climate models, including RegCM4). However, for the surface runoff in the near future, the north and south parts of Burkina Faso almost undergo an increase of surface runoff while a decrease is projected for the eastern region (more important in the RCP4.5) and substantial decreases in the central-western part of Burkina Faso (for the late twenty-first century). Finally, an aridity index has been applied to the historical and future climatologies of precipitation and potential evapotranspiration. It is interesting to note that during the near future, climate change provides some extension of the dry areas in southern Burkina Faso at the expenses of semi-arid zones. However, in the late twenty-first century and under both RCP4.5 and RCP8.5 GHG forcings, almost the whole Burkina Faso, tends to shift toward a generalized arid climate (with less extension in the southern part, especially in the RCP4.5 scenario).

From these results, it is evident that climate change will substantially affect the hydroclimatology of Burkina Faso during the near future toward a lesser surface water amount in the north Burkina Faso and a generalized decrease of water availability during the late twenty-first century (decrease of soil moisture and intensification of the aridity). Such changes will add more stress to irrigated agricultural activities over the country at a period of time where the crops need more water due to aridity intensification.

6.2 Perspectives and recommendations

Available observations constitute a major pillar of any land surface modelling research and climate change assessment for water resources monitoring and management. It is therefore of high importance to use further data along with more sophisticated methods in order to improve model accuracy as well as reduce uncertainties. This appeals the use of state-of-the-science land models, most recent data assimilation technics and regional climate models. Due to novelty approach engaged in this research, the perspectives and recommendations are basically oriented for hydroclimate research purposes. Therefore, the following points are suggested:

6.2.1 Perspectives for further research investigations

In land surface modelling and data assimilation

- The LAI representation could be enhanced even more using more efficient observations and assimilation systems. For example, one single LAI observation was used within a grid cell for all types of vegetation to perform the assimilation, making the Kalman gain and the increment disaggregation rely on the vegetation type as in Barbu et al., (2014).
- This procedure could be improved by performing the assimilation using disaggregated values of LAI for each individual vegetation type. Such a LAI disaggregation method was recently proposed by Munier et al., (2018). Munier et al., (2018) produced disaggregated global LAI maps available every 10 days for each vegetation type available from ECOCLIMAP-II over 1999–2015.
- Assimilating the disaggregated LAI could impact the analyzed LAI and other vegetation related variables, mainly evapotranspiration and GPP as emphasized in Munier et al., (2018).
- Also, LDAS-Monde analyses for the SSM variable could be improved by implementing an observation operator for the ASCAT radar (backscatter coefficients), instead of assimilating a retrieved soil moisture product. This would allow a direct assimilation of level 1 data and the use of all the information contained in these observations (Lievens et al., 2016).

In hydroclimatic change assessment

- The use of statistical bias correction methods in historical RCM simulations: this will potentially reduce the uncertainties in future projections as highlighted by Mbaye et al.

2016 over Senegal River Basin.

- Increasing the resolution of RCMs (e.g. towards ~ 12 Km) appears to provide substantially enhanced information on the magnitude and patterns of hydroclimatic changes. It will be further interesting to assess the new WASCAL high resolution simulations developed for West Africa.
- The contribution of more simulations in building the multi-model ensemble of RCMs simultions: this will enhance the reliability of projections using information from several RCMs and therefore, reduce the associated uncertainties, as highlighted in Mbaye et al. 2019 over Senegal.
- Despite its clear importance on climate changes, vegetation dynamics and/or land use changes are represented in only a few hydroclimatic simulations. Thus, a synchronously coupled regional hydro-climate-vegetation simulations would be of highly importance to investigate the land use changes feedback in futue hydroclimate changes on water resources over Burkina Faso. This will help address the uncertainty in model results related to future hydroclimatic conditions as in Yu et al. (2015).
- The use of RegCM simulations based on the non-hydrostatic dynamical core could potentially provide an added-value in the predictions of hydroclimate variables over Burkin Faso.
- Considering the different sub-basins of Burkina Faso will allow assessing climate change on water resources through estimating a potential water availability considered as the ratio between the precipitation and the potential evapotranspiration. Also, it will be important to analyze each basins's potential—for a better consideration of the water balance—to increase agricultural productivity through assessing changes in crop water deamand, irrigation water need, water availability, and the difference between water availability and irrigation water need, referred as basin irrigation potential as in Sylla et al. (2018).
- Considering soil moisture assessment, the humidity values of the different soil layers have not been considered in this study. Hence, a regression equation must be established to take into account the contribution of the entire root zone, and therefore of the soil to evapotranspiration and ultimately to gross primary production
- Using higher resolution dataset for the gross primary production would help better monitor the agricultural productivity, while considering the different soil heterogeneities in the assessment.

- Quantifying the hydrological water budget components for Burkina Faso would be also relevant, especially when considering the different sub-basins of the country, as highlighted previously.
- For surface runoff projections, land use and land cover change contributions should be taken into account to estimate their impacts on water availability as well as agriculutre in future.
- Information on projected hydroclimatology and drought conditions can help policymakers to develop strategies for the most vulnerable areas. For example, a shift from wet to semi-arid conditions may cause species migration and/or extinction along with increased water stress on managed and unmanaged ecosystems (Colwell et al. 2008; Carr et al. 2014). Thus, the breeding of species more resilient to hotter and drier climates or the implementation of sustainable practices, such as climate-smart agriculture, would be required in order to mitigate the effects of climate change (Loarie et al. 2009; Campbell et al. 2014).
- It is also paramount for the local authorities to develop some adaptation measures and mitigation strategies to cope with the new environmental conditions due to intensifying climate change over Burkina Faso.

6.2.2 Recommandations to researchers

The following recommendations are made for further research involving integrated hydroclimate modelling over Burkina Faso

- Include the impacts of land use/cover changes on regional hydroclimatic changes in order to provide more reliable long-term reanalyses of surface states variables and robust hydroclimate information.
- Extend this study to other regions and/or in the main river basins of West Africa.
- Further application of integrated and multi-disciplinarity approaches in environmental assements in hydrolclimate research

Overall, the results obtained and illustrated throughout this thesis have permited to confirm the hypothesis formulated in Chapter 1. Thus, pointing out the need of elaborating robust LSMs, data assimilation technics as well as reliable ensemble-based climate change projections and related impact/adaptation assessment studies for this highly vulnerable region of West Africa (Burkina Faso). In particular, increased resolution appears to provide substantially enhanced information on the magnitude and patterns of changes in the

hydroclimatology and drought patterns over the region, and this calls for a sustained use of regional climate models coupled with hydrological routines to enhance the reliability of hydrclimatic change projections over West Africa.

References

Agustí-Panareda, A., Beljaars, A., Ahlgrimm, M., Balsamo, G., Bock, O., Forbes, R., Ghelli, A., Guichard, F., Köhler, M., Meynadier, R., 2010. The ECMWF re-analysis for the AMMA observational campaign. *Quarterly Journal of the Royal Meteorological Society* 136, 1457–1472.

Albergel, C., de Rosnay, P., Gruhier, C., Muñoz-Sabater, J., Hasenauer, S., Isaksen, L., Kerr, Y., Wagner, W., 2012. Evaluation of remotely sensed and modelled soil moisture products using global ground-based in situ observations. *Remote Sensing of Environment* 118, 215–226. https://doi.org/10.1016/j.rse.2011.11.017

Albergel, C., Dutra, E., Bonan, B., Zheng, Y., Munier, S., Balsamo, G., de Rosnay, P., Muñoz-Sabater, J., Calvet, J.-C., 2019. Monitoring and Forecasting the Impact of the 2018 Summer Heatwave on Vegetation. *Remote Sensing* 11, 520. https://doi.org/10.3390/rs11050520

Albergel, C., Dutra, E., Munier, S., Calvet, J.-C., Munoz-Sabater, J., de Rosnay, P., Balsamo, G., 2018. ERA-5 and ERA-Interim driven ISBA land surface model simulations: which one performs better? *Hydrology & Earth System Sciences* 22.

Albergel, C., Munier, S., Leroux, D.J., Dewaele, H., Fairbairn, D., Barbu, A.L., Gelati, E., Dorigo, W., Faroux, S., Meurey, C., 2017. Sequential assimilation of satellite-derived vegetation and soil moisture products using SURFEX_v8. 0: LDAS-Monde assessment over the Euro-Mediterranean area. *Geoscientific Model Development* 10, 3889.

Albergel, C., Rüdiger, C., Pellarin, T., Calvet, J.-C., Fritz, N., Froissard, F., Suquia, D., Petitpa, A., Piguet, B., Martin, E., 2008. From near-surface to root-zone soil moisture using an exponential filter: an assessment of the method based on in-situ observations and model simulations. *Hydrology and Earth System Sciences* 12, 1323–1337.

ANAM: Meterological Agency. Rainfall and Temperature Data of Burkina Faso; Meterological Agency: Ouagadougou, Burkina Faso, 2018.

Annuaire Statistique 2013; Institut National de la Statistique et de la Démographie (INSD): Ouagadougou, Burkina Faso, 2014.

Anyamba A, Small JL, Britch SC, Tucker CJ, Pak EW, Reynolds CA, Crutchfield J, Linthicum KJ 2014 Recent weather extremes and impacts on agricultural production and vector-borne disease outbreak patterns. *PLoSONE* 9:e92538. doi:10.1371/journal.pone. 0092538

Balsamo, G., Mahfouf, J.F., Bélair, S., Deblonde, G., 2007. A land data assimilation system for

soil moisture and temperature: An information content study. *Journal of Hydrometeorology* 8, 1225–1242.

Barbu, A.L., Calvet, J.-C., Mahfouf, J.-F., Albergel, C., Lafont, S., 2011. Assimilation of Soil Wetness Index and Leaf Area Index into the ISBA-A-gs land surface model: grassland case study. *Biogeosciences* 8, 1971–1986.

Barbu, A.L., Calvet, J.-C., Mahfouf, J.-F., Lafont, S., 2014. Integrating ASCAT surface soil moisture and GEOV1 leaf area index into the SURFEX modelling platform: a land data assimilation application over France. *Hydrology and Earth System Sciences* 18, 173–192.

Bartalis, Z., Wagner, W., Naeimi, V., Hasenauer, S., Scipal, K., Bonekamp, H., Figa, J., Anderson, C., 2007. Initial soil moisture retrievals from the METOP-A Advanced Scatterometer (ASCAT). *Geophysical Research Letters* 34.

Bechtold, P., 2016. Convection in global numerical weather prediction, in: Parameterization of Atmospheric Convection: Volume 2: Current Issues and New Theories. *World Scientific*, pp. 5–45.

Beck, H.E., Pan, M., Roy, T., Weedon, G.P., Pappenberger, F., van Dijk, A., Huffman, G.J., Adler, R.F., Wood, E.F., 2018. Daily evaluation of 26 precipitation datasets using Stage-IV gauge-radar data for the CONUS. *Hydrol. Earth Syst. Sci. Discuss* 1–23.

Berrisford, P., Dee, D., Fielding, K., Fuentes, M., Kallberg, P., Kobayashi, S., Uppala, S., 2009. The ERA-interim archive. *ERA report series* 1–16.

Beven, K., 2012. Predicting Hydrographs Using Distributed Models Based on Process Descriptions. Rainfall-Runoff Modelling: *The Primer*, Second Edition, John Wiley & Sons, Ltd, Chichester, UK. doi 10, 9781119951001.

Boko M, Niang I, Nyong A, Vogel C, Githeko A, Medany M, Osman Elasha B, Tabo R and Yanda, P Africa Climate change 2007: impacts, adaptation and vulnerability. Contribution of Working Group I I t o the Fourth Assessment Repo r t of the Intergovernmental Panel on Climate Change, Parry ML, Canziani OF, Palutikof J, van der Linden PJ and Hanson CE, Eds., *Cambridge University Press*, Cambridge UK, 433–467.

Boone, A., De Rosnay, P., Balsamo, G., Beljaars, A., Chopin, F., Decharme, B., Delire, C., Ducharne, A., Gascoin, S., Grippa, M., 2009. The AMMA land surface model intercomparison project (ALMIP). *Bulletin of the American Meteorological Society* 90, 1865–1880.

Boone, A., Masson, V., Meyers, T., Noilhan, J., 2000. The influence of the inclusion of soil

freezing on simulations by a soil–vegetation–atmosphere transfer scheme. *Journal of Applied Meteorology* 39, 1544–1569.

Bouttier, F. & Courtier, P. 1999. Lecture notes on data assimilation concepts and methods. Reading, UK: European Centre for Medium-Range Weather Forecasts

Bowen, I.S., 1926. The Ratio of Heat Losses by Conduction and by Evaporation from any Water *Surface. Phys. Rev.* 27, 779–787. https://doi.org/10.1103/PhysRev.27.779

Brooks, R., Corey, T., 1964. HYDRAU uc properties of porous media. *Hydrology Papers*, Colorado State University 24, 37.

Brut, A., Rüdiger, C., Lafont, S., Roujean, J.-L., Calvet, J.-C., Jarlan, L., Gibelin, A.-L., Albergel, C., Moigne, P.L., Soussana, J.F., Klumpp, K., Guyon, D., Wigneron, J.P., Ceschia, E., 2009. Modelling LAI at a regional scale with ISBA-A-gs: comparison with satellite-derived LAI over southwestern France. *Biogeosciences* 6, 1389–1404.

Brutsaert, W., 2005. Hydrology: an introduction. Cambridge University Press.

Calvet, J.-C., Lafont, S., Cloppet, E., Souverain, F., Badeau, V., Le Bas, C., 2012. Use of agricultural statistics to verify the interannual variability in land surface models: a case study over France with ISBA-A-gs. *Geosci. Model Dev.* 5, 37–54. https://doi.org/10.5194/gmd-5-37-2012

Calvet, J.-C., Noilhan, J., Roujean, J.-L., Bessemoulin, P., Cabelguenne, M., Olioso, A., Wigneron, J.-P., 1998. An interactive vegetation SVAT model tested against data from six contrasting sites. *Agricultural and Forest Meteorology* 92, 73–95.

Calvet, J.-C., Rivalland, V., Picon-Cochard, C., Guehl, J.-M., 2004. Modelling forest transpiration and CO2 fluxes—Response to soil moisture stress. *Agricultural and forest meteorology* 124, 143–156.

Campbell, G.S., 1974. A simple method for determining unsaturated conductivity from moisture retention data. *Soil science* 117, 311–314.

Campbell BM, Thornton P, Zougmore R, van Asten P, Lipper L (2014) Sustainable intensification: what is its role in climate smart agriculture? *Curr Opin Environ Sustain* 8:39–43

Canal, N., Calvet, J.-C., Decharme, B., Carrer, D., Lafont, S., Pigeon, G., 2014. Evaluation of root water uptake in the ISBA-A-gs land surface model using agricultural yield statistics over France. *Hydrology and Earth System Sciences* 18, 4979–4999.

Carr JA, Hughes AF and Foden WB (2014) A climate change vulnerability assessment of West African species. *UNEP-WCMC technical report*.

Carrer, D., Roujean, J.-L., Lafont, S., Calvet, J.-C., Boone, A., Decharme, B., Delire, C.,

Gastellu-Etchegorry, J.-P., 2013. A canopy radiative transfer scheme with explicit FAPAR for the interactive vegetation model ISBA-A-gs: Impact on carbon fluxes: CANOPY RT SCHEME FOR ISBA-A-gs LSM. *J. Geophys. Res. Biogeosci.* 118, 888–903. https://doi.org/10.1002/jgrg.20070

Charney, J.G., 1975. Dynamics of deserts and drought in the Sahel. *Quarterly Journal of the Royal Meteorological Society* 101, 193–202.

Chen, J. M., Menges, C. H., & Leblanc, S. G. 2005. Global mapping of foliage clumping index using multi-angular satellite data. *Remote Sensing of Environment*, 97(4), 447-457.

Clapp, R.B., Hornberger, G.M., 1978. Empirical equations for some soil hydraulic properties. *Water Resources Research* 14, 601–604. https://doi.org/10.1029/WR014i004p00601

Cobo, J.G., Dercon, G., Cadisch, G., 2010. Nutrient balances in African land use systems across different spatial scales: A review of approaches, challenges and progress. *Agriculture, Ecosystems & Environment* 136, 1–15. https://doi.org/10.1016/j.agee.2009.11.006

Collatz, G., Ribas-Carbo, M., Berry, J., 1992. Coupled Photosynthesis-Stomatal Conductance Model for Leaves of C4 Plants. *Functional Plant Biol.* 19, 519. https://doi.org/10.1071/PP9920519

Colwell RK, Brehm G, Cardelus CL, Gilman AC, Longino JT (2008) Global warming, elevational range shifts, and lowland biotic attrition in the wet tropics. Science 322:258–261

Crosson, W.L., Laymon, C.A., Inguva, R., Schamschula, M.P., 2002. Assimilating remote sensing data in a surface flux–soil moisture model. *Hydrological processes* 16, 1645–1662.

Dai, Y., Zeng, X., Dickinson, R.E., Baker, I., Bonan, G.B., Bosilovich, M.G., Denning, A.S., Dirmeyer, P.A., Houser, P.R., Niu, G., Oleson, K.W., Schlosser, C.A., Yang, Z.-L., 2003. The Common Land Model. *Bull. Amer. Meteor. Soc.* 84, 1013–1024. https://doi.org/10.1175/BAMS-84-8-1013

De Jeu, R.A., Wagner, W., Holmes, T.R.H., Dolman, A.J., Van De Giesen, N.C., Friesen, J., 2008. Global soil moisture patterns observed by space borne microwave radiometers and scatterometers. *Surveys in Geophysics* 29, 399–420.

De Ridder, K., 2009. Soil temperature spin-up in land surface schemes. *Theor Appl Climatol* 95, 341–347. https://doi.org/10.1007/s00704-008-0011-y

Decharme, B., Douville, H., 2006. Introduction of a sub-grid hydrology in the ISBA land surface model. *Clim Dyn* 26, 65–78. https://doi.org/10.1007/s00382-005-0059-7

Dee, D.P., Uppala, S.M., Simmons, A.J., Berrisford, P., Poli, P., Kobayashi, S., Andrae, U.,

Balmaseda, M.A., Balsamo, G., Bauer, d P., 2011. The ERA-Interim reanalysis: Configuration and performance of the data assimilation system. *Quarterly Journal of the royal meteorological society* 137, 553–597.

Diallo I., Sylla M.B., Giorgi F., Gaye A.T. and Camara M. 2012 Multimodel GCM-RCM ensemble based projections of temperature and precipitation over West Africa for the early 21st century. *Int J Geophys* Article ID 972896. doi:10.1155/2012/972896.

Diallo I., Giorgi F., Deme A., Tall M., Mariotti L., Gaye A.T. 2016 Projected changes of summer monsoon extremes and hydroclimatic regimes over West Africa for the twenty-first century. *Clim Dyn.* doi:10. 1007/s00382-016-3052-4

Diallo, F.B., Hourdin, F., Rio, C., Traore, A.-K., Mellul, L., Guichard, F., Kergoat, L., 2017. The Surface Energy Budget Computed at the Grid-Scale of a Climate Model Challenged by Station Data in West Africa. *Journal of Advances in Modeling Earth Systems* 9, 2710–2738.

Dickinson, R.E., 1984. Modeling evapotranspiration for three-dimensional global climate models, in: Hansen, J.E., Takahashi, T. (Eds.), *Geophysical Monograph Series.* American Geophysical Union, Washington, D. C., pp. 58–72. https://doi.org/10.1029/GM029p0058

Dirmeyer, P.A., Dolman, A.J., Sato, N., 1999. The pilot phase of the global soil wetness project. *Bulletin of the American Meteorological Society* 80, 851–878.

Dirmeyer, P. A., Gao, X., Zhao, M., Guo, Z., Oki, T., & Hanasaki, N. 2006. GSWP-2: Multimodel analysis and implications for our perception of the land surface. *Bulletin of the American Meteorological Society*, *87*(10), 1381-1398.

Draper, C., Mahfouf, J.-F., Calvet, J.-C., Martin, E., Wagner, W., 2011. Assimilation of ASCAT near-surface soil moisture into the SIM hydrological model over France. *Hydrology and Earth System Sciences* 15, 3829–3841.

Draper, C.S., Mahfouf, J.-F., Walker, J.P., 2009. An EKF assimilation of AMSR-E soil moisture into the ISBA land surface scheme. *J. Geophys. Res.* 114, D20104. https://doi.org/10.1029/2008JD011650

Draper, C.S., Reichle, R.H., De Lannoy, G.J.M., Liu, Q., 2012. Assimilation of passive and active microwave soil moisture retrievals: ASCAT AMSR-E ASSIMILATION. *Geophys. Res. Lett.* 39, n/a-n/a. https://doi.org/10.1029/2011GL050655

Drusch, M., Wood, E.F., Gao, H., 2005. Observation operators for the direct assimilation of TRMM microwave imager retrieved soil moisture. *Geophysical Research Letters* 32.

Druyan, L.M. 2011 Studies of 21st-century precipitation trends over West Africa. *Int J Climatol*

31:1415–1572. doi:10.1002/joc.2180

Dunne JP, Jasmin J, Shevliakova E, Stouffer RJ, et al. (2013) GFDL's ESM2 global coupled climate-carbon earth system models part II: carbon system formulation and baseline simulation characteristics. *J Clim* 26(7). doi:10.1175/JCLI-D-12-00150.1

Ek, M.B., Mitchell, K.E., Lin, Y., Rogers, E., Grunmann, P., Koren, V., Gayno, G., Tarpley, J.D., 2003. Implementation of Noah land surface model advances in the National Centers for Environmental Prediction operational mesoscale Eta model. *Journal of Geophysical Research: Atmospheres* 108. https://doi.org/10.1029/2002JD003296

El-Khoury A, O. Seidou, D.R. Lapen, Z. Que, M. Mohammadian, M. Sunohara, D. Bahram (2015) Combined impacts of future climate and land use changes on discharge, nitrogen and phosphorus loads for a Canadian river basin. *J Environ Manag* 151, 76–86.

Emanuel KA (1991) A scheme for representing cumulus convection in large-scale models. *J Atmos Sci* 48:2313–2335

Emanuel KA, Zivkovic-RothmanM(1999) Development and evaluation of a convection scheme for use in climate models. *J Atmos Sci* 56: 1766–1782. doi:10.1175/1520-0469

Entekhabi, D., Asrar, G.R., Betts, A.K., Beven, K.J., Bras, R.L., Duffy, C.J., Dunne, T., Koster, R.D., Lettenmaier, D.P., McLaughlin, D.B., 1999. An agenda for land surface hydrology research and a call for the second international hydrological decade. *Bulletin of the American Meteorological Society* 80, 2043–2058.

Entekhabi, D., Nakamura, H., Njoku, E.G., 1994. Solving the inverse problem for soil moisture and temperature profiles by sequential assimilation of multifrequency remotely sensed observations. IEEE Trans. Geosci. *Remote Sensing* 32, 438–448. https://doi.org/10.1109/36.295058

Entekhabi, D., Njoku, E.G., O'Neill, P.E., Kellogg, K.H., Crow, W.T., Edelstein, W.N., Entin, J.K., Goodman, S.D., Jackson, T.J., Johnson, J., Kimball, J., Piepmeier, J.R., Koster, R.D., Martin, N., McDonald, K.C., Moghaddam, M., Moran, S., Reichle, R., Shi, J.C., Spencer, M.W., Thurman, S.W., Tsang, L., Van Zyl, J., 2010. The Soil Moisture Active Passive (SMAP) Mission. *Proceedings of the IEEE* 98, 704–716. https://doi.org/10.1109/JPROC.2010.2043918

Etchevers, P., Golaz, C., Habets, F., 2001. Simulation of the water budget and the river flows of the Rhone basin from 1981 to 1994. *Journal of Hydrology* 244, 60–85. https://doi.org/10.1016/S0022-1694(01)00332-8

Evensen, G., 2009. Data Assimilation: The Ensemble Kalman Filter. *Springer Science & Business Media.*

Fairbairn, D., Barbu, A.L., Napoly, A., Albergel, C., Mahfouf, J.-F., Calvet, J.-C., 2017. The effect of satellite-derived surface soil moisture and leaf area index land data assimilation on streamflow simulations over France. *Hydrology and Earth System Sciences* 21, 2015–2033.

FAO, World Reference Base for Soil Resources: International Soil Classification System for Naming and Creating Legends for Soil Maps; *FAO*: Rome, Italy, 2015.

Faroux, S., Kaptué Tchuenté, A.T., Roujean, J.-L., Masson, V., Martin, E., Moigne, P.L., 2013. ECOCLIMAP-II/Europe: A twofold database of ecosystems and surface parameters at 1 km resolution based on satellite information for use in land surface, meteorological and climate models. *Geoscientific Model Development* 6, 563–582.

Farquhar, G.D., von Caemmerer, S., Berry, J.A., 1980. A biochemical model of photosynthetic CO2 assimilation in leaves of C3 species. *Planta* 149, 78–90. https://doi.org/10.1007/Burkina Faso00386231

Fatras, C., Frappart, F., Mougin, E., Frison, P. L., Faye, G., Borderies, P., & Jarlan, L. 2015. Spaceborne altimetry and scatterometry backscattering signatures at C-and Ku-bands over West Africa. *Remote Sensing of Environment,* 159, 117-133.

Forzieri, G., Alkama, R., Miralles, D. G., & Cescatti, A. (2017). Satellites reveal contrasting responses of regional climate to the widespread greening of Earth. *Science*, *356*(6343), 1180-1184.

Franks, S.W., Beven, K.J., 1999. Conditioning a multiple-patch SVAT Model using uncertain time-space estimates of latent heat fluxes as inferred from remotely sensed data. *Water Resources Research* 35, 2751–2761.

Gao, H., Wood, E.F., Jackson, T.J., Drusch, M., Bindlish, R., 2006. Using TRMM/TMI to Retrieve Surface Soil Moisture over the Southern United States from 1998 to 2002. *J. Hydrometeor.* 7, 23–38. https://doi.org/10.1175/JHM473.1

Garrigues, S., Allard, D., Baret, F., & Weiss, M. 2006. Influence of landscape spatial heterogeneity on the non-linear estimation of leaf area index from moderate spatial resolution remote sensing data. *Remote Sensing of Environment*, 105(4), 286-298.

Garrigues, S., Olioso, A., Carrer, D., Decharme, B., Calvet, J.-C., Martin, E., Moulin, S., Marloie, O., 2015. Impact of climate, vegetation, soil and crop management variables on multi-year ISBA-A-gs simulations of evapotranspiration over a Mediterranean crop site. *Geosci. Model Dev*. 8, 3033–3053. https://doi.org/10.5194/gmd-8-3033-2015

Georgakakos, K.P., Carpenter, T.M., 2006. Potential value of operationally available and spatially distributed ensemble soil water estimates for agriculture. *Journal of hydrology*

328, 177–191.

Gibelin, A.-L., Calvet, J.-C., Roujean, J.-L., Jarlan, L., Los, S.O., 2006. Ability of the land surface model ISBA-A-gs to simulate leaf area index at the global scale: Comparison with satellites products. *Journal of Geophysical Research: Atmospheres* 111.

Gibelin, A.-L., Calvet, J.-C., Viovy, N., 2008. Modelling energy and CO2 fluxes with an interactive vegetation land surface model-Evaluation at high and middle latitudes. *Agricultural and Forest Meteorology* 148, 1611–1628. https://doi.org/10.1016/j.agrformet.2008.05.013

Giorgi F, Coppola E, Solmon F, Mariotti L, Sylla MB, Bi X, Elguindi N, Diro GT, Nair V, Giuliani G, Turuncoglu UU, Cozzini S, Güttler I, O'Brien TA, Tawfik AB, Shalaby A, Zakey AS, Steiner AL, Stordal F, Sloan LC, Brankovic C (2012) RegCM4: model description and preliminary tests over multiple CORDEX domains. *Clim Res* 52:7–29. doi:10.3354/cr01018

Glenn, E.P., Huete, A.R., Nagler, P.L., Hirschboeck, K.K., Brown, P., 2007. Integrating Remote Sensing and Ground Methods to Estimate Evapotranspiration. *Critical Reviews in Plant Sciences* 26, 139–168. https://doi.org/10.1080/07352680701402503

Goudriaan, J., van Laar, H.H., van Keulen, H., Louwerse, W., 1985. Photosynthesis, CO2 and Plant Production, in: Day, W., Atkin, R.K. (Eds.), Wheat Growth and Modelling. *Springer US, Boston, MA*, pp. 107–122. https://doi.org/10.1007/978-1-4899-3665-3_10

Grell G, Dudhia J, Stauffer DR (1994) A description of the fifth generation Penn State/NCAR Mesoscale Model (MM5). National Center for Atmospheric Research Tech Note NCAR/TN-398 + STR, NCAR, *Boulder, CO*

Greve, P., Orlowsky, B., Mueller, B., Sheffield, J., Reichstein, M., Seneviratne, S.I., 2014. Global assessment of trends in wetting and drying over land. *Nature geoscience* 7, 716.

Gruber, A., Su, C.-H., Zwieback, S., Crow, W., Dorigo, W., Wagner, W., 2016. Recent advances in (soil moisture) triple collocation analysis. *International Journal of Applied Earth Observation and Geoinformation* 45, 200–211.

Guichard, F., Kergoat, L., Mougin, E., Timouk, F., Baup, F., Hiernaux, P., Lavenu, F., 2009. Surface thermodynamics and radiative budget in the Sahelian Gourma: Seasonal and diurnal cycles. *Journal of Hydrology* 375, 161–177.

Guillod, B.P., Orlowsky, B., Miralles, D.G., Teuling, A.J., Seneviratne, S.I., 2015. Reconciling spatial and temporal soil moisture effects on afternoon rainfall. *Nature communications* 6, 6443.

Habets, F., Etchevers, P., Golaz, C., Leblois, E., Ledoux, E., Martin, E., Noilhan, J., Ottlé, C.,

1999. Simulation of the water budget and the river flows of the Rhone basin. *J. Geophys. Res.* 104, 31145–31172. https://doi.org/10.1029/1999JD901008

Hamon W (1963) Computation of direct runoff amounts from storm rainfall. *Int Assoc Sci Hydrol Publ* 63:52–62

Heathman, G.C., Starks, P.J., Ahuja, L.R., Jackson, T.J., 2003. Assimilation of surface soil moisture to estimate profile soil water content. *Journal of Hydrology* 279, 1–17. https://doi.org/10.1016/S0022-1694(03)00088-X

Hersbach, H., Dee, D., 2016. ERA5 reanalysis is in production. ECMWF newsletter 147.

Hogan, R.J., Bozzo, A., 2018. A flexible and efficient radiation scheme for the ECMWF model. *Journal of Advances in Modeling Earth Systems* 10, 1990–2008.

Holm, E.V., 2003. Lecture notes on assimilation algorithms 30.

Houser, P.R., De Lannoy, G.J.M., Walker, J.P., 2010. Land Surface Data Assimilation, in: Lahoz, W., Khattatov, B., Menard, R. (Eds.), Data Assimilation. *Springer Berlin Heidelberg, Berlin, Heidelberg*, pp. 549–597. https://doi.org/10.1007/978-3-540-74703-1_21

Hsieh, C.-I., Huang, C.-W., Kiely, G., 2009. Long-term estimation of soil heat flux by single layer soil temperature. *Int J Biometeorol* 53, 113–123. https://doi.org/10.1007/s00484-008-0198-8

Ibrahim, B., Karambiri, H., Polcher, J., Yacouba, H., & Ribstein, P. 2014. Changes in rainfall regime over Burkina Faso under the climate change conditions simulated by 5 regional climate models. *Climate Dynamics*, 42(5-6), 1363-1381.

Imaoka, K., Kachi, M., Kasahara, M., Ito, N., Nakagawa, K., Oki, T., 2010. INSTRUMENT PERFORMANCE AND CALIBRATION OF AMSR-E AND AMSR2 4.

INSD : Annuaire Statistique 2013; Institut National de la Statistique et de la Démographie (*INSD*): Ouagadougou, Burkina Faso, 2014.

IPCC 2014; Climate change 2014: impacts, adaptation, and vulnerability. WorkingGroup II contribution to the Fifth Assessment Report of the Intergovernmental Panel on Climate Change.Available at: *http://www.ipcc.ch/.* Accessed June 2014

IRIN. Burkina Faso: Population Growth Outstrips Economic Gains. 2009. Available online: *http://www.irinnews.org/report/82501/* (accessed on 8 December 2019).

Jackson, R.B., Canadell, J., Ehleringer, J.R., Mooney, H.A., Sala, O.E., Schulze, E.D., 1996. A global analysis of root distributions for terrestrial biomes. *Oecologia* 108, 389–411.

Jacobs, C.M.J., van den Hurk, B.M.M., de Bruin, H.A.R., 1996. Stomatal behaviour and photosynthetic rate of unstressed grapevines in semi-arid conditions. *Agricultural and*

Forest Meteorology 80, 111–134. https://doi.org/10.1016/0168-1923(95)02295-3

Jarvis, P.G., 1976. The Interpretation of the Variations in Leaf Water Potential and Stomatal Conductance Found in Canopies in the Field. Philosophical Transactions of the Royal Society B: *Biological Sciences* 273, 593–610. https://doi.org/10.1098/rstb.1976.0035

Jenkins G.S., Gaye A.T., Sylla B. 2005 Late 20th century attribution of drying trends in the Sahel from the regional climate model (RegCM3). *Geophys Res Lett* 32:L22705. doi:10.1029/2005GL024225

Jones C, Hughes J, Bellouin N, Hardiman S, Jones G, Knight J, et al. (2011) The HadGEM2-ES implementation of CMIP5 centennial simulations. *Geosci Model Dev* 4:543–570. doi:10.5194/gmd-4-543-2011

Joiner, J., Yoshida, Y., Guanter, L., Middleton, E.M., 2016. New methods for the retrieval of chlorophyll red fluorescence from hyperspectral satellite instruments: simulations andapplication to GOME-2 and SCIAMACHY. *Atmos. Meas. Tech.* 9, 3939–3967. https://doi.org/10.5194/amt-9-3939-2016

Jung, M., Reichstein, M., Schwalm, C.R., Huntingford, C., Sitch, S., Ahlström, A., Arneth, A., Camps-Valls, G., Ciais, P., Friedlingstein, P., 2017. Compensatory water effects link yearly global land CO 2 sink changes to temperature. *Nature* 541, 516.

Kalma, J.D., McVicar, T.R., McCabe, M.F., 2008. Estimating Land Surface Evaporation: A Review of Methods Using Remotely Sensed Surface Temperature Data. *Surv Geophys* 29, 421–469. https://doi.org/10.1007/s10712-008-9037-z

Kalman, R. E. 1960. A new approach to linear filtering and prediction problems. Transaction of the ASME - *Journal of Basic Engineering*, 82, 35-45.

Kaminski, T., Knorr, W., Rayner, P.J., Heimann, M., 2002. Assimilating atmospheric data into a terrestrial biosphere model: A case study of the seasonal cycle. *Global Biogeochemical Cycles* 16, 14-1-14–16.

Keenan, T. F., Carbone, M. S., Reichstein, M. & Richardson, A. D. 2011. The model–data fusion pitfall: assuming certainty in an uncertain world. Oecologia, 167, 587-597.

Kergoat, L., Guichard, F., Pierre, C., Vassal, C., 2017. Influence of dry-season vegetation variability on Sahelian dust during 2002–2015. *Geophysical Research Letters* 44, 5231–5239.

Kerr, Y.H., 2007. Soil moisture from space: Where are we? *Hydrogeology journal* 15, 117–120.

Kerr, Y.H., Waldteufel, P., Wigneron, J.-P., Martinuzzi, J., Font, J., Berger, M., 2001. Soil moisture retrieval from space: The Soil Moisture and Ocean Salinity (SMOS) mission. *IEEE transactions on Geoscience and remote sensing* 39, 1729–1735.

Kinnell, P.I.A., 2010. Event soil loss, runoff and the Universal Soil Loss Equation family of models: A review. *Journal of Hydrology* 385, 384–397. https://doi.org/10.1016/j.jhydrol.2010.01.024

Koster, R.D., Guo, Z., Yang, R., Dirmeyer, P.A., Mitchell, K., Puma, M.J., 2009. On the nature of soil moisture in land surface models. *Journal of Climate* 22, 4322–4335.

Koster, R.D., Mahanama, S.P.P., Yamada, T.J., Balsamo, G., Berg, A.A., Boisserie, M., Dirmeyer, P.A., Doblas-Reyes, F.J., Drewitt, G., Gordon, C.T., 2011. The second phase of the global land–atmosphere coupling experiment: soil moisture contributions to subseasonal forecast skill. *Journal of Hydrometeorology* 12, 805–822.

Koster, R.D., Milly, P.C.D., 1997. The Interplay between Transpiration and Runoff Formulations in Land Surface Schemes Used with Atmospheric Models. *J. Climate* 10, 1578–1591. https://doi.org/10.1175/1520-0442(1997)010<1578:TIBTAR>2.0.CO;2

Koster, R.D., Suarez, M.J., Liu, P., Jambor, U., Berg, A., Kistler, M., Reichle, R., Rodell, M., Famiglietti, J., 2004. Realistic Initialization of Land Surface States: Impacts on Subseasonal Forecast Skill. *J. Hydrometeor.* 5, 1049–1063. https://doi.org/10.1175/JHM-387.1

Kumar, S.V., Jasinski, M., Mocko, D., Rodell, M., Borak, J., LI, B., Kato Beaudoing, H., Peters-Lidard, C.D., 2018. NCA-LDAS land analysis: Development and performance of a multisensor, multivariate land data assimilation system for the National Climate Assessment. *Journal of Hydrometeorology.*

Kumar, S.V., Jasinski, M., Mocko, D.M., Rodell, M., Borak, J., Li, B., Beaudoing, H.K., Peters-Lidard, C.D., 2019. NCA-LDAS Land Analysis: Development and Performance of a Multisensor, Multivariate Land Data Assimilation System for the National Climate Assessment. *J. Hydrometeor.* 20, 1571–1593. https://doi.org/10.1175/JHM-D-17-0125.1

Ladson, A., Weinmann, E., 2008. Hydrology – An Australian Introduction. Australasian Journal of Water Resources 12, 71–72. https://doi.org/10.1080/13241583.2008.11465335

Lal, R., 2001. Soil degradation by erosion. *Land Degrad. Dev.* 12, 519–539. https://doi.org/10.1002/ldr.472

Leroux, D., Calvet, J.-C., Munier, S., Albergel, C., 2018. Using Satellite-Derived Vegetation Products to Evaluate LDAS-Monde over the Euro-Mediterranean Area. *Remote Sensing* 10, 1199.

Le Moigne, P., Boone, A., Calvet, J.-C., Decharme, B., Faroux, S. et al. : SURFEX scientific documentation, Groupe de météorologie à moyenne échelle, *note de centre*, 87, 211p.,

2009.

Lian, X., Piao, S., Huntingford, C. *et al.* Partitioning global land evapotranspiration using CMIP5 models constrained by observations. *Nature Clim Change* **8,** 640–646 2018. https://doi.org/10.1038/s41558-018-0207-9

Li, J., Islam, S., 1999. On the estimation of soil moisture profile and surface fluxes partitioning from sequential assimilation of surface layer soil moisture. *Journal of Hydrology* 220, 86–103. https://doi.org/10.1016/S0022-1694(99)00066-9

Lievens, H., De Lannoy, G.J.M., Al Bitar, A., Drusch, M., Dumedah, G., Franssen, H.-J.H., Kerr, Y.H., Tomer, S.K., Martens, B., Merlin, O., 2016. Assimilation of SMOS soil moisture and brightness temperature products into a land surface model. *Remote sensing of environment* 180, 292–304.

Liu, Q., Reichle, R.H., Bindlish, R., Cosh, M.H., Crow, W.T., de Jeu, R., De Lannoy, G.J.M., Huffman, G.J., Jackson, T.J., 2011. The Contributions of Precipitation and Soil Moisture Observations to the Skill of Soil Moisture Estimates in a Land Data Assimilation System. *J. Hydrometeor.* 12, 750–765. https://doi.org/10.1175/JHM-D-10-05000.1

Loarie SR, Duffy PB, Hamilton H, Asner GP, Field CB, Ackerly DD (2009) The velocity of climate change. Nature 462:1052–1055

Lobell DB, BänzigerM,Magorokosho C, Vivek B (2011) Nonlinear heat effects on African maize as evidenced by historical yield trials. *Nat Climate Change* 1:42–45. doi:10.1038/nclimate1043

Louvet, S., Pellarin, T., Al Bitar, A., Cappelaere, B., Galle, S., Grippa, M., & Mougin, E. 2015. SMOS soil moisture product evaluation over West-Africa from local to regional scale. *Remote Sensing of Environment*, 156, 383-394.

MA 2017: Ministry of Agriculture. Climatic and Agro-ecological Zones of Burkina Faso; *Ministry of Agriculture*: Ouagadougou, Burkina Faso, 2017.

Mahfouf, J.-F., 2010. Assimilation of satellite-derived soil moisture from ASCAT in a limited-area NWP model. *Quarterly Journal of the Royal Meteorological Society*: A journal of the atmospheric sciences, applied meteorology and physical oceanography 136, 784–798.

Mahfouf, J.-F., Bergaoui, K., Draper, C., Bouyssel, F., Taillefer, F., Taseva, L., 2009. A comparison of two off-line soil analysis schemes for assimilation of screen level observations. *Journal of Geophysical Research: Atmospheres* 114.

Martin E., Le Moigne P., and Masson V. Le code de surface externalisée SURFEX de Météo-France. *In Ateliers de Modélisation de l'Atmosphère*, 2007.

Manabe, S., 1969. Climate and the ocean circulation. *Mon. Wea. Rev.* 97, 739–774. https://doi.org/10.1175/1520-0493(1969)097<0739:CATOC>2.3.CO;2

Margulis, S.A., McLaughlin, D., Entekhabi, D., Dunne, S., 2002. Land data assimilation and estimation of soil moisture using measurements from the Southern Great Plains 1997 Field Experiment: SOIL MOISTURE ESTIMATION USING THE EnKF. *Water Resour. Res.* 38, 35-1-35–18. https://doi.org/10.1029/2001WR001114

Mariotti, L., Diallo, I., Coppola, E., Giorgi, F. 2014 Seasonal and intraseasonal changes of African monsoon climates in 21st century CORDEX projections. *Clim Chang.* doi:10.1007/s10584-014-1097-0

Martens, B., Gonzalez Miralles, D., Lievens, H., Van Der Schalie, R., De Jeu, R.A., Fernández-Prieto, D., Beck, H.E., Dorigo, W., Verhoest, N., 2017. GLEAM v3: Satellite-based land evaporation and root-zone soil moisture. *Geoscientific Model Development* 10, 1903–1925.

Masson, V., Champeaux, J.-L., Chauvin, F., Meriguet, C., Lacaze, R., 2003. A Global Database of Land Surface Parameters at 1-km Resolution in Meteorological and Climate Models. *J. Climate* 16, 1261–1282. https://doi.org/10.1175/1520-0442(2003)16<1261:AGDOLS>2.0.CO;2

Masson, V., Le Moigne, P., Martin, E., Faroux, S., Alias, A., Alkama, R., Belamari, S., Barbu, A., Boone, A., Bouyssel, F., 2013. The SURFEXv7. 2 land and ocean surface platform for coupled or offline simulation of earth surface variables and fluxes. *Geoscientific Model Development* 6, 929–960.

Maybeck, P.S., 1988. Stochastic models, estimation, and control. Vol. 1: ..., 5. print. ed, Mathematics in science and engineering. *Acad. Press*, New York.

McKenzie, N.J., Jacquier, D.W., Ashton, L.J., Cresswell, H.P., 2000. Estimation of soil properties using the Atlas of Australian Soils. *CSIRO Land and Water Technical Report* 11, 1–12.

MEE - Ministère de l'Environnement et de l'Eau, 1998 : Politique et stratégies en matière d'eau - Adopté par le Conseil des Ministres en sa séance du 1° Juillet 1998, Ouagadougou, Burkina Faso, Juillet 1998, 119p.

Mertens, J., Madsen, H., Kristensen, M., Jacques, D., Feyen, J., 2005. Sensitivity of soil parameters in unsaturated zone modelling and the relation between effective, laboratory and in situ estimates. *Hydrological Processes*: An International Journal 19, 1611–1633.

Meterological Agency. Rainfall and Temperature Data of Burkina Faso; Meterological Agency: Ouagadougou, Burkina Faso, 2018.

Milly, P.C.D., Shmakin, A.B., 2002. Global Modeling of Land Water and Energy Balances. Part II: Land-Characteristic Contributions to Spatial Variability. *J. Hydrometeor.* 3, 301–310. https://doi.org/10.1175/1525-7541 (2002)003<0301: GMOLWA>2.0.CO; 2

Miralles, D.G., Teuling, A.J., Van Heerwaarden, C.C., de Arellano, J.V.-G., 2014. Mega-heatwave temperatures due to combined soil desiccation and atmospheric heat accumulation. *Nature Geoscience* 7, 345.

Moran, M.S., Peters-Lidard, C.D., Watts, J.M., McElroy, S., 2004. Estimating soil moisture at the watershed scale with satellite-based radar and land surface models. *Canadian Journal of Remote Sensing* 30, 805–826. https://doi.org/10.5589/m04-043

Moss RH, Edmonds JA, Hibbard KA, Manning MR, Rose SK, van Vuuren DP, Carter TR, Emori S, Kainuma M, Kram T, et al. (2010) The next generation of scenarios for climate change research and assessment. *Nature* 463:747–756

Munier, S., Carrer, D., Planque, C., Camacho, F., Albergel, C., Calvet, J.-C., 2018. Satellite Leaf Area Index: global scale analysis of the tendencies per vegetation type over the last 17 years. *Remote Sensing* 10, 424.

Munro, R.; Eisinger, M.; Anderson, C.; Callies, J.; Corpaccioli, E.; Lang, R.; Lefebvre, A.; Livschitz, Y.; Perez Albinana, A. GOME-2 on MetOp: From In-Orbit Verification to Routine Operations. *In Proceedings of the EUMETSAT Meteorological Satellite Conference*, Helsinki, Finland, 12–16 June 2006.

Njoku, E.G., Jackson, T.J., Lakshmi, V., Chan, T.K., Nghiem, S.V., 2003. Soil moisture retrieval from AMSR-E. IEEE transactions on Geoscience and remote sensing 41, 215–229.

Noilhan, J., Mahfouf, J.-F., 1996. The ISBA land surface parameterisation scheme. *Global and planetary Change* 13, 145–159.

Noilhan, J., Planton, S., 1989. A simple parameterization of land surface processes for meteorological models. *Monthly weather review* 117, 536–549.

Overgaard, J., Rosbjerg, D., Butts, M.B., 2006. Land-surface modelling in hydrological perspective ? a review. *Biogeosciences* 3, 229–241.

Owe, M., de Jeu, R., Holmes, T., 2008. Multisensor historical climatology of satellite-derived global land surface moisture. *Journal of Geophysical Research*: Earth Surface 113.

Pagán, B.R., Maes, W.H., Gentine, P., Martens, B., Miralles, D.G., 2019. Exploring the Potential of Satellite Solar-Induced Fluorescence to Constrain Global Transpiration Estimates. *Remote Sensing* 11, 413.

Parry ML, Canziani OF, Palutikof JP, van der Linden PJ, Hanson CE (eds) Climate change 2007: impacts, adaptation and vulnerability. (Contribution of Working Group II to the

Fourth Assessment Report of the Intergovernmental Panel on Climate Change) *Cambridge University Press*, Cambridge.

Peters-Lidard, C.D., Kumar, S.V., Mocko, D.M., Tian, Y., 2011. Estimating evapotranspiration with land data assimilation systems: ESTIMATING EVAPOTRANSPIRATION WITH LAND DATA ASSIMILATION SYSTEMS. *Hydrol. Process.* 25, 3979–3992. https://doi.org/10.1002/hyp.8387

Peugeot, C.;, 2018. *Personal communication*, December.

Pielke, R.A., Sr, Avissar, R., Raupach, M., Dolman, A.J., Zeng, X., Denning, A.S., 1998. Interactions between the atmosphere and terrestrial ecosystems: influence on weather and climate. *Global Change Biology* 4, 461–475. https://doi.org/10.1046/j.1365-2486.1998.t01-1-00176.x

Pierre, C., Grippa, M., Mougin, E., Guichard, F., Kergoat, L., 2016. Changes in Sahelian annual vegetation growth and phenology since 1960: A modeling approach. *Global and Planetary Change* 143, 162–174.

Pinnington, E., Quaife, T., Black, E., 2018. Impact of remotely sensed soil moisture and precipitation on soil moisture prediction in a data assimilation system with the JULES land surface model. *Hydrology and Earth System Sciences* 22, 2575–2588.

Pitman, A.J., 2003. The evolution of, and revolution in, land surface schemes designed for climate models. *International Journal of Climatology*: A Journal of the Royal Meteorological Society 23, 479–510.

Richard W., Seneviratne, S. I., Hirschi, M., Chang, J., Ciais, P., Deryng, D., ... & Henrot, A. J. (2018). Evapotranspiration simulations in ISIMIP2a—Evaluation of spatio-temporal characteristics with a comprehensive ensemble of independent datasets. *Environmental Research Letters*, *13*(7), 075001.

Reichle, R.H., 2005. Global assimilation of satellite surface soil moisture retrievals into the NASA Catchment land surface model. Geophys. *Res. Lett.* 32, L02404. https://doi.org/10.1029/2004GL021700

Reichle, R.H., Crow, W.T., Koster, R.D., Sharif, H.O., Mahanama, S.P.P., 2008. Contribution of soil moisture retrievals to land data assimilation products. *Geophysical Research Letters* 35.

Reichle, R.H., Koster, R.D., 2004. Bias reduction in short records of satellite soil moisture. *Geophysical Research Letters* 31.

Reichle, R.H., Koster, R.D., Dong, J., Berg, A.A., 2004. Global soil moisture from satellite observations, land surface models, and ground data: Implications for data assimilation.

Journal of Hydrometeorology 5, 430–442.

Reichle, R.H., Koster, R.D., Liu, P., Mahanama, S.P., Njoku, E.G., Owe, M., 2007. Comparison and assimilation of global soil moisture retrievals from the Advanced Microwave Scanning Radiometer for the Earth Observing System (AMSR-E) and the Scanning Multichannel Microwave Radiometer (SMMR). *Journal of Geophysical Research: Atmospheres* 112.

Reichle, R.H., Walker, J.P., Koster, R.D., Houser, P.R., 2002. Extended versus Ensemble Kalman Filtering for Land Data Assimilation. *J. Hydrometeor.* 3, 728–740. https://doi.org/10.1175/1525-7541(2002)003<0728:EVEKFF>2.0.CO;2

Riahi K, Krey V, Rao S, Chirkov V, Fischer G, Kolp P, Kindermann G, Nakicenovic N, Rafai P (2011) RCP8.5: Exploring the consequence of high emission trajectories. *Clim Chang.* doi:10.1007/s10584-011-0149-y

Richards, L.A., 1931. Capillary conduction of liquids through porous mediums. *Physics* 1, 318–333.

Richter, H., Western, A.W., Chiew, F.H.S., 2004. The Effect of Soil and Vegetation Parameters in the ECMWF Land Surface Scheme. *J. Hydrometeor.* 5, 1131–1146. https://doi.org/10.1175/JHM-362.1

Rivalland, V., Calvet, J.-Ch., Berbigier, P., Brunet, Y., Granier, A., 2005. Transpiration and CO2 fluxes of a pine forest: modelling the undergrowth effect. *Annales Geophysicae* 23, 291–304.

Rodell, M., Houser, P.R., Jambor, U.E.A., Gottschalck, J., Mitchell, K., Meng, C.-J., Arsenault, K., Cosgrove, B., Radakovich, J., Bosilovich, M., 2004. The global land data assimilation system. *Bulletin of the American Meteorological Society* 85, 381–394.

Rüdiger, C., Albergel, C., Mahfouf, J.-F., Calvet, J.-C., and, Walker, J. P., 2010. Evaluation of Jacobians for Leaf Area Index data assimilation with an extended Kalman filter. *J. Geophys. Res.* https://doi.org/10.1029/2009JD012912, 2010

Sabater, J.M., Rüdiger, C., Calvet, J.-C., Fritz, N., Jarlan, L., Kerr, Y., 2008. Joint assimilation of surface soil moisture and LAI observations into a land surface model. *Agricultural and Forest Meteorology* 148, 1362–1373. https://doi.org/10.1016/j.agrformet.2008.04.003

Sarrat, C., Noilhan, J., Lacarrère, P., Ceschia, E., Ciais, P., Dolman, A., Elbers, J.A., Gerbig, C., Gioli, B., Lauvaux, T., Miglietta, F., Neininger, B., Ramonet, M., Vellinga, O., Bonnefond, J.-M., 2009. Mesoscale modelling of the CO2 interactions between the surface and the atmosphere applied to the April 2007 CERES field experiment.

Biogeosciences 6, 633–646.

Sawada, Y., 2018. Quantifying Drought Propagation from Soil Moisture to Vegetation Dynamics Using a Newly Developed Ecohydrological Land Reanalysis. *Remote Sensing* 10, 1197.

Sawada, Y., Koike, T., 2014. Simultaneous estimation of both hydrological and ecological parameters in an ecohydrological model by assimilating microwave signal. *Journal of Geophysical Research: Atmospheres* 119, 8839–8857.

Sawada, Y., Koike, T., Walker, J.P., 2015. A land data assimilation system for simultaneous simulation of soil moisture and vegetation dynamics. *Journal of Geophysical Research: Atmospheres* 120, 5910–5930.

Schellekens, J., Dutra, E., la Torre, A. M. D., Balsamo, G., van Dijk, A., Weiland, F. S., Fink, G. (2017). A global water resources ensemble of hydrological models: The eartH2Observe Tier-1 dataset. *Earth System Science Data*, *9*, 389-413.

Scipal, K., Drusch, M., Wagner, W., 2008. Assimilation of a ERS scatterometer derived soil moisture index in the ECMWF numerical weather prediction system. *Advances in water resources* 31, 1101–1112.

Sellers, P.J., Dickinson, R.E., Randall, D.A., Betts, A.K., Hall, F.G., Berry, J.A., Collatz, G.J., Denning, A.S., Mooney, H.A., Nobre, C.A., Sato, N., Field, C.B., Henderson-Sellers, A., 1997. Modeling the Exchanges of Energy, Water, and Carbon Between Continents and the Atmosphere. *Science* 275, 502–509. https://doi.org/10.1126/science.275.5299.502

Sellers, P.J., Mintz, Y., Sud, Y.C., Dalcher, A., 1986. A Simple Biosphere Model (SIB) for Use within General Circulation Models. *J. Atmos. Sci.* 43, 505–531. https://doi.org/10.1175/1520-0469(1986)043<0505:ASBMFU>2.0.CO;2

Simonsson, L., Stockholm Environment Institute, 2005. Vulnerability profile of Burkina Faso. *Stockholm Environment Institute (SEI)*, Stockholm.

Sivakumar, M.V.K., 2007. Interactions between climate and desertification. *Agricultural and Forest Meteorology* 142, 143–155. https://doi.org/10.1016/j.agrformet.2006.03.025

Slingo, A., White, H.E., Bharmal, N.A., Robinson, G.J., 2009. Overview of observations from the RADAGAST experiment in Niamey, Niger: 2. Radiative fluxes and divergences. *Journal of Geophysical Research: Atmospheres* 114.

Su, C.-H., Ryu, D., Young, R.I., Western, A.W., Wagner, W., 2013. Inter-comparison of microwave satellite soil moisture retrievals over the Murrumbidgee Basin, southeast Australia. *Remote Sensing of Environment* 134, 1–11.

https://doi.org/10.1016/j.rse.2013.02.016

Sylla M.B., Gaye A.T., Jenkins G.S., Pal J.S., Giorgi F. 2010 Consistency of projected drought over the Sahel with changes in the monsoon circulation and extremes in a regional climate model projection. *J Geophys Res* 115:D16108. doi:10.1029/2009JD012983

Sylla M.B., Gaye AT, Jenkins GS 2012. On the fine-scale topography regulating changes in atmospheric hydrological cycle and extreme rainfall overWest Africa in a regional climate model projections. *Int J Geophys.* doi:10.1155/2012/981649

Sylla M.B., Pal J.S., Wang J.L., Lawrence P. 2015a Impact of land surface characterization on regional climate modeling over West Africa. *Clim Dyn*. doi:10.1007/s00382-015-2603-4

Sylla, M.B., Elguindi N, Giorgi F, Wisser D. 2016 Projected robust shift of climate zones overWest Africa in response to anthropogenic climate change for the late 21st century. *Clim Chang* 134(1–2):241–253

Sylla, M.B., Pal, J.S., Faye, A. *et al.* Climate change to severely impact West African basin scale irrigation in 2 °C and 1.5 °C global warming scenarios. *Sci Rep* 8, 14395 2018. https://doi.org/10.1038/s41598-018-32736-0

Taylor, C.M., Gounou, A., Guichard, F., Harris, P.P., Ellis, R.J., Couvreux, F., De Kauwe, M., 2011. Frequency of Sahelian storm initiation enhanced over mesoscale soil-moisture patterns. *Nature Geoscience* 4, 430.

Taylor K.E., Stouffer RJ, Meehl GA 2012 An overview of CMIP5 and the experiment design. *Bull Am Meteor Soc* 93:485–498

Thomson A.M., Calvin KV, Smith SJ, Kyle GP, Volke A, Patel P, Delgado-Arias S, Bond-Lamberty B, Wise MA, Clarke LE, Edmonds JA 2011 RCP4.5: A pathway for stabilization of radiative forcing by 2100. *Clim Chang.* doi:10.1007/s10584-011-0151-4

Thornthwaite C., Mather J. 1955 The water balance. *Publ Climatol* 8:1–104.

Topp, G.C., Davis, J.L., Annan, A.P., 1980. Electromagnetic determination of soil water content: Measurements in coaxial transmission lines. *Water Resources Research* 16, 574–582. https://doi.org/10.1029/WR016i003p00574

Toy, T.J., Foster, G.R., Renard, K.G., 2002. Soil Erosion: Processes, Prediction, Measurement, and Control. *John Wiley & Sons*.

Ulaby, F.T.M., 1986. Microwave remote sensing: Active and passive. *Volume 3 - From theory to applications*.

Ulaby, F.T.M., 1982. Microwave remote sensing: Active and passive. *Volume 2 - Radar remote*

sensing and surface scattering and emission theory.

United Nations Environmental Programme (UNEP). *Global Environment Outlook 4: UNEP; UNEP:* Valletta, Malta, 2012.

Urraca, R., Huld, T., Gracia-Amillo, A., Martinez-de-Pison, F.J., Kaspar, F., Sanz-Garcia, A., 2018. Evaluation of global horizontal irradiance estimates from ERA5 and COSMO-REA6 reanalyses using ground and satellite-based data. *Solar Energy* 164, 339–354.

Van Den Hurk, B., Jia, L., Jacobs, C., Menenti, M., Li, Z.-L., 2002. Assimilation of land surface temperature data from ATSR in an NWP environment--a case study. *International Journal of Remote Sensing* 23, 5193–5209.

Van Genuchten, M.Th., 1980. A Closed-form Equation for Predicting the Hydraulic Conductivity of Unsaturated Soils. *Soil Science Society of America Journal* 44, 892–898. https://doi.org/10.2136/sssaj1980.03615995004400050002x

Van Vuuren DP, Edmonds J, Kainuma MLT, Riahi K, et al. (2011) Representative concentration pathways: an overview. *Clim Chang.* doi:10.1007/s10584-011-0148-z

Vicente-Serrano, S. M., Miralles, D. G., Domínguez-Castro, F., Azorin-Molina, C., El Kenawy, A., McVicar, T. R. & Peña-Gallardo, M. (2018). Global assessment of the Standardized Evapotranspiration Deficit Index (SEDI) for drought analysis and monitoring. *Journal of Climate*, *31*(14), 5371-5393.

Viterbo, P., Beljaars, A.C.M., 1995. An Improved Land Surface Parameterization Scheme in the ECMWF Model and Its Validation. *J. Climate* 8, 2716–2748. https://doi.org/10.1175/1520-0442(1995)008<2716:AILSPS>2.0.CO;2

Vrugt, J.A., Gupta, H.V., Nualláin, B., Bouten, W., 2006. Real-Time Data Assimilation for Operational Ensemble Streamflow Forecasting. *J. Hydrometeor.* 7, 548–565. https://doi.org/10.1175/JHM504.1

Wagner, W., Blöschl, G., Pampaloni, P., Calvet, J.-C., Bizzarri, B., Wigneron, J.-P., Kerr, Y., 2007. Operational readiness of microwave remote sensing of soil moisture for hydrologic applications. *Hydrology Research* 38, 1–20.

Wagner, W., Hahn, S., Kidd, R., Melzer, T., Bartalis, Z., Hasenauer, S., Figa-Saldaña, J., de Rosnay, P., Jann, A., Schneider, S., 2013. The ASCAT soil moisture product: A review of its specifications, validation results, and emerging applications. *Meteorologische Zeitschrift* 22, 5–33.

Wagner, W., Lemoine, G., Rott, H., 1999. A Method for Estimating Soil Moisture from ERS Scatterometer and Soil Data. *Remote Sensing of Environment* 70, 191–207. https://doi.org/10.1016/S0034-4257(99)00036-X

Walker, J.P., Houser, P.R., 2004. Requirements of a global near-surface soil moisture satellite mission: accuracy, repeat time, and spatial resolution. *Advances in Water Resources* 27, 785–801. https://doi.org/10.1016/j.advwatres.2004.05.006

Walker, J.P., Houser, P.R., Houser, P.R., 2005. Hydrologic Data Assimilation [WWW Document]. *Advances in Water Science Methodologies.* https://doi.org/10.1201/9780203086841-12

Wang, K., Liang, S., 2009. Evaluation of ASTER and MODIS land surface temperature and emissivity products using long-term surface longwave radiation observations at SURFRAD sites. *Remote Sensing of Environment*, Monitoring Protected Areas 113, 1556–1565. https://doi.org/10.1016/j.rse.2009.03.009

Waongo, M., Laux, P., Traoré, S.B., Sanon, M., Kunstmann, H., 2014. A crop model and fuzzy rule-based approach for optimizing maize planting dates in Burkina Faso, West Africa. *Journal of Applied Meteorology and Climatology* 53, 598–613.

Weiss, M., Baret, F., Myneni, R., Pragnère, A., & Knyazikhin, Y. 2000. Investigation of a model inversion technique to estimate canopy biophysical variables from spectral and directional reflectance data.

Williams, J., Ross, P. J. & Bristow, K. L. Prediction of the Campbell water retention function from texture, structure and organic matter. In: Van Genuchten, M. T., Leij, F. J. & Lund, L. J., eds. *Proceedings of the International Workshop on Indirect Methods for Estimating the Hydraulic Properties of Unsaturated Soils*, 1992 University of California, Riverside, California. 427-441.

Willmott C, Feddema J (1992) A more rational climatic moisture index. *Prof Geogr* 44(1):84–88.

Wilson CO,Weng Q (2011) Simulating the impact of future land use and climate changes on surface water quality in the Des Plaines River watershed Chicago metropolitan statistical area Illinois. *Sci Total Environ* 409(20):4387–4405

World Bank Country and Lending Groups". datahelpdesk.worldbank.org. *World Bank*. Retrieved 29 September 2019

Yates, D.N., Chen, F., Nagai, H., 2003. Land surface heterogeneity in the Cooperative Atmosphere Surface Exchange Study (CASES-97). Part II: Analysis of spatial heterogeneity and its scaling. *Journal of Hydrometeorology* 4, 219–234.

Zhang, Y., Peña-Arancibia, J.L., McVicar, T.R., Chiew, F.H., Vaze, J., Liu, C., Lu, X., Zheng, H., Wang, Y., Liu, Y.Y., 2016. Multi-decadal trends in global terrestrial evapotranspiration and its components. *Scientific reports* 6, 19124.

Yu, M., Wang, G. & Pal, J.S. Effects of vegetation feedback on future climate change over West Africa. *Clim Dyn* 46, 3669–3688 (2016). https://doi.org/10.1007/s00382-015-2795-7

Zhan, S., Song, C., Wang, J., Sheng, Y., & Quan, J. (2019). A global assessment of terrestrial evapotranspiration increase due to surface water area change. *Earth's future*, 7(3), 266-282.

Annexe 1: List of figures

A1.1: *Annual average maps of LAI [$m^2 \cdot m^{-2}$] over January 2001 to June 2018. From left to right: LAI model, LAI analysis, LAI analysis-model difference.*

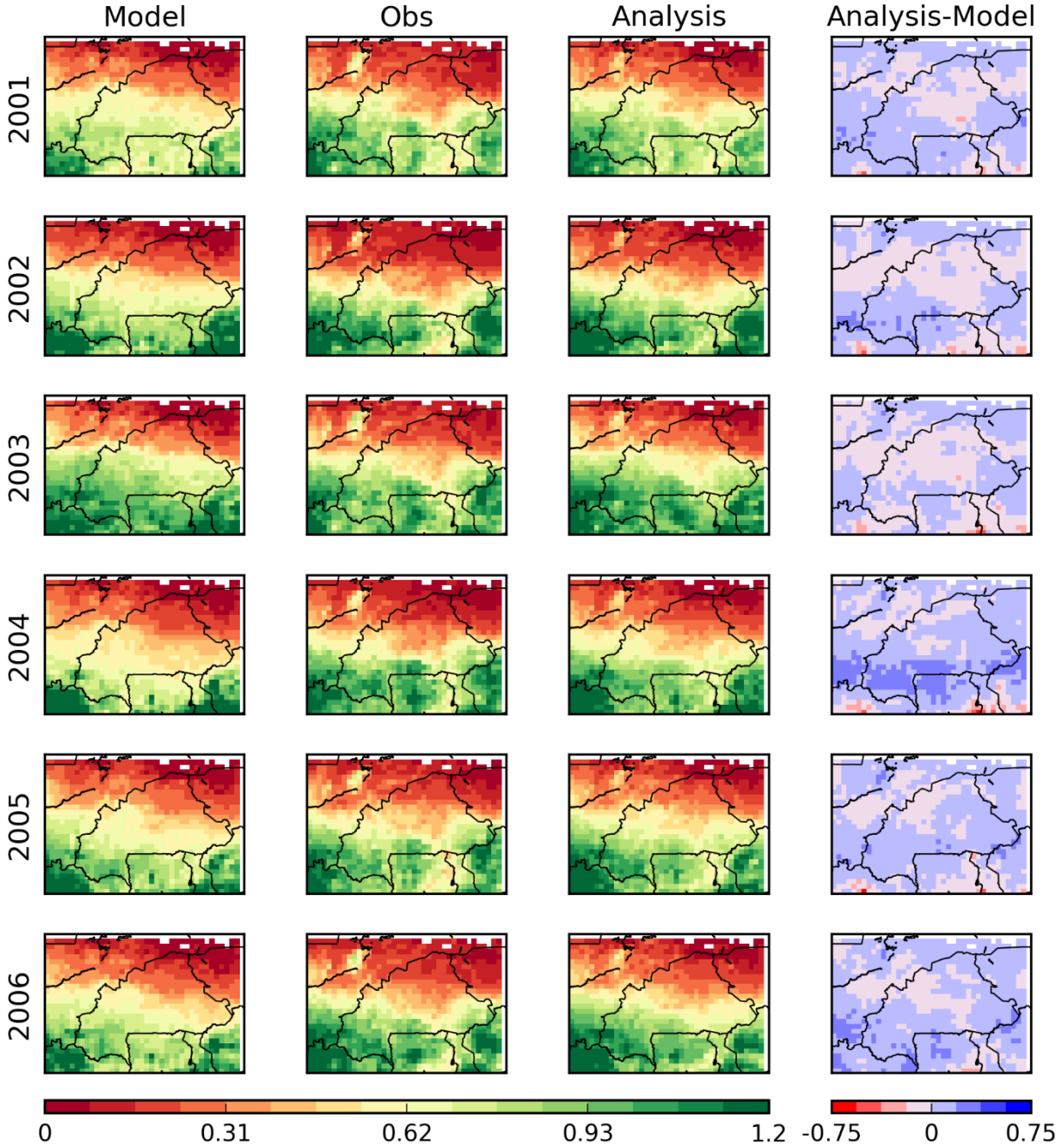

A1.2: *ctd.*

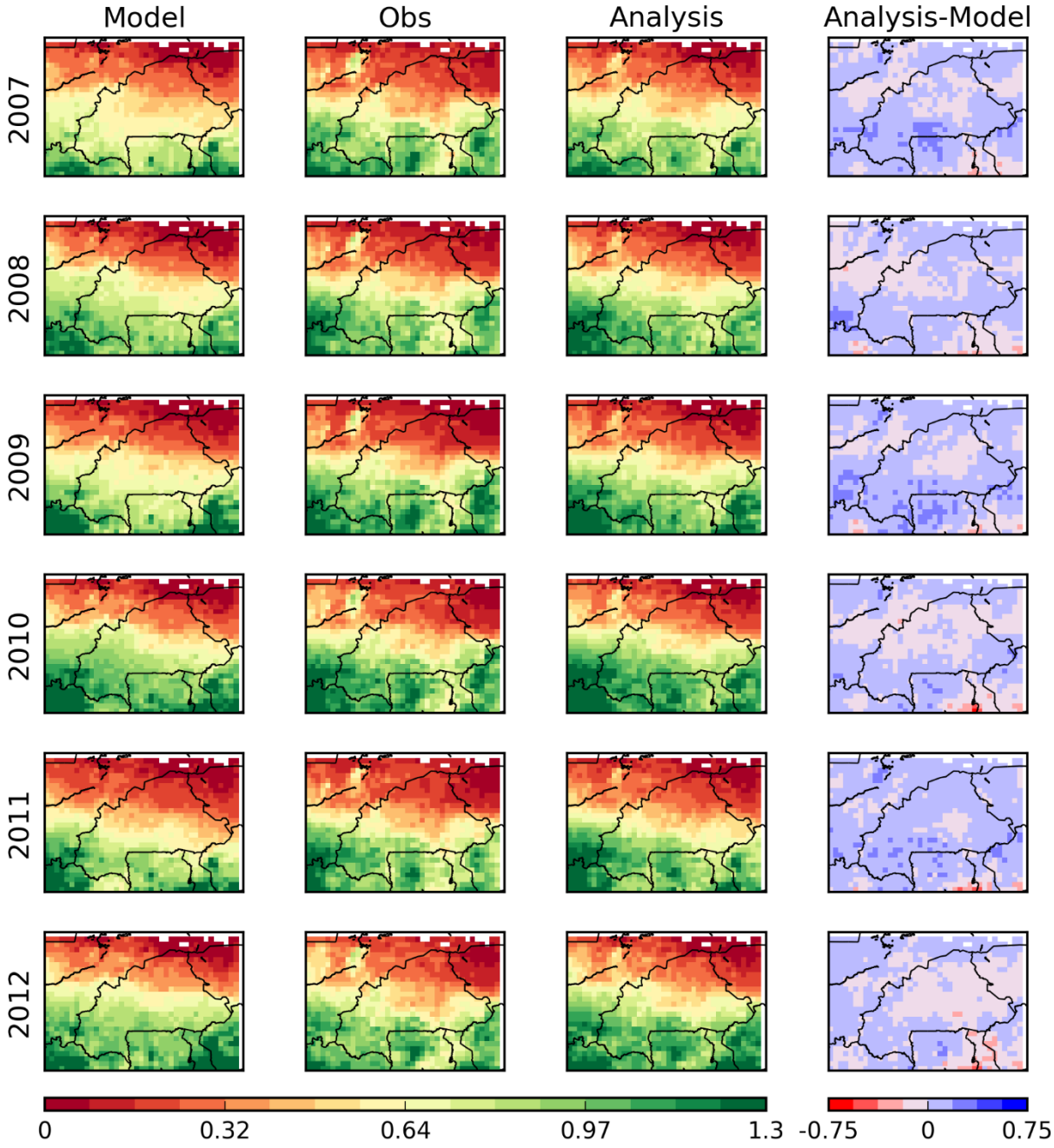
Model
Obs
Analysis
Analysis-Model
2007
2008
2009
2010
2011
2012
0
0.32
0.64
0.97
1.3
-0.75
0
0.75

A1.3: *ctd.*

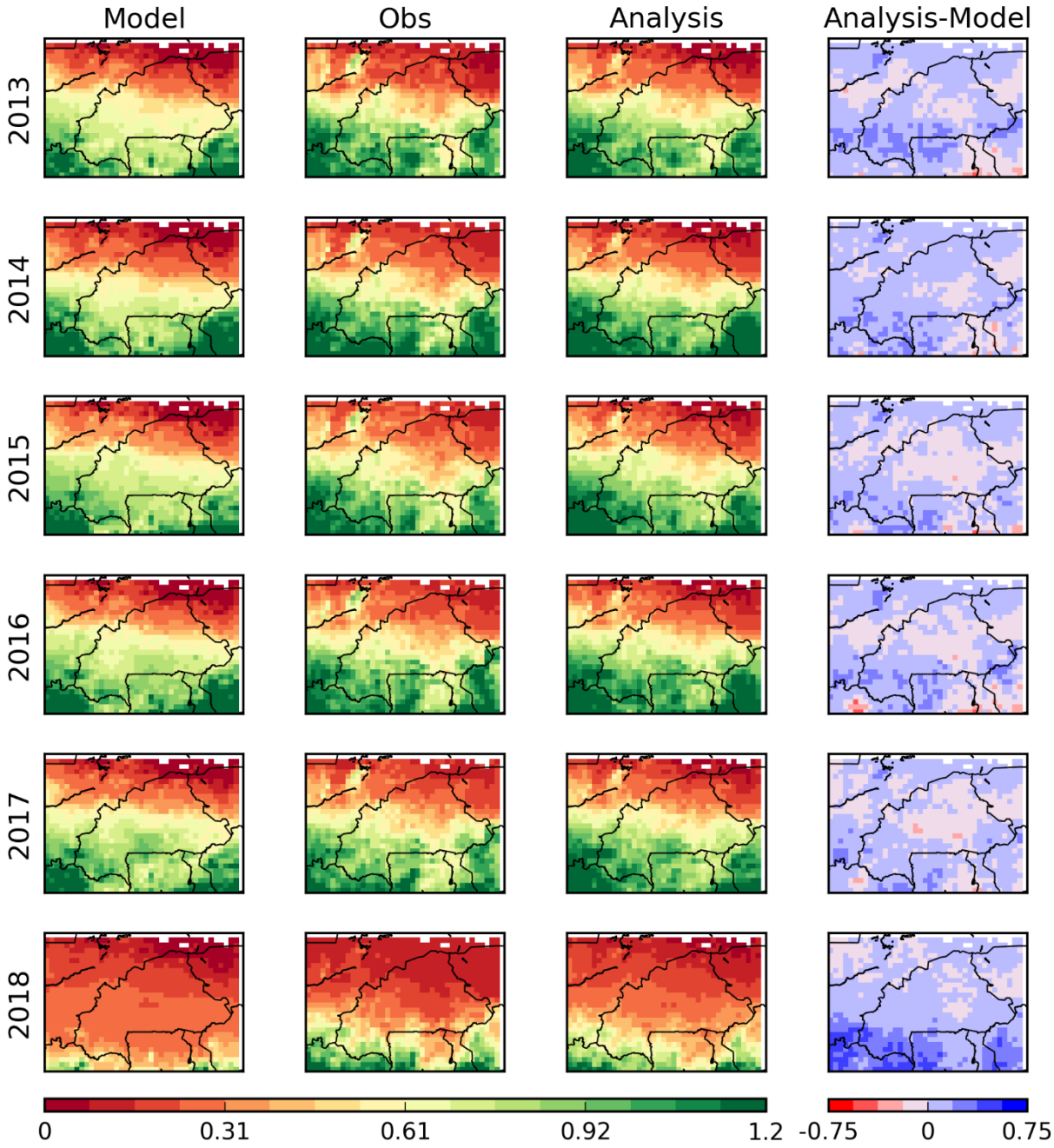
Model
Obs
Analysis
Analysis-Model
2013
2014
2015
2016
2017
2018
0
0.31
0.61
0.92
1.2
-0.75
0
0.75

A1.4: *Annual average maps SSM [$m^3 \cdot m^{-3}$] over January 2001 to June 2018. From left to right: SSM model, SSM analysis, SSM analysis-model difference.*

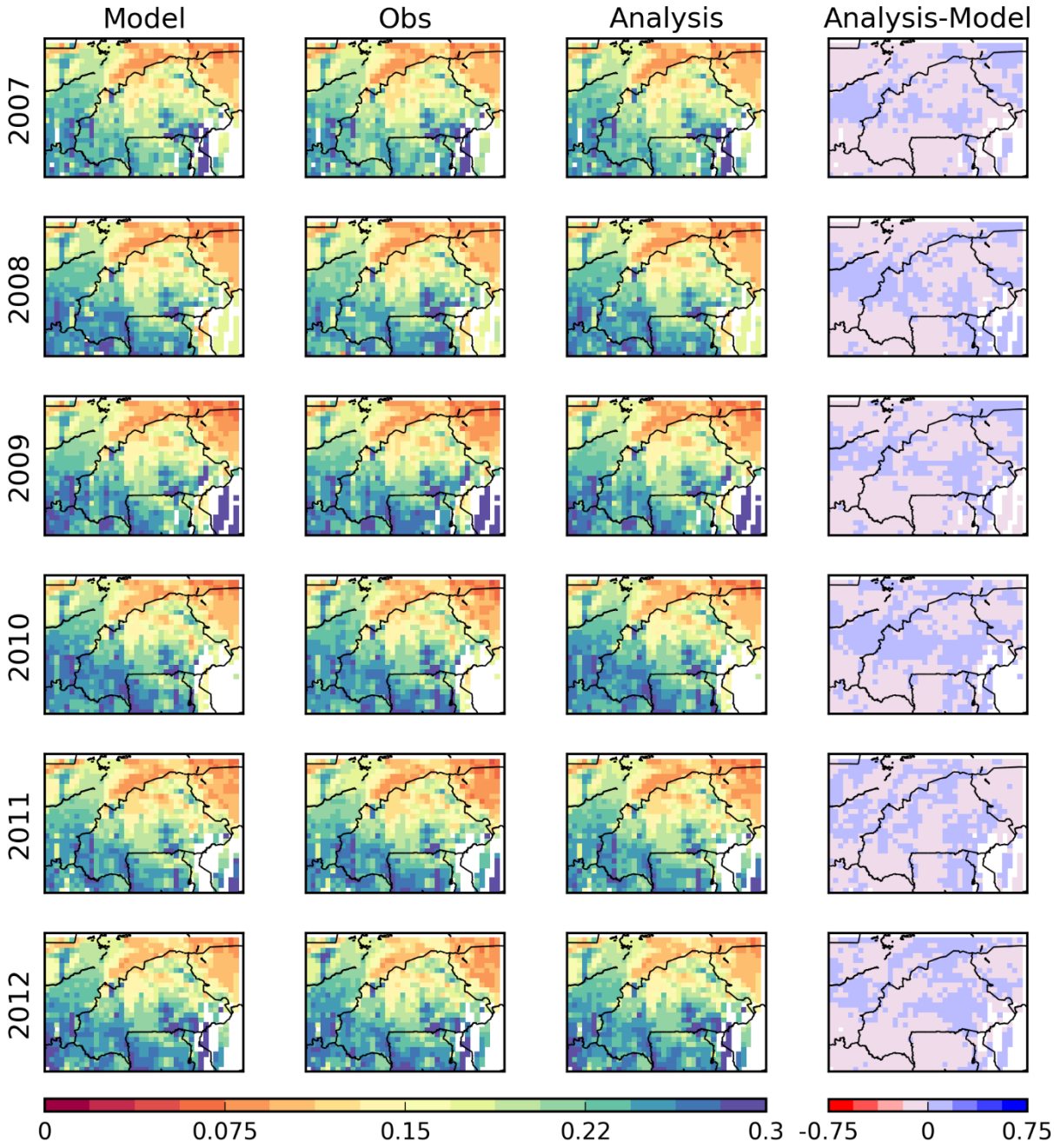

A1.5: *ctd.*

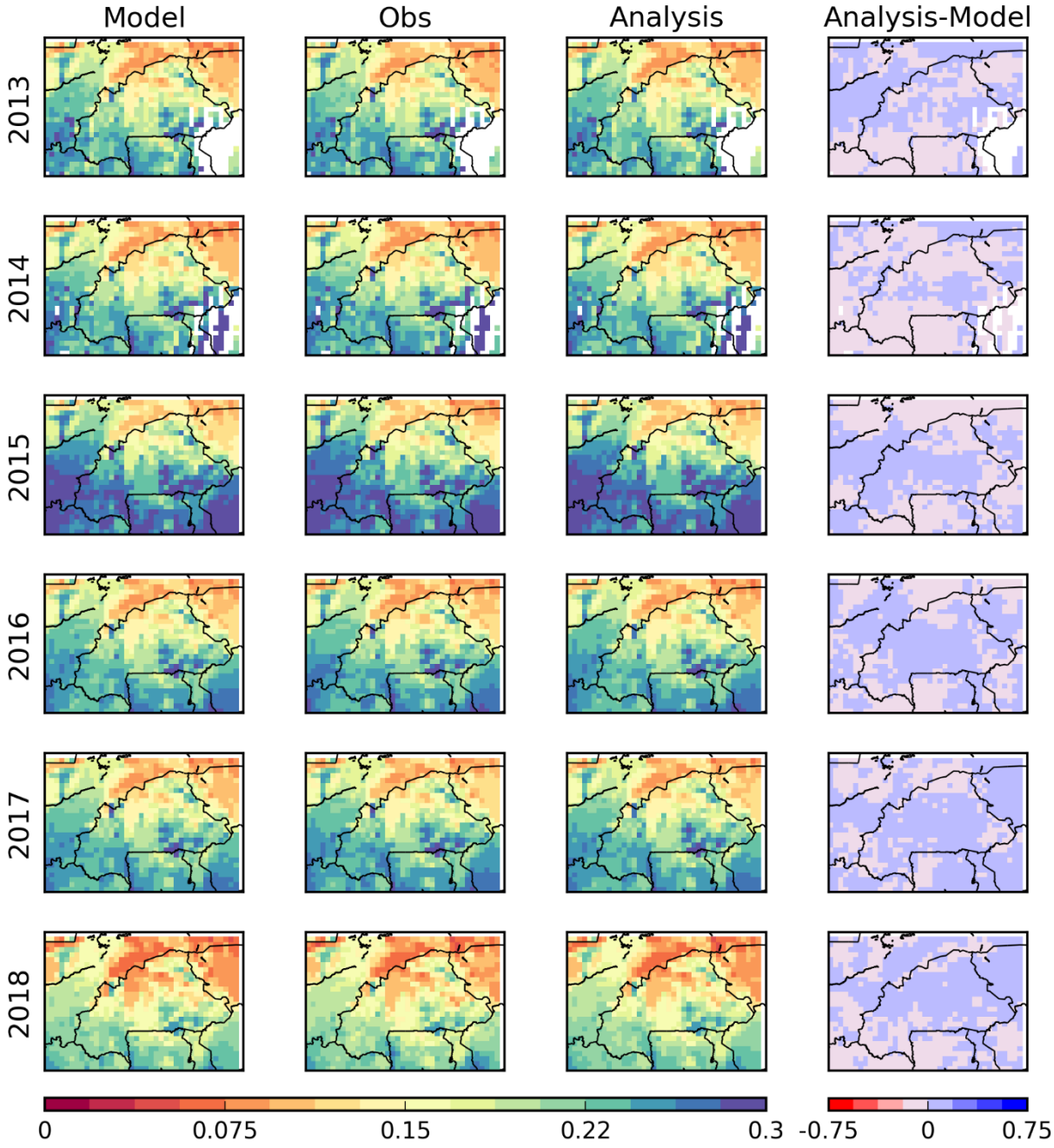
Model
Obs
Analysis
Analysis-Model
2013
2014
2015
2016
2017
2018
0
0.075
0.15
0.22
0.3
-0.75
0
0.75

A1.6: *Seasonnal correlation maps of LAI over January 2001 to June 2018.*

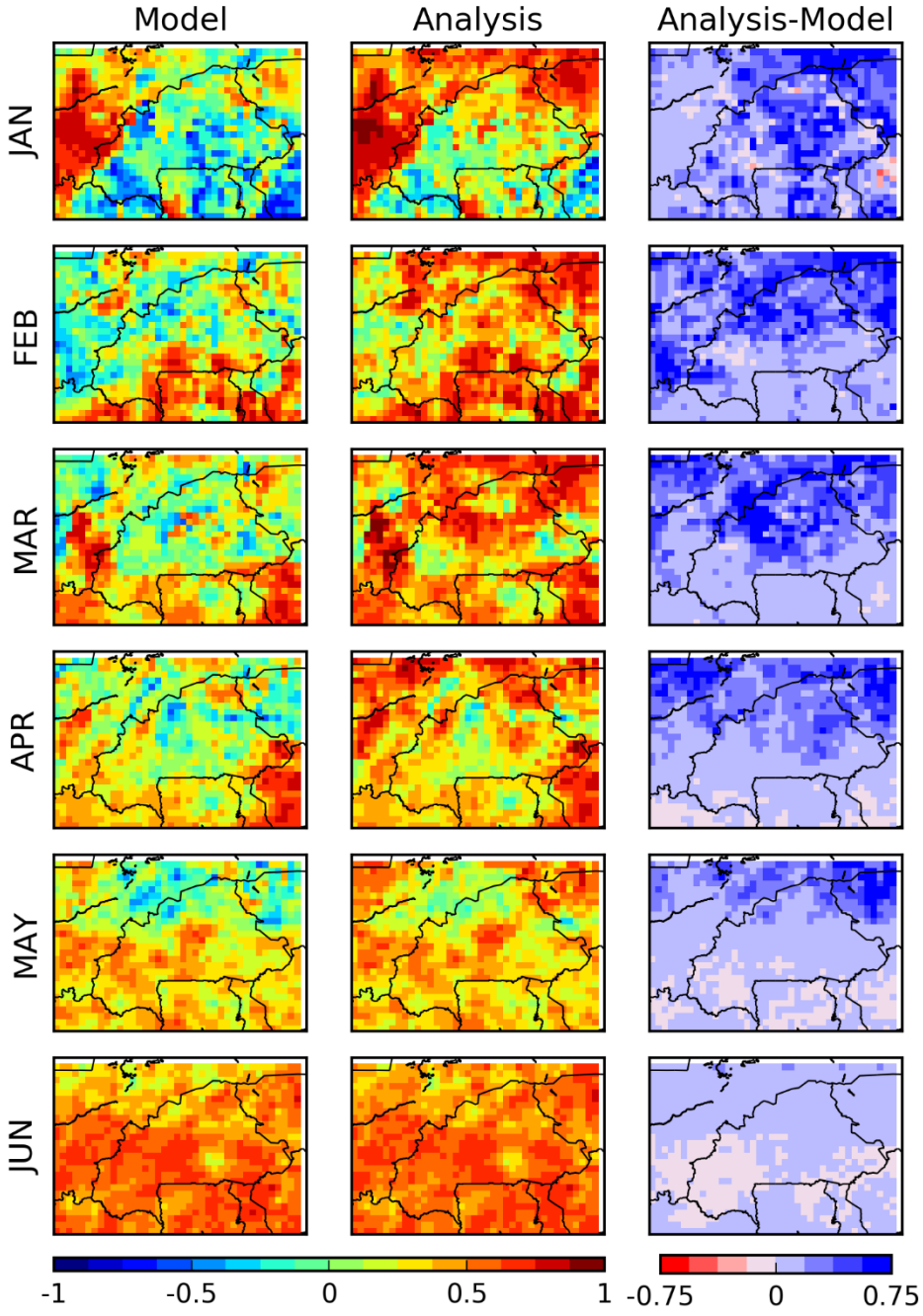

A1.7: *ctd.*

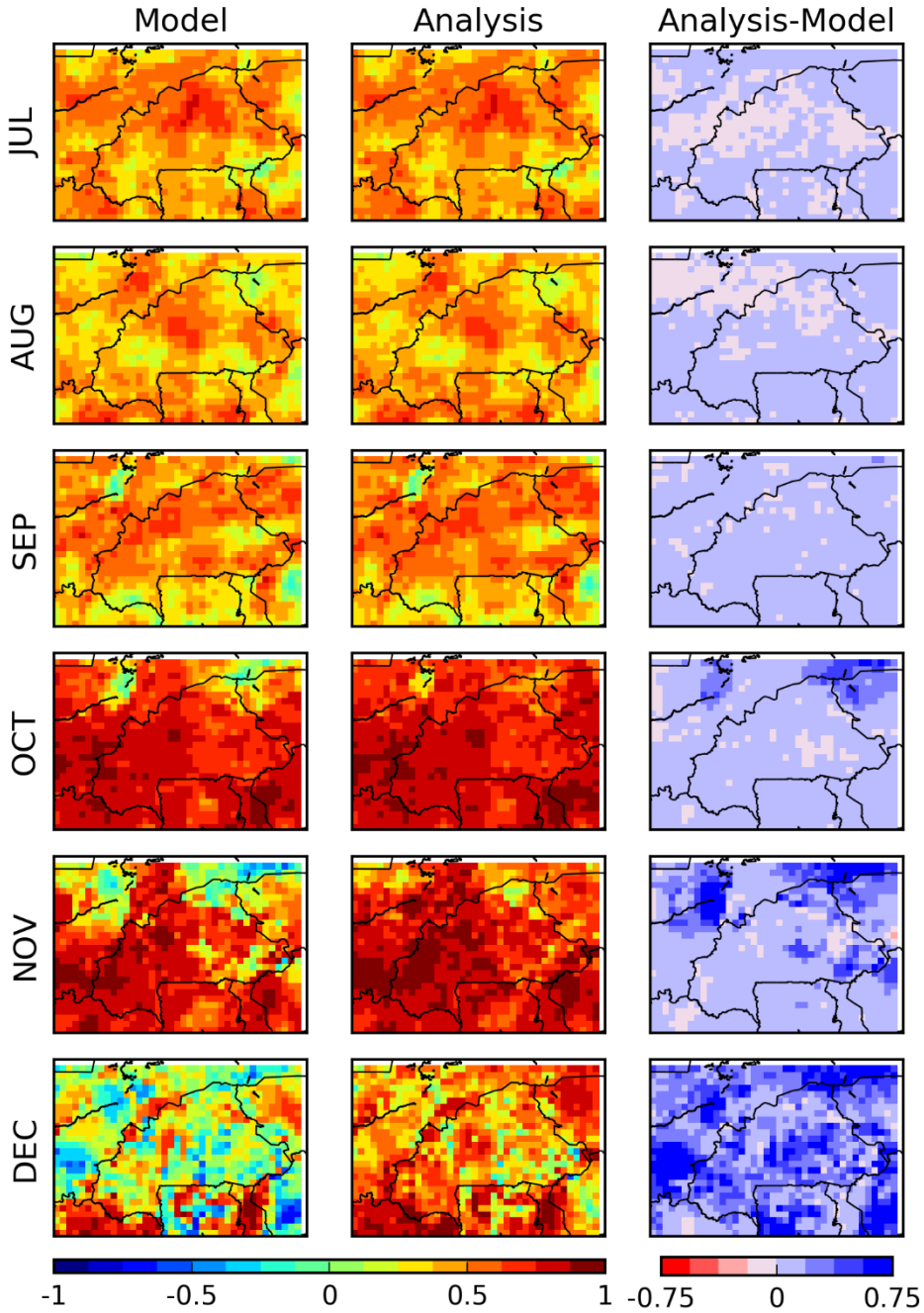
Model
Analysis
Analysis-Model
JUL
AUG
SEP
OCT
NOV
DEC
-1
-0.5
0
0.5
1
-0.75
0
0.75

A1.8: *Climatological maps of SSM from ESACCI-COMBINED and Evapotranspiration from GLEAM along with their respective standard deviation over 2017-08/2019.*

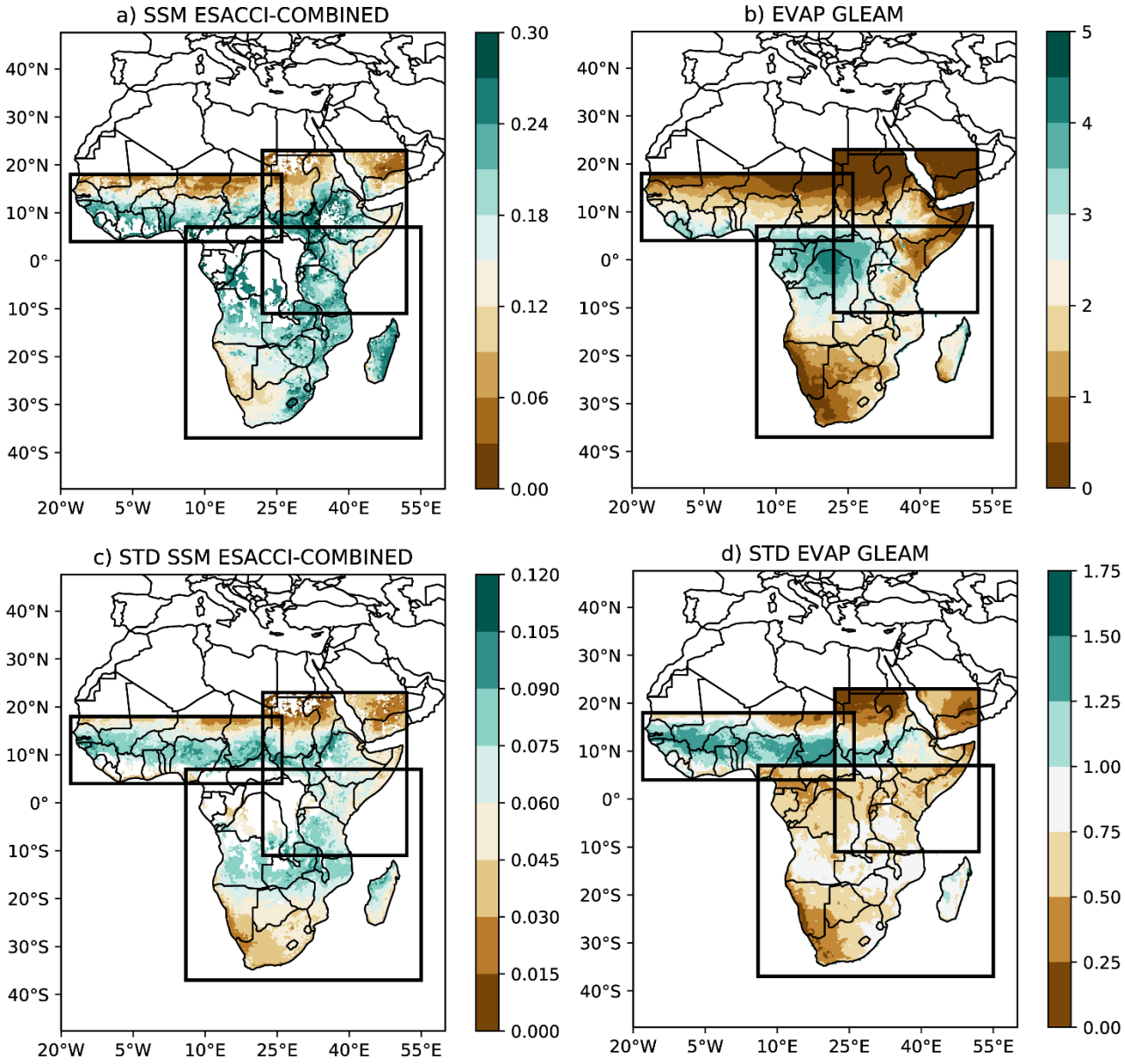

A1.10: *(a), (b), (c) maps of SSM correlation for LDASMonde, ERA5Land FLDAS respectively; (d), (e), (f) differences in correlation between LDASMonde and ERA5Land, LDASMonde and FLDAS and FLDAS and ERA5Land, respectively.*

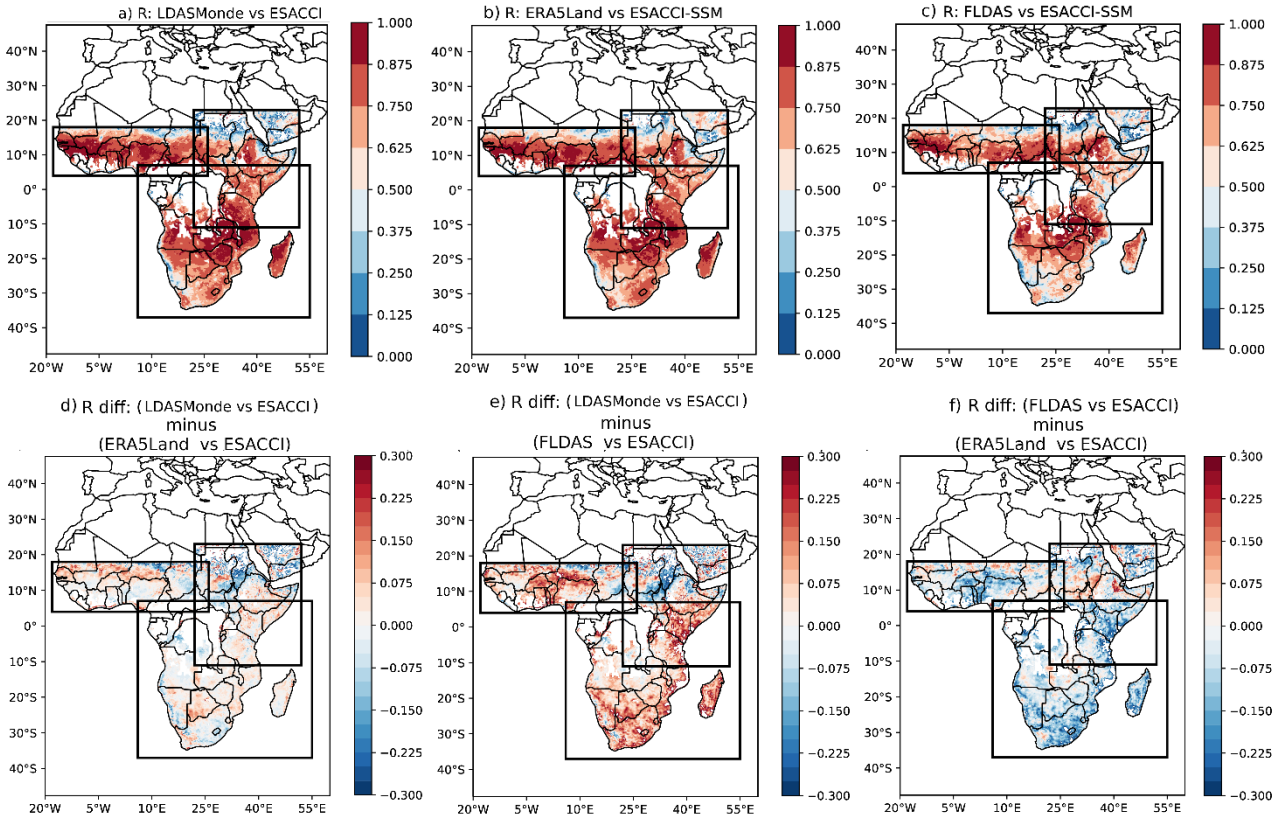

A1.11: *Seasonnal correlation of SSM and Evapotranspiration for LDASMonde, ERA5Land, ERA5 and FLDAS for West (a,d), East (b,e) and (c,f) South Africa.*

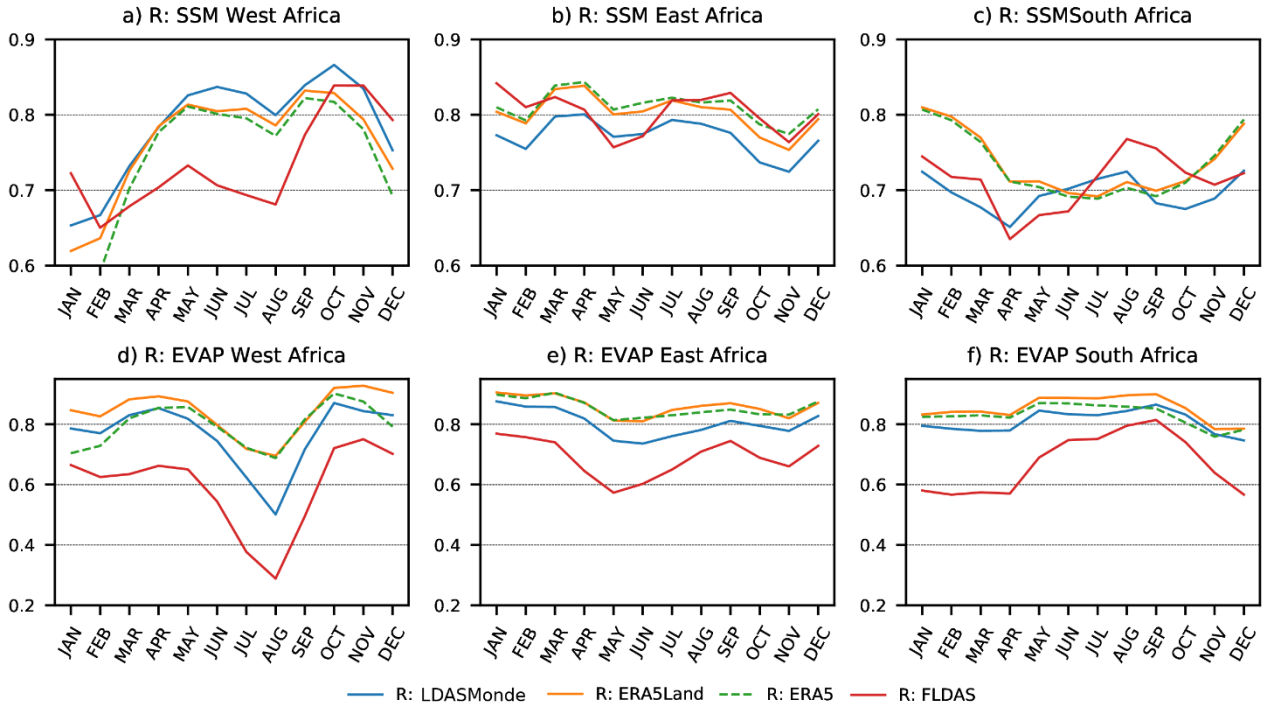

A1.12: *Seasonnal correlation of Evapotranspiration for LDASMonde (with and without vegetation filtered), ERA5Land (with and without vegetation filtered) for West (a), East (b) and (c) South Africa.*

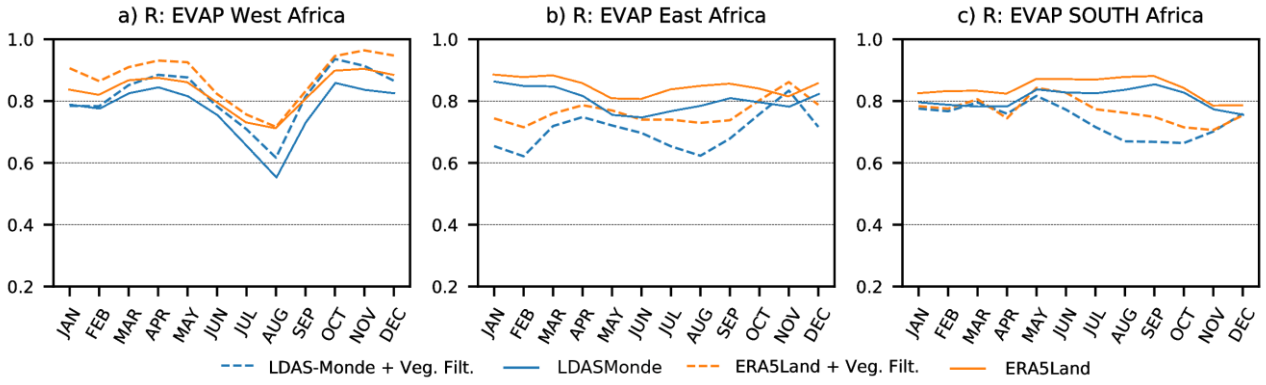

Annexe 2: List of publications and conferences

Publications

Tall, M.; Albergel, C.; Bonan, B.; Zheng, Y.; Guichard, F.; Dramé, M.S.; Gaye, A.T.; Sintondji, L.O.; Hountondji, F.C.C.; Nikiema, P.M.; Calvet, J.-C. Towards a Long-Term Reanalysis of Land Surface Variables over Western Africa: LDAS-Monde Applied over Burkina Faso from 2001 to 2018. *Remote Sens.* **2019**, *11*, 735.

Koubodana, H.D., Adounkpe J., **Tall, M.**, Amoussou, E., Mumtaz, M., Adounkpe, J., Atchonouglo, K. 2019b. Trend Analysis of Hydroclimatic Historical Data and Future Scenarios of Climate Extreme Indices over Mono River Basin in West Africa. Am. J. Rural Dev. 8, 37–52. https://doi.org/10.12691/ajrd-8-1-5

Tall, M.; Albergel, C.; Sintondji, L.O.; Hountondji, Gaye A. T., Guichard Francoise. ERA5Land, FLDAS and ISBA representation of soil moisture and evapotranspiration over Sub-Saharan Africa: an assessment using satellite derived datasets (in prep).

Tall, M.; Sintondji, L.O.; Hountondji F., Gaye A. T. Impact of anthropogenic climate change on the hydroclimatology of Burkina Faso by using an ensemble-based regional climate models. (in prep).

Conferences

(i) African Climate Risks Conference ACRC. 7-9 October 2019. Addis Ababa, Ethiopia (oral presentation).

(ii) AMMA-CATCH 30 years Workshop 12-14 November 2018. Niamey, Niger (oral presentation).

(iii) Ninth ICTP Workshop on the Theory and Use of Regional Climate Models, 28 May – 8 June 2018, Trieste, Italy (oral presentation).

Candidate biography

Mr Moustapha Tall is engaged in the West African Science Service Center on Climate Change and Adapted Land Use (WASCAL) Doctoral program for his doctoral thesis in Climate change and water resources at the Université of Abomey-Calavi (UAC) in Bénin Republic since 2016. His research interests are climate change implications on water resources, extreme events such as droughts and floods, land surface modelling as well as data assimilation. Prior to his PhD studies, he completed a Master's Degree in Meteorology at the Laboratory of Atmospheric and Ocean Physics at the Université Cheikh Anta Diop (UCAD) of Dakar in Senegal. Most of his research involves the use of stand-alone models, regional climate models coupled with hydrological routines to provide hydroclimatic information that are potentially relevant for future water resources planning as well as to cope with global changes. He is also an IPCC contributing author for the AR6 (Chapter 12: Climate change information for regional impact and for risk assessment).

Abstract: This thesis aims to assess past and future hydroclimatic conditions over Burkina Faso using an integrated approach involving land surface modelling, data assimilation and climate change. To this end, high-resolution simulations from the CO_2-responsive versions of the Interactions between Soil, Biosphere, and Atmosphere (ISBA), the global Land Data Assimilation System (LDAS-Monde) and a multi-model ensemble based on the most recent version of the Regional climate Model (RegCM4) under two Representative Concentration Pathways (RCP4.5 and RCP8.5) are used. ISBA estimates are assessed through its forcings (ERA5 and ERA-Interim reanalyses) for precipitation and solar radiation variables. First, it is shown that both reanalyses present a good performance in representing precipitation variability and incoming solar radiation (with better score for ERA5). This highlits a good calibration and potential of ISBA to provide good quality estimates of land surface estimates such as Leaf Area Index (LAI) and Surface Soil Moisture (SSM). Then, within LDAS-Monde, SSM and LAI observations from the Copernicus Global Land Service (CGLS) are assimilated with a simplified extended Kalman filter (SEKF) using ISBA over a long period (2001-2018). Results of four experiments are then compared: Open-loop simulation (i.e., model run with no assimilation) and analysis (i.e., joint assimilation of SSM and LAI) both forced by either ERA5 or ERA-Interim. After jointly assimilating SSM and LAI, sensitivity study of the model to the observations permits to notice that the assimilation is able to impact soil moisture in the first top soil layers (mainly up the first 20 cm), but also in deeper soil layers (from 20 cm to 60 cm and below), as reflected by the structure of the SEKF Jacobians. The benefit of using ERA5 reanalysis over ERA-Interim when used in LDAS-Monde is highlighted. The assimilation is able to improve the simulation of both SSM and LAI: the analyses add skill to both configurations, indicating the healthy behaviour of LDAS-Monde. For LAI in particular, the southern region of Burkina Faso (dominated by a Sudan-Guinean climate) highlights a strong impact of the assimilation compared to the other two sub-regions of Burkina Faso (dominated by Sahelian and Sudan-Sahelian climates). In the southern part of the domain, differences between the model and the observations are the largest, prior to any assimilation. These differences are linked to the model failing to represent the behaviour of some specific vegetation species, which are known to put on leaves before the first rains of the season. The LDAS-Monde analysis is very efficient at compensating for this model weakness. Evapotranspiration estimates from the Global Land Evaporation Amsterdam Model (GLEAM) project as well as upscaled carbon uptake from the FLUXCOM project and sun-induced fluorescence from the Global Ozone Monitoring Experiment-2 (GOME-2) are used in the evaluation process, again demonstrating improvements in the representation of evapotranspiration and gross primary production from assimilation. Finally, the impact of anthropogenic climate change in the hydroclimatology of Burkina Faso for the middle (2041– 2060) and late twenty-first century (2080–2099) has been investigated with regard the historical period (2001-2018). The results indicate that an elevated warming, leading to substantial increase of atmospheric water demand, is projected over the whole of Burkina Faso. In addition, mean precipitation unveils contrasting changes with wetter conditions by the middle of the century and drier conditions during the late twenty-first century. Such changes cause more/less evapotranspiration and soil moisture respectively during the two future periods. Furthermore, surface runoff shows a tendency to increase and decrease over short distances regardless whether the region receives more or less precipitation. Finally, it is found that while dry and semi-arid conditions develop in the RCP4.5 scenario, generalized arid conditions prevail over the whole Burkina Faso for RCP8.5. It is thus evident that these future climate conditions substantially threaten water resources availability for the country as well as agricultural activities. Therefore, strong governmental politics are needed to help design response options to cope with the challenges posed by the projected climate change for the country.

Key words: Land surface modelling, data assimilation, evapotranspiration; leaf area index, runoff, surface soil moisture.

PhD	Moustapha Tall	Integration of land surface modelling, data assimilation and climate change in assessing past and future hydroclimatic conditions over Burkina Faso, West Africa	GRP/CCWR/INE/WASCAL – UAC 01, 2021